INFORMATION TO USERS

This manuscript has been reproduced from the microfilm master. UMI films the text directly from the original or copy submitted. Thus, some thesis and dissertation copies are in typewriter face, while others may be from any type of computer printer.

The quality of this reproduction is dependent upon the quality of the copy submitted. Broken or indistinct print, colored or poor quality illustrations and photographs, print bleedthrough, substandard margins, and improper alignment can adversely affect reproduction.

In the unlikely event that the author did not send UMI a complete manuscript and there are missing pages, these will be noted. Also, if unauthorized copyright material had to be removed, a note will indicate the deletion.

Oversize materials (e.g., maps, drawings, charts) are reproduced by sectioning the original, beginning at the upper left-hand corner and continuing from left to right in equal sections with small overlaps.

Photographs included in the original manuscript have been reproduced xerographically in this copy. Higher quality 6" x 9" black and white photographic prints are available for any photographs or illustrations appearing in this copy for an additional charge. Contact UMI directly to order.

Bell & Howell Information and Learning
300 North Zeeb Road, Ann Arbor, MI 48106-1346 USA
800-521-0600

Université d'Ottawa • University of Ottawa

The Effect of the Substrate Membrane on the Performance of Sulfonated Poly(2,6 - dimethyl - 1,4 - phenylene oxide) - Polyetherimide Thin Film Composite Membranes for Low Pressure Reverse Osmosis

Anuradha P. Boucher-Sharma

A thesis submitted to the Faculty of Graduate and Postdoctoral Studies
in partial fulfillment of the requirement for the degree of
M. A. Sc. In Chemical Engineering
Department of Chemical Engineering
University of Ottawa
Canada

June, 2000

ABSTRACT

Thin film composite (TFC) membranes were prepared by coating sulfonated poly(2,6 - dimethyl - 1,4 - phenylene oxide) (SPPO) of ion-exchange capacity value of 1.8 meq/g on top of substrate polyetherimide (PEI) membranes with various mean pore sizes which were also laboratory prepared. Both substrate membranes and TFC membranes were characterized by the mean pore size and pore size distribution, which were determined by analyzing the reverse osmosis separation data for aqueous solutions of polyethylene glycols of different molecular weights. Low pressure reverse osmosis performance of the composite membranes was also investigated by using aqueous electrolyte solutions.

It was found that the solvent/nonsolvent ratio in the casting solution for the preparation of the substrate membranes did not affect the molecular weight cutoff (MWCO) of the substrate membranes, but had a significant effect on the pure water permeation flux of the substrate membranes. Also, the different morphologies of the substrate membranes resulted in various types of coatings of SPPO which influenced the MWCO of the prepared TFC membranes.

A parameter, N/δ, representing the pore density divided by the total thickness of both the thin coated film of the TFC membrane and the skin of the porous substrate membrane, was calculated for both the substrate and the thin film composite membranes. Strong correlations were found between N/δ of the porous substrate membranes and N/δ of the TFC membranes as well as between N/δ of the substrate membrane and the MWCO of the TFC membranes. Another interesting observation was that the solvent

used for the preparation of the casting solution had a decisive effect on the parameter N/δ for the substrate membranes.

No clear correlation was found between the MWCO of the thin film composite membranes and the pure water flux of the substrate membranes.

The MWCO of the substrate membranes did not have much effect on the electrolyte separation. The mean pore size and pore size distribution of the substrate membranes did not appear to control the performance of the TFC membranes in terms of flux.

It was also found that the performance of the TFC membranes was governed primarily by Donnan equilibrium. The separation data obtained using single salt solutions indicated a decrease in retention with an increase in the valency of the anion. It was therefore concluded that the polyvalent cations mask the charge character of the TFC membranes.

Scanning electron microscopy was utilized to investigate the morphological structure of the substrate membranes. It was found that the solvent used in the casting solution had a definite effect on the membrane structures.

RÉSUMÉ

Des membranes composites à fine couche furent préparées en recouvrant la partie supérieure de membranes supportives en polyetherimide (PEI) de poly 2,6-diméthyl-1,4-phénylène oxyde sulfoné (SPPO) ayant une capacité d'échange ionique de 1,8 méq/g. Les supports de PEI furent également fabriqués au laboratoire, et ce avec des diamètres moyens de pores différents. Le diamètre moyen et la distribution de taille des pores des supports et des membranes composites furent évalués via les données d'osmose inverse obtenues avec des solutions aqueuses de polyéthylène glycol de différentes masses moléculaires. Les membranes composites furent également l'objet d'études par osmose inverse à basse pression avec d'autres solutions électrolytiques.

Il apparut que le rapport solvant/nonsolvant dan la solution à base de polymères servant à la préparation de supports n'influençait pas leur seuil de coupure mais affectait significativement leur perméabilité à l'eau pure. Il fut trouvé aussi que le seuil de coupure de chacune des membranes composites fabriquées dépendait de la structure originale du support; cet effet résultant probablement de revêtements différents de SPPO.

Le paramètre, N/δ, la densité de pores divisée par l'épaisseur totale de la couche sélective, fut calculé à la fois pour le support et pour les membranes composites. Une grande corrélation fut observée entre le paramètre N/δ du support et le paramètre N/δ de la membrane composite, de même qu'entre le paramètre N/δ du support et le seuil de coupure de la membrane composite. Une observation intéressante de cet étude concerne

le fait que le paramètre N/δ du support est principalement déterminé par le solvant utilisé dans la solution à base de polymères.

Le seuil de coupure du support n'a toutefois pas d'effet sur la séparation des électrolytes par la membrane composite. La distribution des diamètres moyen des pores du support ne semblent pas non plus influencer les performances de perméabilité de la membrane composite.

Il est également montré que la performance des membranes dépendait essentiellement des équilibres de Donnan. Les données de filtration utilisant des solutions avec un seul sel indiquent une diminution de la rétention avec un accroissement de la valence de l'anion. It fut ainsi inféré que les cations polyvalents masquait les charges des membranes composites.

ACKNOWLEDGMENTS

The author would like to express her sincere thanks to Dr. Takeshi Matsuura for having the opportunity to learn from his expertise and profound understanding of membranes and membrane separation processes as well as his guidance throughout this endeavor. The author is also thankful to Dr. Geeta Chowdhury for her continuous encouragement and advice. Furthermore, it should be acknowledged that this project was initiated by Zenon Environmental and the author is therefore grateful to have made a contribution to this project.

Dedicated to my dear family for their unceasing support in all my undertakings.

TABLE OF CONTENTS

LIST OF TABLES

LIST OF FIGURES

NOMENCLATURE

List of symbols

a	Einstein-Stokes radius, cm
c	concentration, g/dL
C_p	solute concentration in permeate solution, ppm
C_f	solute concentration in feed solution, ppm
D_{AB}	diffusion coefficient of A in an infinitely dilute solution of A in B, cm^2/s
d_p	pore size diameter, nm
f_i	fraction of pores of diameter d_i, dimensionless
J	total product flux through membrane, m^3/m^2s
k	Boltzmann's constant, J/K
M	molecular weight, g/mol
M_B	molecular weight of solvent B, g/mol
N	number of pores per unit area, pores/μm^2
N/δ	pore density by effective membrane thickness, pores/μm^3
N_o	Avogadro's number, 6.022045×10^{23}/mol
PF	product flux, m^3/m^2h
Q(g)	weight of polymer, g
R_o	macromolecular radius of polymer in solution of infinite dilution, cm
S_p	surface porosity, %
T	temperature, K
T_c	temperature correction factor, dimensionless
T_g	glass transition temperature, °C
V_A	molar volume of solute A at its normal boiling temperature, cm^3/mol
W (g)	weight of chlorosulfonic acid required, g

Greek letters

η	solvent viscosity, kg/m s
ϕ	association factor of solvent B, chosen as 2.6 if solvent is water
δ	skin layer (selective layer) thickness, nm
η_B	viscosity of solvent B, g/cms
σ_g	geometric standard deviation, dimensionless
ΔP	pressure difference across the membrane, psig
μ_s	mean Einstein-Stokes radius for which solute separation = 50%, nm
η_{sp}	specific viscosity, dimensionless
$[\eta]$	intrinsic viscosity, dL/g

Abbreviations

AFM	atomic force microscopy
CA	cellulose acetate
CN	cellulose nitrate
DMAc	N,N-dimethylacetamide
DMF	dimethylformamide
ESR	Einstein-Stokes radius
GBL	γ-butyrolactone
IEC	ion exchange capacity
MWCO	molecular weight cutoff
NF	nanofiltration
NMP	N-methylpyrrolidinone
NS-100	commercial membrane
NS-200	commercial membrane
PDMS	polydimethylsiloxane
PEG	polyethylene glycol
PEI	polyetherimide
PPO	polyphenylene oxide
PS	polysulfone
PWF	pure water permeation flux
RO	reverse osmosis
SEM	scanning electron microscopy
SPPO	sulfonated poly(2,6-dimethyl-1,4-phenylene) oxide
TFC	thin film composite
TOC	total organic carbon
UF	ultrafiltration
ULTEM1000	trade name of polyetherimide produced by General Electric Co.

CHAPTER ONE

INTRODUCTION

1.1. Membrane Separation Processes (Reverse Osmosis, Nanofiltration and Ultrafiltration)

Over the last 20 years, membranes and membrane separation techniques have evolved from simple laboratory scale uses to industrial processes. Membrane processes have been widely adopted by different industries for purposes such as the production of potable water, the cleaning of industrial effluents, the fractionation of macromolecular solutions in the food and drug industry, the removal of urea and other toxins from blood streams, the removal of heavy metals from wastewaters and process waters in the electroplating and metal-finishing industries, the recovery of hydrogen, the dehydration of organic mixtures, etc. Such a wide range of applications for membrane processes reflects the importance of membranes in our lives. Today, membranes in large-scale commercial applications are increasingly taking the places of conventional processes. The reason for such a shift is that membrane separation processes offer many advantages over conventional processes. Due to their lower energy requirements, membrane separation processes are more economically competitive. Membrane units can also be integrated into existing processes with relative ease and generally operate under mild conditions. Moreover, the properties of membranes can be varied to fit the separation objectives.

A membrane is a thin barrier between two bulk phases and may be one or a combination of the following materials: nonporous solid, microporous or macroporous solid, a liquid phase, or a gel (Ho and Sirkar, 1992). The membrane separating the two bulk phases controls the mass transfer between the two phases. Each phase is a mixture and the membrane is preferentially permeable to some components of the mixture compared to others. Solute separation and permeate flux are governed by both the chemical nature of the membrane polymer and the physical structure of the membrane. The separation of solutes occurs at the skin layer of the membrane. The skin layer is a thin, dense layer responsible for the separation, and therefore often called the active surface layer or selective layer.

Membrane separation processes are driven by the force caused by one of the following three gradients: concentration gradients, electric potential gradients and pressure gradients. Ultrafiltration and reverse osmosis are pressure-driven membrane processes and membranes used in these two processes are classified according to the range of pore diameters and the size of particles which they retain. The approximate diameters for ultrafiltration (UF) and reverse osmosis (RO) regimes are 10-200 Å and 3-10 Å, respectively (Kesting, 1989). Ultrafiltration is used to treat solutions of high molecular weight solutes and low concentration, therefore the osmotic pressure is negligible. On the other hand, reverse osmosis treats highly concentrated solutions of low molecular weight solutes; hence, osmotic pressure is important and high driving pressures are required for the transport of fluid. Of course, it would be desirable to operate at pressures as low as possible. It is for this reason that membrane researchers have started

recently to develop new membranes (Cadotte et al. 1988, Eriksson 1988, Rudie et al. 1993) that may be operated at lower pressures and their rejections are tailored for specific applications. These membranes have been termed "nanofilters" to differentiate them from ultrafiltration and reverse osmosis membranes. The dividing line between ultrafiltration and reverse osmosis is arbitrary, therefore the range of nanofiltration (NF) membranes may overlap both ultrafiltration and reverse osmosis. Unlike UF membranes, NF membranes are capable of rejecting some salts and their operating pressures are situated between those for UF and RO membranes.

1.2. Thin Film Composite Membranes

Loeb and Sourirajan's (1964) invention of the first integrally-skinned membrane resulted in a burst of interest in membrane separations. An integrally-skinned and asymmetric membrane consists of a very dense top layer called a dense skin layer with a thickness of 0.1 to 0.5 μm and a thick porous sublayer with a thickness of about 50 to 150 μm. The skin layer is the functional portion of the membrane and the resistance to mass transfer is determined primarily by this layer. The porous sublayer merely serves as a mechanical support for the skin. Although integrally-skinned asymmetric membranes can serve as separation membranes without any additional layer, they are sometimes used to obtain thin film composite (TFC) membranes. Such composite membranes consist of an integrally-skinned asymmetric membrane and a thin film which lies on the skin layer of the asymmetric membrane. Both the asymmetric membrane and the thin film are

prepared from different polymeric materials. A typical thin film composite membrane is shown schematically in Figure 1. There are some advantages of thin film composite membranes over asymmetric membranes. In thin film composite membranes each layer can be optimized independently to obtain the best membrane performance, i.e., the thin film may be optimized for selectivity and permeability, while the porous sublayer can be optimized for maximum strength combined with minimum resistance to flow. Moreover, a wide variety of polymers may be used to form the thin film. The thin film composite membranes, however, have the disadvantage of being more expensive to manufacture in comparison to integrally-skinned asymmetric membranes. Several methods have been adopted to coat a thin film on a porous sublayer. Dip-coating, interfacial polymerization, grafting and plasma polymerization are some of the examples. Except for dip-coating, all these techniques involve in-situ formation methods.

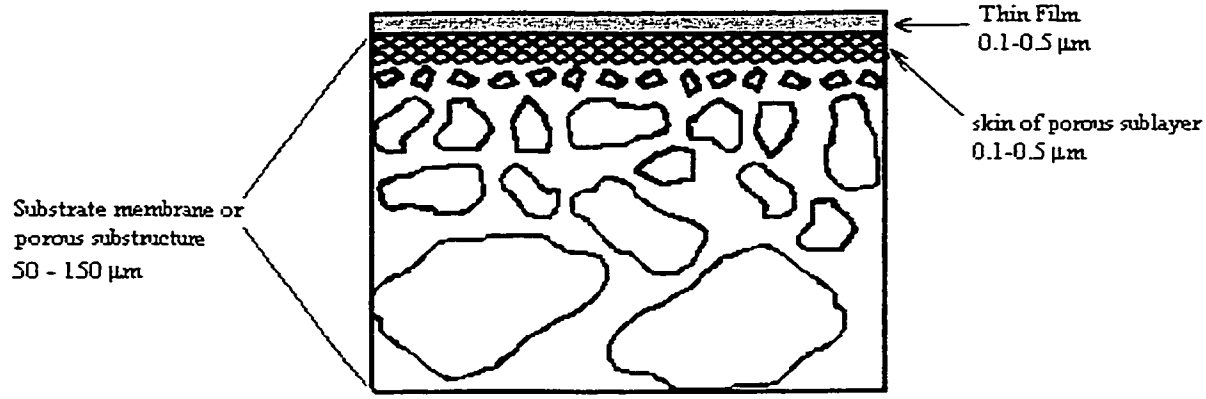

Figure 1. Schematic representation of the cross-section of a thin film composite membrane.

1.3. Charged Composite Membranes

Charged membranes contain in the thin film ionic groups such as sulfonate or quaternary ammonium groups (Strathmann, 1992) which show electric repulsion to solutes having a charge of the same sign as that of the membrane. In this respect, charged membranes can show specific separation abilities. Moreover, because of the repulsive force working on the solute, the pore sizes of charged membranes can be larger than those of neutral membranes to maintain a given separation. As a result, charged reverse osmosis membranes can reject inorganic salts at a lower pressure than neutral membranes.

Some recently developed loose reverse osmosis membranes, which have an intermediate separation ability between those of ultrafiltration and reverse osmosis membranes, are also charged membranes since their skin layer is a polyelectrolyte (Ikeda et al., 1988; Rautenbach and Grosehl, 1990; Petersen, 1993; Tsuru et al., 1994). These charged composite membranes are often termed nanofiltration (NF) membranes. The rejection of substances by these membranes is primarily controlled by two principles: the rejection of neutral species by size (steric effect) and the rejection of ionic solutes by electrostatic interactions between the ions and the membrane (Rudie et al., 1993; Linde and Jönsson, 1995; Rosa and Depinho,1994). There is a wide variety of commercial NF membranes each with differing separation performances. In general, most are thin film composite membranes which contain negatively charged groups fixed to the polymer matrix of the thin film. For negatively charged membranes (cation-exchange

membranes), it is the repulsive force working on the anion which mainly determines the solute retention of salt solutions. The repulsive forces working between ions and the surface of a charged membrane are long-range electrical forces far greater than the dielectric repulsive forces which exist between ions and a neutral membrane. It is for this reason that charged membranes can reject charged solutes whose sizes are smaller than the membrane pore size but cannot reject neutral ones (Jitsuhara and Kimura, 1983; Nakao et al., 1988). Moreover, in the case of negatively charged membranes the degree of retention generally increases with increasing valency of the anions due to stronger repulsion by the membrane (Hamza et al. 1995). In order to maintain electroneutrality, the cations are rejected to the same extent. The reduced thickness of the thin film combined with a charged surface results in charged thin film composite membranes capable of achieving a higher flux at a lower operating pressure than neutral membranes.

1.4. Objectives of this Research

Many investigations have been carried out regarding the effect of materials and coating conditions of the thin film on the overall performance of composite membranes; i.e., the effect of the counterion of sulfonated polyphenylene material (Chowdury et al., 1994) and the effect of the solvent used in making the coating solution (Hamza et al., 1997). Not much attention has been paid, however, to the effect of the porous substrate membrane on the performance of thin film composite membranes, where the porous substrate membrane is the porous sublayer upon which the thin film lies (see Figure 1). There exists therefore a lack of understanding concerning the true role of the substrate

membrane in the performance of thin film composite membranes. Until recently, the substrate membranes were regarded simply as a support for the thin film of composite membranes. Hence, the primary objective of this work is to investigate the effect of the substrate membranes on the performance of thin film composite membranes in which such substrate membranes are used. Polyetherimide (PEI) substrate membranes with a range of pore sizes are prepared in this study by using different compositions of casting solutions. This array of casting solution compositions naturally results in a variety of mean pore size, pore size distribution and porosity of substrate membranes prepared. Charged composite membranes are then prepared by coating the porous PEI substrates so prepared with dilute solutions of sulfonated poly(2,6-dimethyl-1,4-phenylene oxide) (SPPO) in hydrogen form. Low pressure reverse osmosis performance of the composite membranes is then investigated by using aqueous solutions with various solutes.

More specifically, the research objectives of this work are:

1. To investigate the effect of the casting solution composition of porous substrate membranes on their UF performance and porous structure by examining:
   - mean pore size
   - molecular weight cutoff
   - pure water flux
   - membrane structure
   - surface porosity;
2. To characterize porous structures of both substrate and thin film composite membranes in terms of:

- molecular weight cutoff
- mean pore size
- pore size distribution;

3. To investigate the relationship between the substrate membrane and corresponding thin film composite membranes through:
   - molecular weight cutoff
   - mean pore radii
   - parameter N/δ
   - pure water flux
   - configuration of the thin polymer coating;
4. To investigate the effect of the substrate membrane on the reverse osmosis performance of thin film composite membranes by examining:
   - molecular weight cutoff
   - mean pore size
   - pore size distribution
   - rejection
   - pure water flux;
5. To investigate the effect of the electrolyte solutes in the feed solution on the performance of thin film composite membranes by examining:
   - flux
   - rejection.

CHAPTER TWO

LITERATURE SURVEY

2.1. Phase Inversion Membranes

There are several ways to prepare porous polymeric membranes, such as sintering, stretching, track etching and phase separation processes. The final morphology of the membranes will vary greatly depending on the properties of the materials and the process conditions. The majority of membranes are prepared by controlled phase separation of polymer solutions into two phases: one with a high polymer concentration and one with a low polymer concentration. Phase inversion is a process whereby a polymer is transformed from a liquid state to a solid state. The process of solidification is often initiated by the transition from one liquid state into two liquids (liquid-liquid demixing). At a certain stage during demixing, one of the liquid phases (the high polymer concentration phase) will solidify so that a solid matrix is formed. The transitions which occur during the phase inversion process are schematically depicted in Figure 2. By controlling the initial stage of phase transition the membrane morphology can be controlled. This is a very important aspect since the performance of the resulting membrane depends strongly on the morphology formed during phase separation.

There are four main techniques for the preparation of polymeric membranes by controlled phase separation: 1) thermal precipitation; 2) precipitation by solvent evaporation; 3) precipitation from the vapor phase and 4) immersion precipitation. Most commercially available membranes are prepared by immersion precipitation, therefore this technique was employed for the preparation of the substrate membranes used in this study.

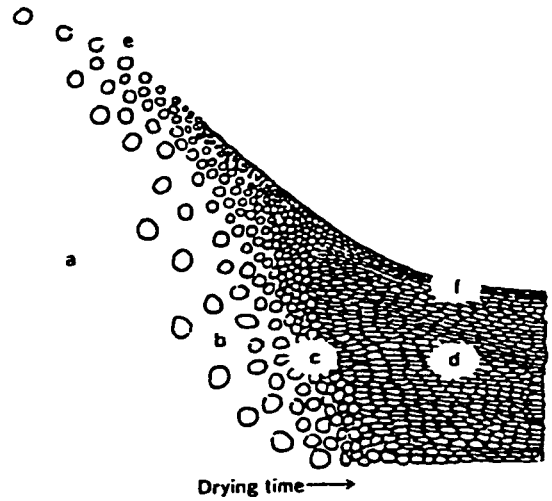

Figure 2. Mechanism of formation of phase inversion membranes: a)sol 1; b) sol 2; c) primary gel; d) secondary gel; e) air-solution interface; f) skin (Kesting, 1985).

2.1.1. Immersion Precipitation

The growth of membrane science was initiated by the invention of the asymmetric membrane (Loeb and Sourirajan, 1962) which can be formed by the technique known as

immersion precipitation. The basic procedure of immersion precipitation involves spreading a casting solution consisting of a polymer and a solvent using a doctor's knife on a support (eg. glass plate) as a thin film. The thin film of polymer solution is either 1) allowed to partially evaporate after which it is immersed in a nonsolvent gelation bath; or 2) immersed directly into the nonsolvent gelation bath. During this, many mass transfer processes occur. Solvent and nonsolvent are exchanged (Zhang et al., 1995; Smolders et al., 1992) between the thin film layer and bath in an interdiffusion-type process, see Figure 3. The resultant loss of solvent power in the casting solution induces a process of demixing (phase separation). Demixed phases undergo further transformations such as dilution, solidification, gelation, etc. Rates of the above mentioned processes greatly influence the final membrane structure and properties. In particular, in solvent-nonsolvent exchange and in demixing, diffusion plays a key role.

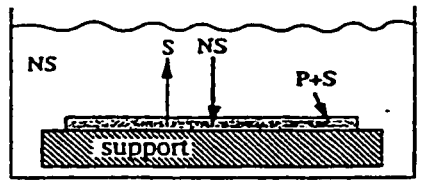

Figure 3. Schematic illustration of immersion precipitation: P, polymer; S, solvent; NS, nonsolvent.

2.1.2. Ternary phase diagrams and phase separation in polymer solutions

The state and equilibrium compositions of polymer solutions can be well depicted in ternary phase diagrams. These phase diagrams and the thermodynamic expressions for the chemical potentials in the system are necessary to properly describe the diffusion process upon immersion in a nonsolvent bath. One has to conclude that a sound thermodynamic analysis is a necessary prerequisite for even a qualitative description of a membrane formation process. It is somewhat surprising that relatively few serious attempts at such analysis have been reported.

Looking at the isothermal ternary phase diagram, Figure 4, the corners represent the pure components (solvent, nonsolvent and polymer), the axes the three binary combinations, and a point in the triangle a ternary composition. Within the triangle, a binodal and spinodal curve can be observed. The tie lines connect the points on the binodal curve that are in equilibrium. A composition within this two-phase region always lies on a tie line and splits into two phases represented by the two intersections between the tie line and the binodal curve. One endpoint in the tie line represents the polymer rich phase while the other represents the polymer lean phase. The area between the binodal and spinodal curves is known as the metastable region. The critical point is the location where the binodal and spinodal curves join.

The location of the binodal curve in the ternary phase diagram can be found experimentally by cloud-point measurements or by measuring the light-scattering of the polymer solutions for various compositions. The binodal curve can also be obtained

mathematically through Flory-Huggins formalism and the proper interaction parameters (Flory, 1953).

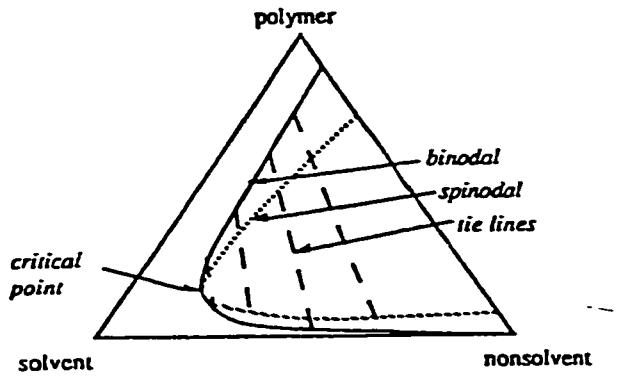

Figure 4. Schematic representation of a tenary system.

The initial procedure for membrane formation from a ternary system is always to prepare a homogeneous (thermodynamically stable) polymer solution. This often corresponds to a point on the polymer-solvent axis (although sometimes some nonsolvent is added to the polymer solution in an amount where the composition of the polymer solution still remains outside the binodal envelope). Demixing will occur by the addition of nonsolvent in an amount that the solution becomes thermodynamically unstable. When the binodal curve is reached, liquid-liquid demixing will occur. When the metastable gap is entered, at a composition above the critical point, nucleation of the polymer-lean phase occurs. The tiny droplets formed consist of a mixture of solvent and nonsolvent and very little polymer. These droplets grow further until the surrounding continuous phase solidifies.

During the process of immersion precipitation, a polymer solution will start on the polymer-solvent axis and when it is immersed in a nonsolvent bath it will follow a specific composition path from its original point on the ternary diagram to its final composition. Composition paths are determined by mass transfer models to describe the diffusion process. From this discussion, it can be understood that changes in the polymer casting solution such as use of different solvents, additives and varying concentrations of the components as well as changes in environmental variables such as use of different gelation baths, gelation bath temperatures and surrounding humidity will indeed result in various composition paths in a ternary phase diagram. Hence, such variables permit control over the ultimate structure and performance of phase inversion membranes.

Moreover, for a specific polymer/solvent/nonsolvent system and temperature, there is a corresponding binodal line. Therefore, if any of these is changed, the binodal line will be different and may be shifted towards the polymer-solvent axis or towards the polymer-nonsolvent axis. Such a change will undoubtedly have an effect on the precipitation of the polymer and hence the resulting membrane morphology.

2.1.3. Estimation of binary liquid diffusion coefficients at infinite dilution

During the process of membrane formation solvent and nonsolvent are exchanged in an interdiffusion-type process. Diffusion of the solvent and nonsolvent in the gelation bath plays a key role in the final morphology of the resulting membrane. Therefore, knowledge of the diffusion coefficients for each of the components in the casting solution is very important.

For a binary mixture of solute A in solvent B, the diffusion coefficient, D_{AB}, of A diffusing in an infinitely dilute solution of A in B implies that each molecule is in an environment of essentially pure B. An old but still widely used correlation for D_{AB}, the Wilke-Chang equation (Wilke and Chang, 1955), is an empirical modification of the Stokes-Einstein relation:

$$D_{AB} = \frac{7.4 \times 10^{-10} (\phi M_B)^{1/2} T}{\eta_B V_A^{0.6}} \qquad (1)$$

where D_{AB} is the mutual diffusion coefficient of solute A at very low concentration in solvent B, M_B is the molecular weight of the solvent B, T is the temperature, η_B is the viscosity of the solvent B, V_A is the molar volume of solute A at its normal boiling temperature, ϕ is an association factor of solvent B and 7.4×10^{-6} is a constant with units of $g^{0.5} cm^{2.8} K^{-1} mol^{-0.1} s^{-2}$. Wilke and Chang recommend that ϕ be chosen as 2.6 if the solvent is water.

2.2. Donnan Exclusion

The theory of the ionic distribution in and outside the membrane was established by considering ion transport through ion-exchange membranes. It is called Donnan exclusion. The same theory is applicable for reverse osmosis by charged membranes. Ion-exchange membranes are characterized by the presence of fixed charges in their component polymer molecules. Ion-exchange membranes can be subdivided into anion-exchange and cation-exchange membranes. Anion-exchange membranes contain positively charged groups attached to the polymer, for example those derived from

quaternary ammonium salts. Positively charged cations are repelled from the membrane because of this fixed charge. This type of exclusion is called Donnan exclusion. Polyelectrolytes that contain a fixed negatively charged group, for example $-SO_3^-$, are called cation-exchange membranes because they are capable of exchanging positively charged ions. The mobile ions which possess a charge opposite that of the fixed charges are known as counter-ions whereas those of the same charge are co-ions. For the case of cation-exchange membranes, in order to maintain electroneutrality, the membranes will have a stoichiometric amount of exchangeable cations in the vicinity of the fixed anions. These mobile cations can be replaced by other cations in an external solution.

In electrolyte separation, a Donnan effect stemming from the membrane charge leads to a difference in rejection according to ionic charge. This Donnan effect will be illustrated using the Figure 5 representing a cation-exchange membrane which is placed in a dilute solution of strong electrolyte. The cations in solution are attracted to the fixed negatively charged groups of the membrane. This results in a higher cation concentration in the membrane and a higher mobile-anion concentration in the solution. The emerging concentration differences cannot be settled by diffusion because electroneutrality would not be maintained. An accumulation of positive charge in the solution and negative charge in the membrane arises due to the flux of cations into the solution and the flux of anions into the membrane. As a result of the first diffusing ions, a potential difference between the two phases is created. Such potential is called Donnan potential. The Donnan potential draws cations back into the membrane and anions back into the solution. An equilibrium between the electric field and concentration difference is eventually found. The counter-ion concentration in the membrane is higher than in the

external solution while the co-ion concentration is lower. As the co-ions are repelled from the membrane, the entire electrolyte is repelled as well in order to maintain electroneutrality. Such exclusion of the electrolyte from the membrane is called Donnan exclusion.

The sorption and transport of the electrolyte primarily depend upon the distribution of the co-ion. The Donnan potential, and hence Donnan exclusion, is influenced by parameters such as the ion-exchange capacity of the dry resin, the degree of swelling or shrinkage, the cross-linking density, the concentration of the solution and the ion charge density. Counter-ions of high charge density (small size and/or high valence) and co-ions of low density tend to decrease the exclusion of the electrolyte. This phenomenon occurs because there is maximum attraction and minimum repulsion by the membrane's fixed ionic groups of counter-ions and co-ions respectively.

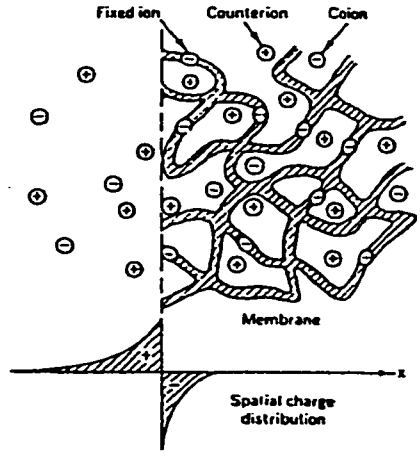

Figure 5. Schematic representation of the distribution of ions in the vicinity of the membrane-solution interface (Kesting, 1985).

2.3. Membrane Characterization by Solute Transport

The performance, flux and rejection, of porous membranes is strongly dependent on the structure of membranes. Therefore, it is of great interest to find the relationship between the porous structure of the membrane, i.e. mean pore size, pore size distribution, number of pores per unit area, etc., and the performance of the membrane. Various methods for characterizing porous membranes have been developed, such as combined bubble pressure and solvent permeability, gas permeability, permporometry, thermoporometry and microscopy observation. A thorough review of these methods was presented by Nakao (1994). There have been a number of studies in which the relationship between solute separation and the solute size has been examined in an attempt to obtain information about the pore size distribution of the membrane. The log-normal probability density function was introduced for correlating separation data with pore size and pore size distribution of ultrafiltration membranes by Michaels (1980). In the present study, membranes were characterized in terms of the mean pore size, geometric standard deviation of the pore size distribution and number of pores per unit area based on solute transport data by following the method presented by Singh et al. (1998). This method is outlined below.

Some of the most common probe solutes used for describing the sieving behavior of polymeric membranes are monodisperse purified proteins and polydisperse, linear macromolecules such as dextrans and their derivatives, poly(vinyl pyrrolidone) and polyethyleneglycol. The Einstein-Stokes radius (ESR) is the parameter generally employed to characterize the probe solute macromolecules. It is defined as the apparent

equivalent spherical radius of the macromolecule and is calculated using the Einstein-Stokes equation:

$$D = \frac{kT}{6\pi\eta a} \tag{2}$$

where D is measured diffusion coefficient, T is the absolute temperature, η is the viscosity of the solvent, k is Boltzmann's constant, and a is the ESR. The diffusivity can also be calculated by using the following equation (Itsieh et al., 1979),

$$D = \frac{2.5\times 10^{6}\, kT}{\left\{\eta\left(M[\eta]\right)^{1/3}\right\}} \tag{3}$$

where M is the molecular weight of the polymer, $[\eta]$ is the intrinsic viscosity of the polymer and the constant 2.5×10^{6} has units of $cm^{2}dL^{1/3}m^{-3}mol^{-1/3}$. By equating these two equations the following is obained,

$$a = 2.122\times 10^{-8}\left(M[\eta]\right)^{1/3} \tag{4}$$

where a is in cm, M is in g/mol , $[\eta]$ is in dL/g and the constant 2.122×10^{-8} has units of $cm\ mol^{1/3}dL^{-1/3}$. The intrinsic viscosity of polyethylene glycol (PEG) of known molecular weight can be calculated by the following equation which is applicable when water is used as the solvent (Meireles et al., 1995),

$$[\eta] = 4.9\times 10^{-4} M^{0.672} \tag{5}$$

where the constant 4.9×10^{-4} has units of $dL\ mol^{0.672}/g^{1.672}$. Combining equations (4) and (5), we obtain,

$$a = 16.73\times 10^{-10} M^{0.557} \tag{6}$$

where the constant 16.73×10^{-10} has units of $cm\ g^{-0.557}\ mol^{0.557}$. The Stokes radii of PEG macromolecules can be calculated from their molecular weights using equation 6.

If the concentration polarization effect is assumed to be negligible, the percent solute separation can be defined as,

$$f = \left(1 - \frac{C_p}{C_f}\right) \times 100 \qquad (7)$$

where C_p and C_f are the solute concentrations in the permeate and bulk feed solutions, respectively. For the system used in this study, the effect of the concentration polarization can be ignored as the mass transfer coefficient for the system is 50×10^{-6} m/s for polyethylene glycols (Matsuura and Sourirajan, 1985). According to Michaels (1980), when the solute separation (%) is plotted versus the Einstein-Stokes radius on a log-normal probability paper, a straight line is generated. Solute separations which are linearly correlated with solute diameters on log-normal probability coordinates are completely defined by two characteristic constants:

1) the mean ESR, μ_s, for which f = 50%, and
2) the geometric standard deviation, σ_g, which can be determined from the ratio of the solute diameter at f = 84.13% and f = 50%

where μ_s is the pore size at which 50% separation is obtained and σ_g is the ratio of the pore sizes at which 84.13% and 50% separation are obtained.

Using these two constants, the pore size distribution of a membrane can be expressed by the following probability density function (Singh et al., 1998),

$$\frac{df(d_p)}{dd_p} = \frac{1}{d_p \ln \sigma_p \sqrt{2\pi}} \exp\left[-\frac{\left(\ln d_p - \ln \mu_p\right)^2}{2\left(\ln \sigma_p\right)^2}\right] \qquad (8)$$

where d_p is the pore size diameter. The pore density, number of pores per unit area, can be determined from the permeability data using the Hagen-Poiseuille equation and

modifying for the total flux by adding all the fluxes through the pores of different sizes (Singh et al., 1998) to obtain,

$$N = \frac{128\eta\delta J}{\pi\Delta P\sum_{d_{min}}^{d_{max}} f_i d_i^4} \tag{9}$$

where N is the total number of pores per unit area, η is the solvent viscosity, δ is the length of the pores, ΔP is the pressure difference across the pores, J is the total flux through the membrane and f_i is the fraction of the number of pores with diameter d_i. The pore length is generally considered to be the thickness of the skin layer of the membrane. Since this value cannot be obtained accurately, equation 9 is modified as follows,

$$\frac{N}{\delta} = \frac{128\eta J}{\pi\Delta P\sum_{d_{min}}^{d_{max}} f_i d_i^4} \tag{10}$$

Note that N/δ now represents the pore density by the effective thickness of the membrane. Similarly, the expression for surface porosity (S_p), which is defined as the ratio between the area of pores to the total membrane surface area, can be derived as,

$$S_p = \left(\frac{N\pi}{4}\sum_{d_{min}}^{d_{max}} f_i d_i^2\right)\times 100 \tag{11}$$

2.4. Origin and Development of Thin Film Composite Membranes

As mentioned in the introduction, there are currently four general methods to prepare composite membranes:

1. separately casting an ultrathin dense membrane film and subsequently laminating it to a microporous support;

2. interfacially polymerizing reactive monomers on the surface of a microporous support;

3. depositing a barrier layer directly from a gas-phase monomer plasma;

4. dip-coating a polymer solution onto a support film followed by drying.

A brief historical review is presented for each method. Petersen (1993) and Petersen and Cadotte (1990) have written very thorough reviews of composite reverse osmosis membranes.

2.4.1. Lamination

The concept and making of the first composite reverse osmosis membrane was developed by Peter Francis of North Star Research Institute in 1964 (Francis, 1966). In his approach, membranes were formed by float-casting ultrathin films of cellulose acetate on a water surface, laminating them to microporous supports and then drying to bond the membranes to the supports. Initially, the microporous support films used were asymmetric Loeb-Sourirajan cellulose acetate membranes. Later, after research for a better support film, microporous polysulfone film proved to have the best properties. The float casting procedure was conducted by first preparing a casting dope of cellulose acetate that was dissolved in a solvent with a slight water solubility such as cyclohexane. When this solution was allowed to flow onto a water surface with mechanical drawing, ultra-thin membranes were spontaneously produced on the water surface. Such cellulose acetate composite membranes are of historical interest only because since then composite membranes of much higher performance have been developed.

2.4.2. Dip-coating

Dip-coating is one of the simplest techniques to obtain a thin film on a porous substrate asymmetric membrane. A coating solution, which generally consists of polymer dissolved in a solvent, is used to produce the thin film. The thin film is formed by contacting the skin layer of the substrate membrane with the coating solution and withdrawing the surface vertically. The membrane is left to dry, resulting in a thin film composite membrane. Additional variations of this method might include incorporation of crosslinking agents in the polymer solution or the use of reactive monomers in place of the polymer.

One of the earliest membranes formed by the dip-coating technique was prepared by Lonsdale, Riley and coworkers (1971). A cellulose acetate - cellulose nitrate (CA/CN) microfilter support was first coated with a layer of aqueous polyacrylic acid solution in order to protect the CA/CN film from the following step. A chloroform solution of cellulose triacetate was then over-coated and dried. This generated a three-layer composite membrane.

A membrane designated as NS-200 was discovered by Cadotte (1975) and consisted of a sulfonated polyfuran barrier layer formed on the surface of a porous polysulfone support. This membrane was produced by dip-coating the polysulfone support in an aqueous solution containing furfuryl alcohol and sulfuric acid. The coated support was then oven-dried at 125-140°C to produce a black composite membrane which was simultaneously sulfonated. The resulting membrane demonstrated high salt

rejections of greater than 99.9% at 20 gfd for synthetic seawater at an operating pressure of 1000 psig.

The PEC-1000 membrane of Toray Industries, Inc. is also apparently prepared by the dip-coating method. This membrane has been described by Kurihara et. al. (1980); however, the composition and preparation conditions are not disclosed. It was prepared by an acid-catalyzed condensation reaction on a microporous polysulfone support. Extremely high rejection of organic compounds were reported for this membrane, typically exceeding 95% from 4-5% feed concentrations.

2.4.3. Gas phase deposition of the barrier layer

Yasuda and Lamaze (1973) have been the pioneers of the use of plasma polymerization to prepare very thin membranes. They observed that certain organic vapors, when exposed to temperature and pressure conditions that will produce a partially ionized gas or plasma, will deposit very thin polymeric films on nearby solid surfaces. In the presence of a finely porous substrate, plasma polymerization results in a thin film which is deposited in a manner in which it can be handled and tested. Many researchers (Yasuda, 1984) have examined a number of organic vapors and plasma conditions. Some of the successfully polymerized monomers and the rate of film deposition are shown in the following table. The main drawback with plasma polymerization is its poor reproducibility.

Table 1. Plasma-polymerized thin films (Gazicki and Yasuda, 1984).

Monomer	Deposition rate (Å/min)
Isobutylene	2.6
Propylene	3.9
Cyclohexane	6.2
Tetrafluoro-1,3-dithiethane	7
Hexamethylcyclotrisilazane	11
Carbondisulfide	31
Thiophene	38
Hexamethylcyclotrisiloxane	46
Tetrafluoroethylene	55
Thiazole	62

2.4.4. Interfacial polymerization

The introduction of microporous polysulfone as a support layer for composite membranes enabled one to use highly acidic or alkaline coating solutions which are often required for interfacial polymerization. The subject of interfacial polymerization was reviewed in a book by Morgan (1965) which dealt with 1) solution polycondensation methods in which equimolar amounts of a diamine and diacid chloride plus tertiary amine were dissolved in an inert solvent; and 2) interfacial polycondensation in which the diamine was dissolved in water and the diacid chloride in a non-water miscible solvent. Interfacially formed membranes were found to be leaky to small molecules such as salts and small dyes.

In 1970 a different approach was taken by Cadotte (Rozelle et al., 1977) which resulted in a significant improvement in membrane properties. A water-saturated microporous polysulfone sheet was immersed in an aqueous solution of polyethyleneimine, then positioned vertically to drain. It was then reacted with toluene diisocyanate or isophthaloyl chloride in hexane. The hexane solution was drained off and

the coated substrate was heat-cured at 110°C. This membrane gave salt rejections in seawater tests in excess of 99% with a flux of 18 gfd at an operating pressure of 1500 psig. This membrane, NS-100, was the first successful example of a noncellulosic composite membrane and the first example of an interfacially formed membrane demonstrating high rejections of small salts. The success of the NS-100 membrane set the direction for several years in the area of interfacially formed membranes. Many additional polymeric amine compositions have been synthesized and evaluated for the production of interfacially formed composite membranes (Petersen 1993).

As the above mentioned methods are all capable of successfully producing thin film composite membranes, the method of dip-coating is used in this study due to its simplicity relative to the other methods and the ease of introducing ionic charge.

2.5. Polyetherimide - Properties and Applications

Aromatic polyetherimide (PEI), constituting the repeat unit shown in Figure 6, is a very attractive polymeric membrane material. It is a resin introduced in 1982 by General Electric Company under the trade name of Ultem® which has since then been used in electrical, electronics, transportation and appliance applications (Serfaty, 1984). It is an amorphous, high performance engineering thermoplastic based on the regular repeating units of ether and imide linkages. The aromatic imide units provide stiffness and high heat resistance while the flexible ether linkages allow for easy processability. Polyetherimide is an attractive polymeric membrane material because of its high physical

strength, chemical resistance to aliphatic hydrocarbons, acids and dilute bases, high temperature stability (glass transition temperature, Tg = 215°C) and good film forming properties. Chemical stability is of great importance in the preparation of composite membranes because the morphology of the substrate could otherwise be changed or damaged during the coating process by the solvents used in the coating solutions.

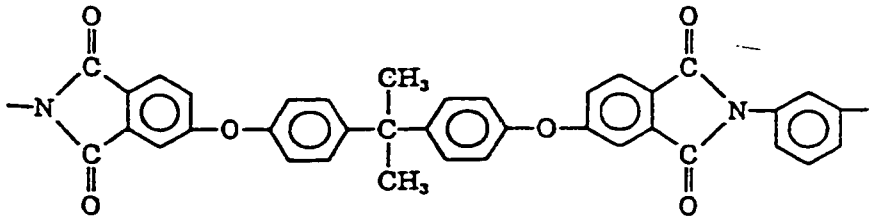

Figure 6. Structural formula of polyetherimide.

Polyetherimide has been used to prepare membranes for gas-gas separations. Kneifel and Peinemann (1992) developed integral asymmetric polyetherimide hollow fiber membranes both with a microporous skin and with a dense skin on the bore side of the fibers. The microporous types were used as substrate membranes for the preparation of composite membranes. The effect of the composition of the polymer solution was studied. In their work, γ-butyrolactone (GBL) was used as an additive and it was found that the number and size of cavities present in the porous sublayer was reduced as the GBL content was increased. Using N-methylpyrrolidinone (NMP) as the solvent, at 25% PEI and with no GBL a large number of finger-like cavities which extended over nearly the entire thickness of the wall were obtained. A reduction in the number and size of the

cavities was observed by adding 30% GBL and at a GBL content of 40% a pure sponge structure was obtained. The oxygen permeability of both the substrate and composite membranes (coated with 1% silicone solution) was strongly affected by the GBL nonsolvent. Optimum permeabilities were obtained at a GBL concentration of 10% for the substrate membrane. For the silicone coated membranes, however, the oxygen permeability increased with increasing GBL content while the O_2/N_2 selectivity decreased with increasing GBL content. The effect of the solvent was also studied. It was found that the morphological structure is also influenced by the type of solvent. A structure with large cavities was obtained when NMP was used as the solvent while the use of dimethylacetamide (DMAc) resulted in a reduction in the number and size of the cavities. The use of dimethylformamide (DMF) as a solvent led to a sponge structure. The effect of increasing the polymer concentration on both the substrate membranes and silicone composite membranes demonstrated that, as expected, the oxygen permeability of the substrate membranes was very much affected by the polymer concentration. The reason for this is that increasing polymer concentration resulted in a densification of the membrane structure. The permeability of the silicone composite membranes, however, remained constant over the range of PEI concentration (22-25%). According to Kneifel and Peinemann (1992), the different behavior of the substrate and composite membranes demonstrated that the permeation characteristics of the composite membranes were determined only by the properties of the silicone film. Therefore, the substrate membrane had no effect on the final properties of the silicone composite membrane.

Park and Lee (1995) also prepared polyetherimide asymmetric hollow fiber membranes and studied the permeation characteristics of carbon dioxide and nitrogen

gases through these membranes. Similarly to Kneifel and Peinemann's (1992) observations, they found that as the concentration of the GBL in the dope solution increased, the structure of the hollow fiber was changed from finger to sponge type.

Many of the studies on polyetherimide membranes were for pervaporation purposes. Huang and Feng have carried out extensive studies on the formation of asymmetric polyetherimide membranes (Huang and Feng, 1995) and the use of PEI membranes for pervaporation of isopropanol/water mixtures (Huang and Feng, 1993). In one study, Huang and Feng (1993) prepared aromatic polyetherimide membranes by the phase inversion method and tested these for the pervaporation separation of water from isopropanol. It was found that the membrane selectivity was enhanced by partial evaporation prior to gelation of the membrane which suggests that the membrane selectivity depends on the membrane structure. In another study (Huang and Feng, 1993), they applied the resistance model approach to polyetherimide asymmetric membranes for pervaporation. It was shown that the overall membrane selectivity is influenced not only by the relative resistance of the skin layer and the substrate but also by the relative resistance of the polymer matrix and the pores in the substrate. Based on their analysis, it was shown as well that for substrates of a given porosity, the smaller the pore size, the better the separation performance, provided that the overall resistance due to the substrate does not change significantly.

Bai et al. (1993) studied the effect of the pore size of the microporous support layer as well as the method of coating the thin film on the pervaporation performance of a composite membrane where polyetherimide was the material used for the microporous support and polydimethylsiloxane (PDMS) was used for the top layer. These membranes

were tested for the pervaporation separation of acetic acid-water mixtures. The permeability of air was measured through dry PEI support membranes made from polymer solutions of varying PEI concentrations (9-30 wt%). It was observed that the permeability decreased with an increase in the PEI concentration, indicating that the pore size of the PEI substrate membranes decreased as the polymer concentration in the casting solution increased. From pervaporation of acetic acid-water mixtures it was also found that the water selectivity increased as the pore size of the PEI membrane decreased. Air permeation and pervaporation experiments were conducted on porous PEI substrates coated with PDMS multilayers. Four PEI substrate membranes with different pore sizes were used and up to five layers of PDMS coatings were applied. It was found that the composite membrane could become either water selective or acetic acid selective, depending on the pore size of the substrate membrane and the method of PDMS coating. Therefore, the performance of these composite membranes could be controlled by changing the characteristics of either the coating layer or the substrate membrane.

Page et al. (1994) studied the pervaporation performance of PDMS spin- and dip-coated polyetherimide membranes for acetic acid-water mixtures. Similarly to Bai et. al. (1993), they found that the coating increased the water selectivity of the membranes for all PEI membranes (20, 23, 25 and 27 wt%) and that the effect was stronger for membranes with smaller pore sizes prepared from casting solutions having higher polymer concentrations. It was also observed that the water selectivity increased as the concentration of PDMS coating solutions increased. The thickness of the coated layer was estimated by weight measurement and compared to that calculated by two versions of the resistance model approach. For the spin-coated membrane, the thickness estimated by

the resistance models was greater than that measured by the weighing method. A comparison of all three coating thickness estimation methods with scanning electron microscopy (SEM) of the membranes revealed that the weighing technique and resistance model approaches overpredicted the coating thickness. This large difference in estimation suggests that the coating solution penetrates the membrane pores to a larger extent than expected.

Finally, polyetherimide has also been used to prepare membranes for organic vapor-gas separations. Deng et al. (1995) effectively separated hydrocarbon mixtures from nitrogen using flat-sheet, asymmetric, aromatic polyetherimide membranes. Deng et al. (1997) prepared hollow fibers from polyetherimide polymer for the separation of volatile organic vapors (n-pentane) from nitrogen, and Fouda et al. (1993) successfully recovered benzaldehyde from a nitrogen stream using silicone (Sylgard 184) coated polyetherimide membranes.

The aforementioned studies show that polyetherimide is a very versatile polymer material to prepare membranes for various applications. However, to date, one area of application where polyetherimide membranes have not been employed is separation of aqueous solutions by ultrafiltration and reverse osmosis.

2.6. Sulfonated Poly(2,6-dimethyl-1,4-phenylene oxide)

Poly(2,6-dimethyl-1,4-phenylene oxide), PPO, is a well-known versatile polymer with a high glass transition temperature, Tg = 220°C (Toi et al., 1982). Due to its hydrophobic nature, PPO does not dissolve in most dipolar solvents and therefore must be

chemically modified. One type of chemical modification of PPO is its sulfonation. Sulfonated poly(2,6-dimethyl-1,4-phenylene oxide) (SPPO) membranes have negative sulfonate ions anchored onto the polymer chains which repulse like charges. Asymmetric SPPO membranes were first attempted by Plummer et al. (1970) for reverse osmosis application where the membrane casting procedure as well as the physical/chemical properties such as film thickness, water content, water permeability and ion exchange capacity (IEC) were optimized. The relationships between membrane properties and reverse osmosis performance were studied in great detail. In this work, PPO of an intrinsic viscosity of 0.45 dL/g was used. Their findings show that the solubility characteristics and water susceptibility varied greatly and depend primarily upon the degree of sulfonation: i.e. at low IECs the polymer is soluble in high chloroform/low methanol solutions, whereas at high IEC values, the polymer is completely soluble in pure methanol and moreover tends to swell excessively in water. It was observed that the water content and IEC of SPPO membranes primarily controlled the reverse osmosis performance, i.e., flux increased with an increase in IEC of the polymer due to the increase of water content which then led to lower rejections. Plummer et al. (1970) also prepared composite membranes using SPPO as the thin film supported by various microporous substrates. Experiments in which both concentration and composition of the feed were varied were performed. Consistent with the Donnan mechanism, the rejections decreased for different feed electrolytes in the following order: $Na_2SO_4 > MgSO_4 > NaCl > MgCl_2$, that is, the higher valence co-ions (anions) and lower valence counter-ions (cations) are best rejected. It was found as well that the concentration of $MgSO_4$ in the feed solution had very little effect on either the flux or the salt rejection. The greatest

advantage demonstrated by the SPPO membranes was their long-term (500 hours) resistance to high pressure (1100 psi) compaction.

LaConti (1977) described the progress that has been made in developing practical sulfonated PPO composite film modules and systems starting from the work of Plummer et al. (1970). The data presented show how these membranes are favored over conventional RO membranes in applications where stability and long-term life is expected. Some of the best suited applications include space station wash water at sterilization temperatures, treatment of highly caustic effluents such as alkaline cyanide plating rinse water and purification of waste water containing organic components.

Further investigations have been carried out by Huang and Kim (1984) on the preparation and reverse osmosis performance of thin film composite membranes. The synthesis of sulfonated polyphenylene oxide polymer as well as the kinetics of this reaction were investigated in an initial study (Huang and Kim, 1984). The preparation of thin film composite membranes of sulfonated polyphenylene oxide - polysulfone (PS) (SPPO-PS) and its applications for the purification of Alberta tar sands waste waters was studied and described in a following study (Huang and Kim, 1984). In this work, various substrates were examined for the preparation of the thin film composite membranes made from polysulfone or polypropylene polymers and it was concluded that the best results were achieved with PS substrate prepared from a casting solution consisting of 12.5 wt% PS in 75 wt% dimethylformamide and 12.5 wt% methyl cellosolve. The cast film was then quenched in an aqueous solution containing 15 wt% NaCl. Similarly to the results obtained by Plummer et al. 1970, Huang and Kim found that for membranes cast under identical conditions, the membrane water content as well as the permeation rate increased

with increasing IEC value. The greatest salt rejections were obtained between IEC values of 2.0 and 2.3 meq/g. The salt rejections were consistent with the Donnan mechanism. SPPO-PS composite membranes with IEC of 2.1-2.3 meq/g were tested under reverse osmosis conditions (600 psig, 20°C) for synthetic and natural waste water from Alberta heavy oil fields. The results obtained regarding rejections and production rate were excellent.

Thin film composite membranes prepared by coating a thin layer of SPPO on the surface of a polysulfone ultrafiltration membrane were studied by Chowdhury et al. (1994) as well. When the sulfonate in the coating was maintained in hydrogen form the permeation rate in the presence of an electrolyte solute in the feed was greater than the pure water permeation rate, with the exception of lithium chloride solute, for which the permeation rate was almost equal to the pure water permeation rate. Chowdhury et al. (1994) interpreted this by the proton (H^+) - alkali metal cation (Me^+) exchange:

$$—SO_3H + Me^+hy = —SO_3^-Me^+ + H^+hy$$

where the right side of the above reaction is increasingly favored as the cationic radius of the electrolyte solute increases as $Li^+ > Na^+ > K^+ > Cs^+$. As the reaction moves from left to right, the number of molecular and/or ionic species increases and more water is drawn into the membrane due to the osmotic pressure effect. Hence, more water is drawn into the membrane as the cationic radius of the electrolyte solute increases due to enhanced ion exchange, thus resulting in a higher permeation rate. When the sulfonate ion in the coating layer of the thin film composite membrane was loaded with an alkali metal cation, however, the pure water permeation rate was highest for Li^+ form and decreased

as follows: $Li^+ > Na^+ > K^+$. Chowdhury et al. (1994) explained these results by relating higher permeation rates to higher hydration number of the loaded alkali metal cation.

Following the above work, Hamza et al. (1995) then studied the effect of the IEC as well as the solvent used for the coating layer on the reverse osmosis performance of sulfonated polyphenylene oxide membranes when solutions of various electrolyte solutes were used in reverse osmosis experiments. The product rate was affected by the IEC value and showed a maximum at an IEC of 1.98 meq/g. The solute separation on the other hand was little affected by the IEC value. Using chloroform-methanol mixtures as the solvent for the coating layer, it was found that the permeability of the SPPO-coated membranes decreased as the chloroform content increased.

Hamza et al. (1997) further investigated the effect of the composition of solvent mixtures used for the preparation of coating solutions on the microscopic structure of thin film composite membranes and their reverse osmosis performance. Scanning electron microscopy (SEM) was used to study the cross-sections of 4 different composite membranes prepared using different solvent mixtures for the coating solution. The thickness of the skin layer could not be clearly distinguished on the micrographs and it appeared that the various chloroform-methanol solvent mixtures did not affect the structure of the substrate membrane. The electrolyte separation of the composite membranes increased slightly as the chloroform content in the coating solution increased, whereas the permeability of the composite membranes decreased. This was attributed to the change in the morphology of the coated layer. Intrinsic viscosity measurements of the polymer solutions in various solvent mixtures revealed that the intrinsic viscosity increased as the methanol content increased and therefore polymer-polymer interactions

decreased. This explained the more open structure of the top layer as the methanol content in the coating solution increased. The latter idea was further confirmed by atomic force microscopy (AFM) measurements which demonstrated that a higher methanol content in the solvent system resulted in a larger nodule size.

CHAPTER THREE

EXPERIMENTAL METHODS

3.1. Material Development and Membrane Preparation

3.1.1. Sulfonation of poly(2,6-dimethyl-1,4-phenylene oxide)

Poly(2,6-dimethyl-1,4-phenylene oxide) (PPO) having an intrinsic viscosity of 1.58 dL/g in chloroform at 25°C was obtained from General Electric Co. Chloroform (Omnisolve), methanol (BDH) and chlorosulfonic acid were all used as received. The sulfonation was carried out in a chloroform solvent system at ambient conditions using chlorosulfonic acid as the sulfonating agent. Ten grams of PPO were added to chloroform to get an approximately 2 wt% solution and was dissolved by stirring for approximately 30 minutes. The amount of chlorosulfonic acid required was calculated for 10 g of polymer and targeting an IEC of 2.0 meq/g using the following formula:

$$W(g) = 116.5 \times Q(g)\left[\frac{\text{target IEC}}{1000 - 80(\text{target IEC})}\right] \qquad (12)$$

where W(g) is the weight of chlorosulfonic acid required and Q(g) is the weight of polymer. Finally the proper amount of chlorosulfonic acid was mixed in approximately 50 ml of chloroform and introduced via an additional funnel dropwise over a period of 3 minutes with constant stirring. The solution was allowed to react by continuously stirring

for a period of 45 minutes. An inert environment was maintained in the reaction vessel by a nitrogen blanket. As the reaction progressed, sulfonated poly(2,6-dimethyl-1,4-phenylene oxide) (SPPO), insoluble in chloroform, precipitated from the solution. The precipitated polymer was then separated and the residual liquid discarded. The polymer was dissolved in methanol, poured onto a Pyrex glass tray forming a film of about 2-3 mm thickness and left to air-dry overnight at room temperature. The dried polymer sheet was then shredded into pieces of about 1 cm^2 and washed with deionized water twice a day until the wash water had a pH above 4. The SPPO was then vacuum dried at room temperature for two days prior to the ion exchange capacity determination. To ensure storage stability, the acid form of the product is generally converted to the sodium form by stirring with saturated NaCl solution (Plummer et al. 1970). However, as the polymer was used to prepare the thin film coating solution within two weeks after it was made, it was kept in acid form in a vacuum oven until use. The sulfonation of PPO conformed to the following chemical reaction:

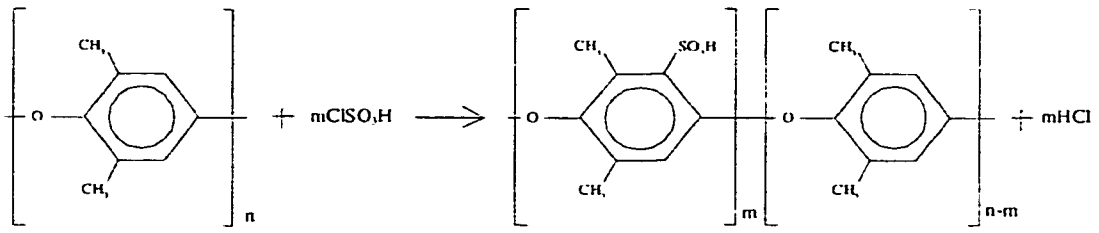

Figure 7. Sulfonation of polyphenylene oxide using chlorosulfonic acid as the sulfonating agent.

3.1.2. Determination of ion exchange capacity

The exact ion exchange capacity (IEC) of the SPPO polymer was determined by using acid-base titration. A weighed amount of SPPO polymer, 0.5 g, was put in an excess measured amount of 0.1 N NaOH solution (25 ml) and stirred for at least one day. The H^+ present in the polymer exchanges with the sodium, liberating H^+ ions which consume a stoichiometric amount of hydroxide. Back titrating the excess sodium hydroxide with 0.1 N HCl then gives the meq (milliequivalents) of hydroxide consumed per unit of dry resin. Using this method, the IEC was found to be 1.8 meq/g dry polymer.

3.1.3. Preparation of integrally skinned asymmetric ultrafiltration substrate membranes

Aromatic polyetherimide (Ultem 1000) was obtained from General Electric Company and was dried at 150 °C for 4 hours prior to use. Reagent grade 1-methyl-2-pyrrolidinone (NMP) and N,N-dimethylacetamide (DMAc) solvents were obtained from Aldrich Chemical Co. and used as received. γ-butyrolactone (GBL) was also obtained from Aldrich Chemical Co. and used as a nonsolvent additive without further purification. Deionized water was used for the gelation medium.

3.1.3.1. Preparation of the polymer solutions

Polymer solutions of various compositions (Table 2) were prepared by mixing polymer, solvent and nonsolvent. The solutions were stirred overnight, filtered using a 10 μm Teflon filter (Millipore), and then degassed for one day by allowing the bottle to sit.

Table 2. Compositions of polymer solutions used for the preparation of substrate membranes (wt %).

Solution #	PEI	NMP	DMAc	GBL
1	22	58	-	20
2	20	70	-	10
3	20	65	-	15
4	20	60	-	20
5	20	55	-	25
6	20	50	-	30
7	20	-	50	30
8	22	-	68	10
9	22	-	58	20
10	22	-	48	30

3.1.3.2. Casting of the substrate membranes

The membranes were cast by immersion precipitation: that is, the substrate membranes were cast by hand on a glass plate using a casting bar (wet thickness 200 μm) and the resulting cast films were immersed in a gelation bath. Water at a temperature of 20.5-21°C acted as the gelation medium. The cast films were left in the water bath for a period of 1 hour, then placed in a 90 °C water bath for 45 minutes and finally stored overnight in a 30 % glycerol solution. The membranes were then air dried for 1 day and stored in plastic bags ready to be used.

All such hand-cast films were visually inspected for pinholes or defects, and good areas chosen for subsequent composite membrane preparations. Inspection was performed by holding up the glycerol-dried film to a strong light source and looking for any points of light passing through defects.

3.1.4. Preparation of thin film composite membranes

A 0.5 wt% or 1 wt% SPPO solution in methanol was prepared and filtered using a Pasteur pipette packed with extra low-lint Kimwipes. Approximately 0.7 ml of the filtered solution was poured and evenly spread onto the skin side of the asymmetric substrate membrane. The excess solution was removed by holding the membrane vertically resulting in a thin layer of SPPO solution. The coated membrane was allowed to dry overnight under ambient conditions.

3.2. Membrane Testing and Characterization Procedures

3.2.1. Experimental reverse osmosis apparatus

Experiments were conducted by using six laboratory reverse osmosis permeation cells each with an effective membrane area ranging between 10.75 cm^2 and 13.2 cm^2, the details of which were described by Sourirajan and Matsuura (1985). The cells were connected in series and therefore six membranes could be tested simultaneously. A schematic diagram of the reverse osmosis apparatus is shown in Figure 8. Prior to characterization, the thin film composite membranes were compacted at 400 psig using deionized water until the permeation rate reached a stable value. After compaction was completed the pressure was decreased to 150 psig, the system was allowed to run for 30 minutes under this condition before the pure water flux (PWF) was measured and recorded.

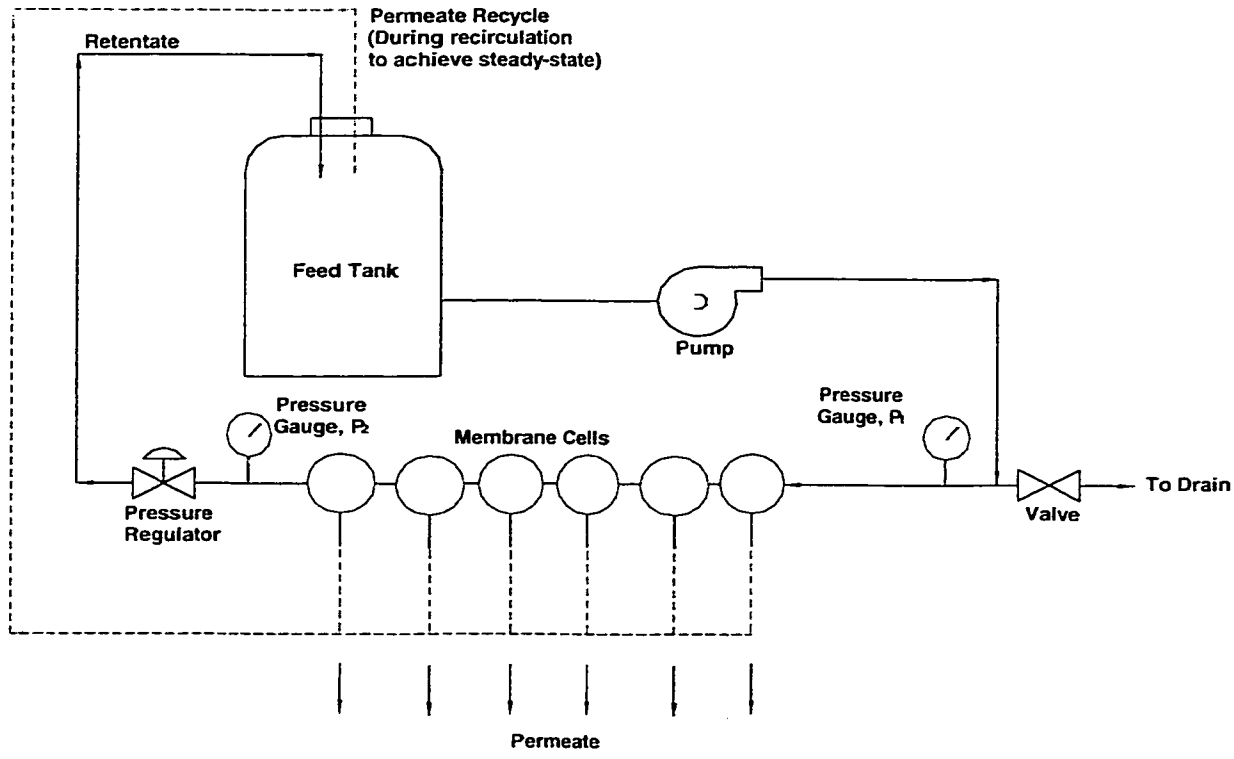

Figure 8. Schematic diagram of reverse osmosis apparatus.

3.2.2 Membrane testing and performance measurement

The reverse osmosis performance of the thin film composite membranes was evaluated in terms of permeation flux as well as solute separation. The experiments were conducted at an operating pressure of 150 psig and at room temperature. During experiments, a pressure drop of less than 10 psig was observed between the pressure gauges. Therefore, the upstream and downstream pressure gauges were adjusted to maintain an average of 150 psig. The feed solution was circulated through the feed chamber of the permeation cells at a flow rate of 800 mL/min. The solution concentrations were 500 ppm for NaCl, 500 ppm and 1500 ppm for $MgSO_4$ and 200 ppm for polyethylene glycols (PEG). The feed solutions were allowed to circulate in the system for a period of one hour in order to reach steady state during which the permeate was recycled to the feed tank to maintain the initial feed concentration. Following this period of time, permeate samples were collected from each cell. A one hour period was chosen as the attainment of steady state conditions as no significant differences in solute separation were observed after 45 min. during preliminary trials performed where permeate samples were analyzed at different times. For each experiment pure water flux (PWF), product flux (PF) in the presence of the solute, and the solute separation, f, in % defined as

$$f(\%) = 1 - {C_p}/{C_f} \qquad (13)$$

were determined, where C_p and C_f are the concentrations of the solute in the permeate and feed solutions respectively. The fluxes were converted to those at 25°C by using density and viscosity data for water. The concentrations of the electrolyte solutes were determined using a Radiometer Copenhagen CDM 80 conductivity meter and the

concentrations of the PEG solutes were measured using a DC-190 Total Organic Carbon Analyzer obtained from Folio Instruments Inc.

The testing of substrate membranes was performed by first subjecting these to compaction using deionized water at 80 psig for 3 hours. The substrate membranes were then tested for pure water flux at 150 psig and PEG solute separation at 50 psig.

3.2.3 Intrinsic viscosity measurement

The intrinsic viscosity of SPPO, having an IEC value of 1.8 meq/g dry polymer, in methanol solvent was measured at 25 °C using a CUSM DC 50 capillary Ubbelohde viscometer obtained from Jupiter Instrument Company. The starting polymer concentration in the viscometer was 0.5 dL/g and was thereafter diluted four times in order to obtain a total of five experimental data points. The experimental flow times were measured as many times as required until a difference of less than 0.5 % between subsequent measurements was obtained. The intrinsic viscosity was determined using Huggin's method (Huggins, 1942) which typically involves extrapolation of experimental data in the form of the quotient η_{sp}/c versus concentration to zero polymer concentration. The intrinsic viscosity was also determined using an alternative method proposed by Kozicki and Kuang (1996). Since the alternative method does not involve extrapolation, it does not require a theoretical equation for use in evaluations. An analytical expression containing the point $\eta_{sp} = 0$ at $c = 0$ which provides a good fit of the experimental data and yields a first derivative at $c = 0$ is sufficient for an independent evaluation of the intrinsic viscosity. The method does not suffer from a magnification of error at low

concentrations. The macromolecular radius in solution of infinite dilution was then obtained by the following equation (Wood and Sourirajan, 1991)

$$R_o^3 = \frac{3[\eta]M}{2.5N_o(4\pi)} \tag{14}$$

where R_o is the macromolecular radius in a solution of infinite dilution, $[\eta]$ is the solution intrinsic viscosity, M is the number average polymer molecular weight, and N_o is Avogadro's number. The number average molecular weight of the SPPO polymer, 157128 Da, was obtained by gel permeation chromatography using dimethylformamide as the solvent. A 0.3 wt% solution was used. The analysis was performed at the Korea Research Institute of Chemical Technology, Korea and the parameters were: HT6E53 gel permeation chromatography column, 200 μL volume, 40 minutes run time, 80 °C and 1 mL/min flow rate.

3.2.4. Scanning electron microscopy

Micrographs of the cross sections of the substrate membranes were obtained by scanning electron microscopy (SEM) at the Institute for Chemical Process and Environmental Technology, National Research Council of Canada. Small samples were cut and broken after cooling in liquid nitrogen. These were mounted on carbon tape on SEM stubs and sputter coated with gold. Analysis was by Jeol JSM 5300 scanning microscope. Photographs of the cross sections were taken at X 2000, X 5000, X 7500 and X 10000 magnifications.

CHAPTER FOUR

RESULTS AND DISCUSSION

A variety of substrate membranes were used to prepare thin film composite membranes. The compositions of polymer solutions for the preparation of the substrate membranes differed in their polymer concentrations, solvents, as well as in their solvent/nonsolvent ratios as indicated in section 3.1.3.1. The use of such different compositions results in a variability of pore size and pore size distribution of the substrate membranes. The charged composite membranes were prepared by coating the porous PEI substrate membranes with dilute solutions of SPPO in hydrogen form. Low pressure reverse osmosis performance of the thin film composite membranes was investigated by using aqueous solutions with various electrolyte solutes. The results of the experiments are presented in this chapter along with appropriate discussions.

4.1. Determination of Molecular Weight Cutoff, Mean Pore Size and Pore Size Distribution

The molecular weight cutoff (MWCO), mean pore size, pore size distribution and geometric standard deviation of the pore size distribution of the various substrate membranes as well as of the thin film composite membranes were determined by applying the sieving model to the separation of polyethylene glycols of different

molecular weights as can be seen in Figure 9 for PEI/DMAc/GBL:20/50/30 - 1 layer 1wt% SPPO. It was assumed that a log-normal probability distribution was applicable for the pore size distributions. Therefore, in order to determine the exact molecular weight cutoff value at 90% separation, the mean pore size at 50% separation and the geometric standard deviation, the results were transferred to a log-normal probability plot where the molecular weights of the polyethylene glycols were converted to Einstein-Stokes radii using equation 6. An example is shown for the PEI/DMAc/GBL:20/50/30 - 1 layer 1wt% SPPO thin film composite membrane in Figure 10. The log-normal probability plots for all membranes can be found in Appendix D. It can be seen in some of these plots that the error bars are somewhat large. The uncertainty involved in the determination of these plots results from a combination of different membrane coupons tested. For the determination of molecular weight cutoff, mean pore size and geometric standard deviation of pore size distribution of each substrate membrane and thin film composite membrane, 3 and 6 membrane coupons were tested respectively.

4.2. Effect of the Solvent/Nonsolvent Ratio in the Casting Solution Used for the Preparation of the Substrate Membranes

Two different solvents were used separately in the casting solutions used to prepare the substrate membranes: 1-methyl-2-pyrrolidinone (NMP) and N,N-dimethylacetamide (DMAc). The polymer, polyetherimide, and the nonsolvent (additive), γ-butyrolactone (GBL), were dissolved into each solvent to make the casting solutions for the preparation of the substrate membranes. A range of solutions was prepared where the

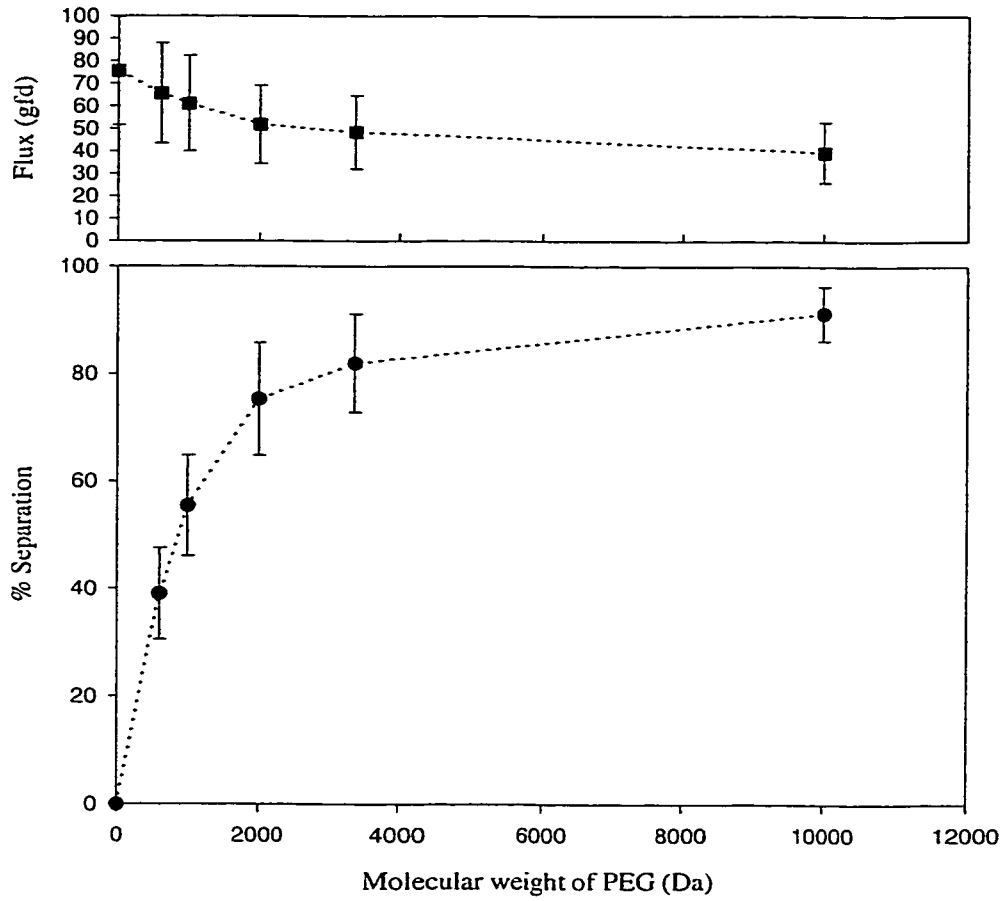

Figure 9. Molecular weight cutoff and flux data for PEI/DMAc/GBL:20/50/30 - 1 layer 1 wt% SPPO.

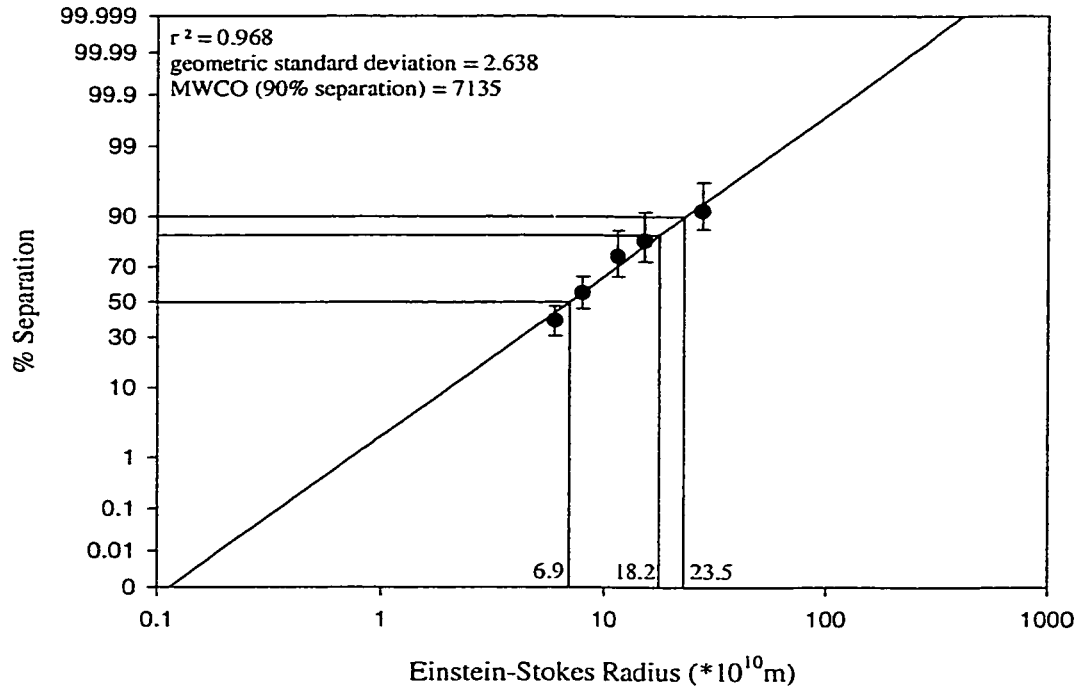

Figure 10. Log-normal probability plot of PEG separation versus Einstein-Stokes radius for PEI/DMAc/GBL:20/50/30 - 1 layer 1 wt% SPPO-H.

ratio of solvent to nonsolvent was varied. In this work, GBL was chosen as an additive because it is a mild solvent that can be added to PEI solutions in a wide concentration range. Furthermore, it greatly increased the viscosity of the polymer solutions which made the process of forming a polymer film on a glass plate easier.

Three substrate membranes were prepared and tested from each of the casting solutions, except for PEI/NMP/GBL:20/60/20 and PEI/NMP/GBL:20/65/15 casting solutions, for which only two defect-free substrate membranes were manufactured and tested. Figure 11 illustrates the effect of the solvent/nonsolvent ratio on the molecular weight cutoff of the substrate membranes. Although there are no clear correlations which can be observed between the molecular weight cutoff of the substrate membranes and the solvent/nonsolvent ratio, some comparisons can be made between substrate membranes prepared using different solvents. A detailed discussion on this comparison will be dealt with in the following section.

The influence of the polymer concentration on the MWCO can be observed in Figure 11. The figure indicates that different MWCOs were obtained for the substrate membranes which were cast from solutions of similar solvent/nonsolvent ratios but two different polymer concentrations (20 wt% and 22 wt%) when DMAc was used as the solvent. For example, looking at the data for membranes PEI/DMAc/GBL:22/48/30 and PEI/DMAc/GBL:20/50/30, which were prepared from casting solutions that have similar solvent/nonsolvent ratios of 1.67 and 1.6, the former membranes corresponding to a polymer concentration of 22 wt% exhibited a lower MWCO. This is understandable on the basis that an increase in the polymer concentration results in densification of the membrane structure and thus a decrease in the MWCO. Interestingly, however, the

substrate membranes prepared from the PEI/DMAc/GBL:22/48/30 polymer solution exhibited also a higher pure water permeation flux (see Figure 12). This is because the surface porosity of PEI/DMAc/GBL:22/48/30 membranes was greater than PEI/DMAc/GBL:20/50/30 membranes. The surface porosities for the substrate membranes were calculated using equation 11 and are presented in Table 3. Moreover, it can be seen from the table that the mean pore radius of the substrate membranes prepared from the casting solution with higher polymer concentration was greater (59.5×10^{-10}m) than that prepared from the lower polymer concentration (22.5×10^{-10}m). This is contradictory to the MWCO data and this can be explained by recalling that molecular weight cutoff is the pore size at which 90% separation is achieved and mean pore size is the size at which 50% separation is achieved. It will be seen in section 4.6 that the geometric standard deviation of the pore size distribution for the PEI/DMAc/GBL:22/48/30 membranes was much smaller than that of PEI/DMAc/GBL:20/50/30. Consequently, although the latter substrate membranes had greater MWCO, their mean pore sizes were smaller than PEI/DMAc/GBL:22/48/30 due to the broader pore size distribution. The differences in mean pore radii obviously has an effect on the pure water permeation flux of the substrate membranes as well.

In the case of the substrate membranes prepared using NMP in the casting solution, for similar solvent/nonsolvent ratios (2.9 and 3) the effect of the polymer concentration on the MWCO appears to be negligible. The decrease in polymer concentration, however, had a definite influence on the pure water permeation flux. The lower concentration of PEI in the casting solution resulted in an increased pure water permeation flux. For example, PEI/NMP/GBL:20/60/20 membranes exhibited a higher

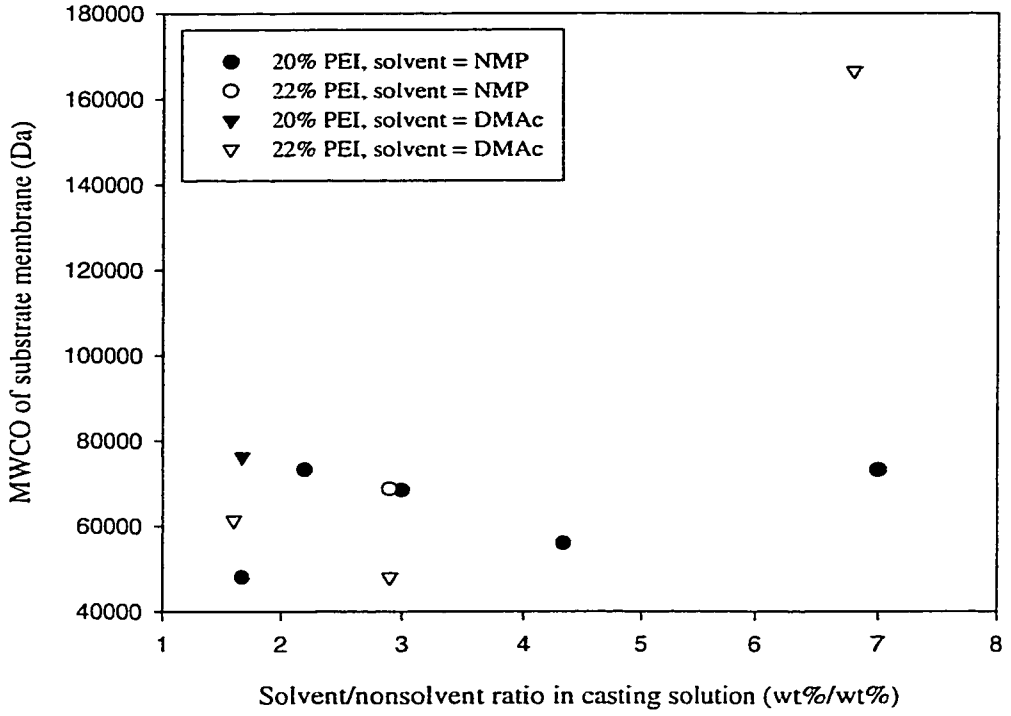

Figure 11. Molecular weight cutoff of the substrate membrane versus the solvent/nonsolvent ratio in the casting solution.

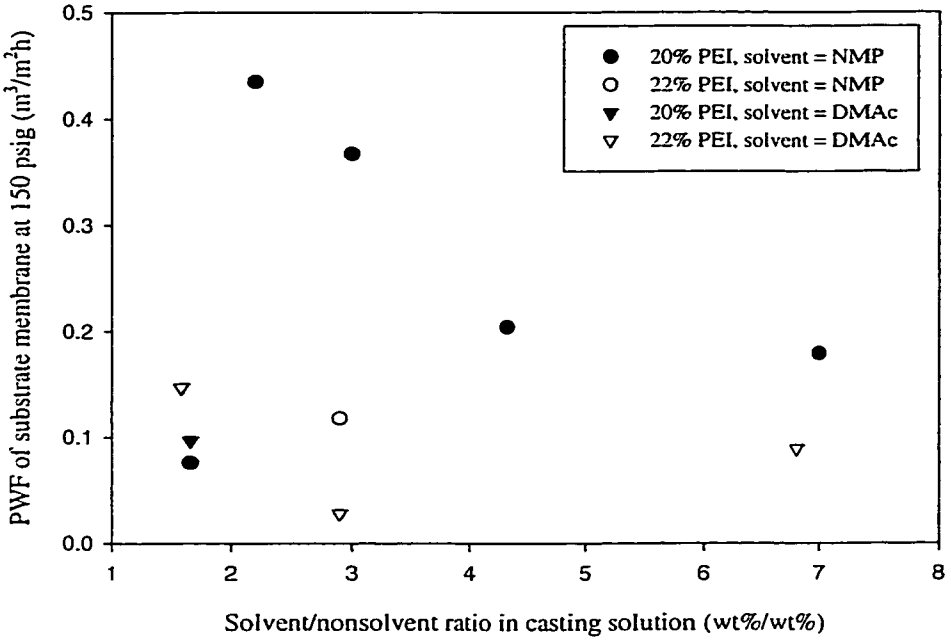

Figure 12. Pure water permeation flux of the substrate membrane at 150 psig versus the solvent/nonsolvent ratio in the casting solution.

pure water permeation flux than PEI/NMP/GBL:22/58/20 substrate membranes. This increase is the result of a greater surface porosity (0.425 %) for the former substrate membranes, in contrast to 0.152 % of the latter substrate membranes. On the other hand, the mean pore sizes of these two sets of membranes were comparable.

Table 3. Mean Einstein-Stokes radii and surface porosities of the substrate membranes.

Composition of Substrate Membrane	Solvent/Nonsolvent Ratio	Mean Einstein-Stokes Radius (10^{-10}m)	% Surface Porosity
PEI/NMP/GBL:22/58/20	2.90	41	0.152
PEI/NMP/GBL:20/70/10	7.00	54	0.340
PEI/NMP/GBL:20/65/15	4.33	57	0.595
PEI/NMP/GBL:20/60/20	3.00	38.6	0.425
PEI/NMP/GBL:20/55/25	2.20	66.5	0.899
PEI/NMP/GBL:20/50/30	1.67	34.5	0.149
PEI/DMAc/GBL:20/50/30	1.67	22.5	0.017
PEI/DMAc/GBL:22/68/10	6.80	51.5	0.020
PEI/DMAc/GBL:22/58/20	2.90	14.8	0.005
PEI/DMAc/GBL:22/48/30	1.60	59.5	0.373

Figure 12 shows also that the pure water permeation flux is affected by the solvent/nonsolvent ratio when PEI concentration and solvent are fixed to 20 wt% and NMP, respectively. The figure shows that there exists an optimal solvent/nonsolvent ratio beyond which the pure water permeation flux of the substrate membranes will decline. The maximum occurs approximately at a solvent/nonsolvent ratio of 2.2. This can be explained in the following way. Suppose you start from the highest solvent/nonsolvent ratio and decrease the ratio gradually by increasing the amount of nonsolvent in the casting solution. The interactions between the polymer and the solvent/nonsolvent mixture will become weaker since the solvent power of the

solvent/nonsolvent mixture is gradually lowered. On the other hand, the polymer-polymer interactions will become stronger. Enhanced polymer-polymer interactions tend to increase the size of the polymer aggregates in the casting solution, leading to the formation of larger aggregate pores on the membrane surface. However, when the solvent/nonsolvent ratio is further lowered to 1.67, this will cause a delay in the demixing of the polymer solution, resulting in densification of polymer in the skin layer. This will lead to a lower pure water permeation flux. A possible explanation for the delay in the demixing is that as the GBL concentration in the casting solution is increased beyond 25 wt%, it stops behaving as an additive. At this point, the GBL concentration is so large that it begins to behave as a weak solvent. Therefore, the polymer-polymer_interactions are decreased and the polymer-solvent as well as polymer-nonsolvent (weak solvent) interactions are increased once more, leading to smaller aggregate pores.

Kneifel and Peinemann (1992) also observed an optimal permeability for hollow fibers produced from polymer solutions containing 25% PEI, NMP and 0-40% GBL. In their study, the hollow fibers used for substrate membranes increased in oxygen permeabilities by the addition of GBL up to 10%, corresponding to a solvent/nonsolvent ratio of 6.5. At higher concentrations decreasing permeability values were obtained. Kneifel and Peinemann concluded from these results that the addition of a certain amount of GBL increased the permeability of the substrate membranes due to an increase in the surface porosity, but at higher GBL concentrations the permeability decreased due to densification of the skin layer of the substrate membranes. The substrate membranes in this study also showed an increase in surface porosity as the solvent/nonsolvent ratio decreased (increasing nonsolvent) up to a ratio of 2.2.

When the substrate membranes were prepared using casting solutions with 22 wt% PEI in DMAc, the influence of the solvent/nonsolvent ratio on the pure water permeation flux of the substrate membranes was less pronounced. Contrary to the substrate membranes prepared from casting solutions in which NMP was the solvent, the pure water permeation flux appears to go through a minimum near a solvent/nonsolvent ratio of 2.9. These results can be interpreted in the following way. This time we will proceed from left to right on Figure 12. As the solvent/nonsolvent ratio in the polymer casting solution increases, the weight fraction of the nonsolvent decreases. This reduction in nonsolvent leads to decreased polymer-polymer interactions, therefore hindering the growth of polymer aggregates and resulting in the formation of smaller aggregate pores on the membrane surface. This can be observed as a decrease in the molecular weight cutoff (see Figure 11) as well as in the mean pore radius (see Table 3), when the solvent/nonsolvent ratio was changed from 1.6 to 2.9. Consequently, the reduction in the pore sizes on the surface of the substrate membranes leads to a decrease in the pure water permeation flux. An increase in the pure water permeation flux can then be observed when solvent/nonsolvent ratio is changed from 2.9 to 6.8. This is due to an increase in dissolving power of the solvent/nonsolvent mixture as the amount of solvent in the mixture increases. More water will be tolerated before polymer precipitation will occur, giving a sufficient amount of time for the polymer lean phase to grow. As a result the pore size will increase. It can be seen from Table 3 that the surface porosity increased from 0.005% to 0.020% when the solvent/nonsolvent ratio was increased from 2.9 (PEI/DMAc/GBL:22/58/20) to 6.8 (PEI/DMAc/GBL:22/68/10).

4.3. Effect of the Solvent in the Casting Solution Used for the Preparation of the Substrate Membranes

The solvent in the casting solution itself may have an influence on the mean pore size, surface porosity and pure water permeation flux of the substrate membranes. A study performed by Huang and Feng (1995) in which the phase separation data for systems PEI/NMP/H_2O and PEI/DMAc/H_2O with and without lithium nitrate additive were determined using the turbidimetric titration method resulted in the data presented in Figure 13. The phase separation data obtained in this figure, in the form of a phase diagram, consist of a boundary curve (polymer precipitation curve) which distinguishes the homogeneous and heterogeneous regions. As was discussed in Chapter Two, the homogeneous region which lies in the space between the polymer-solvent axis and the precipitation curve can be considered as a measure of the system's resistance to polymer precipitation by the nonsolvent water. It is clear from the figure that NMP is a more potent solvent than DMAc for PEI polymer.

Figure 12 shows that membranes prepared from the NMP solution exhibited higher pure water permeation flux than those prepared from the DMAc solution, when solvent/nonsolvent ratio and polymer concentration were fixed to 2.9 and 22 wt%, respectively. As demonstrated by Huang and Feng's data (1995), NMP is a more powerful solvent than DMAc. In casting a membrane from a given polymer, the more powerful the solvent is, the more water will be imbibed in the polymer precipitate, rendering the membrane structure more porous. This phenomena is confirmed by the mean pore radii and surface porosities obtained for these membranes.

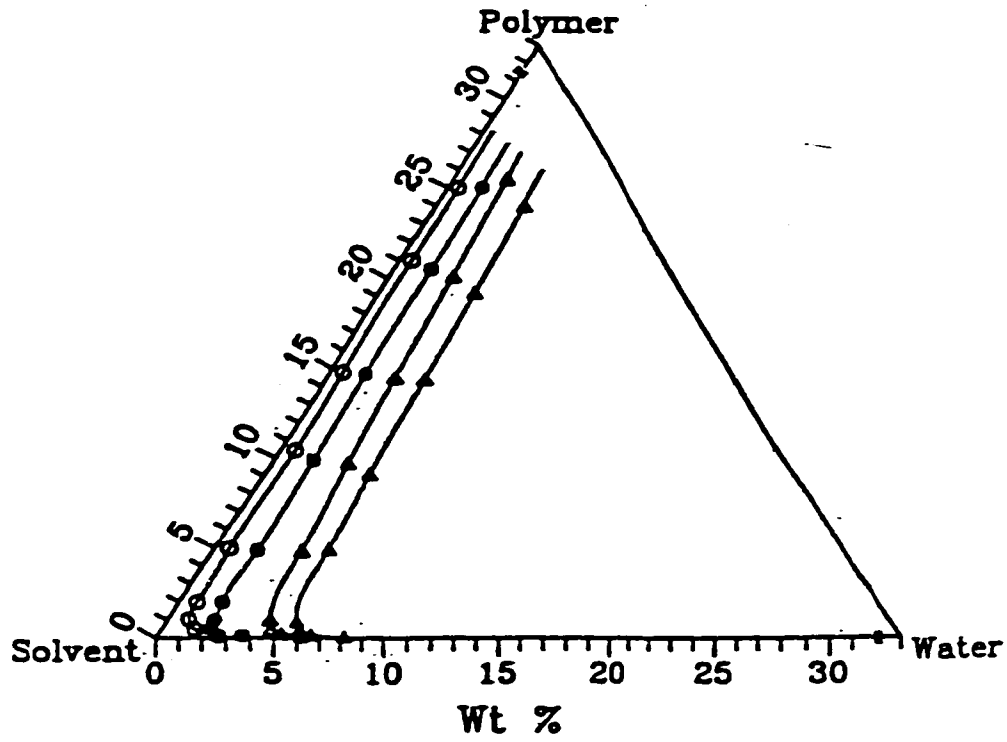

Figure 13. Phase separation data for PEI/solvent/water systems. Temperature, 25°C. Solvent, (O, ●) DMAc and (Δ, ▲) NMP; open keys indicate 2 wt% $LiNO_3$ present in the original polymer solution. (Huang and Feng, 1995).

PEI/NMP/GBL:22/58/20 substrate membranes had a mean pore radius of 41×10^{-10}m and a surface porosity of 0.152%, compared to PEI/DMAc/GBL:22/58/20 substrate membranes which had a mean pore radius of 14.8×10^{-10}m and a surface porosity of 0.005% (see Table 3). Similarly to this study, Huang and Feng (1995) found as well that the amount of water imbibed in the polymer during polymer precipitation affects the morphology of the resulting membranes directly.

For the substrate membranes produced at a lower solvent/nonsolvent ratio of 1.67 and a constant PEI weight fraction of 20% in the casting solution, the pure water permeation flux of the substrate membranes produced using DMAc as the solvent was slightly greater than that of the membranes produced using NMP as the solvent. This is contrary to the results obtained at a solvent/nonsolvent ratio of 2.9 and cannot be explained in terms of mean pore radius or surface porosity. This will be discussed later using the parameter N/δ. Briefly, N/δ was greater for the membranes prepared from the casting solution of the above composition when the solvent was DMAc. The pure water permeation flux, of course, will increase when the number of pores per unit membrane area, N, increases and the effective thickness of the membrane, δ, decreases.

4.4 Characterization by Scanning Electron Microscopy (SEM)

Pore structure in a membrane is influenced by both thermodynamic and kinetic factors of the casting solution and the casting process. These include polymer configuration just before the polymer is precipitated by the entrance of nonsolvent in the quench step. There is a general consensus among researchers that, in the case of

immersion precipitation, liquid-liquid demixing processes are largely responsible for the membrane morphology. The specific structures in the membrane attributed to phase separation processes are even more complicated for ternary systems than for binary systems. The reason for these difficulties is that the diffusion processes change the initial composition of the film directly after immersion. Moreover, the composition is not the same throughout the solution.

Scanning electron microscopy (SEM) was used to investigate the cross-sections of substrate membranes prepared from casting solutions in which the polymer, solvent and nonsolvent concentrations varied. Figure 14 shows the cross-sections of PEI/NMP/GBL substrate membranes where the polymer concentration was held constant at 20 wt% and the GBL content was decreased following 30 wt%, 20 wt% and 10 wt% respectively. The first observation that can be made from these photomicrographs is that the substrate membranes are of asymmetric nature, demonstrating a skin layer and a porous substructure consisting of fingerlike cavities. The effect of the solvent/nonsolvent ratio on the morphology of the substrate membranes can be seen in these figures as well. The following observations can be made as the solvent/nonsolvent ratio increases: (i) there is a decrease in the length and size of the fingerlike cavities; (ii) as they are narrower structures, there is an increase in the number of cavities; (iii) the walls of the fingerlike cavities lose their smooth appearance and become rougher. Although it is rather difficult to assess, comparing Figures 14(b) and 14(c), it appears as though the skin layer thickness of the PEI/NMP/GBL:20/70/10 substrate membrane is smaller or the fingerlike structure begins closer to the top layer of the substrate membrane.

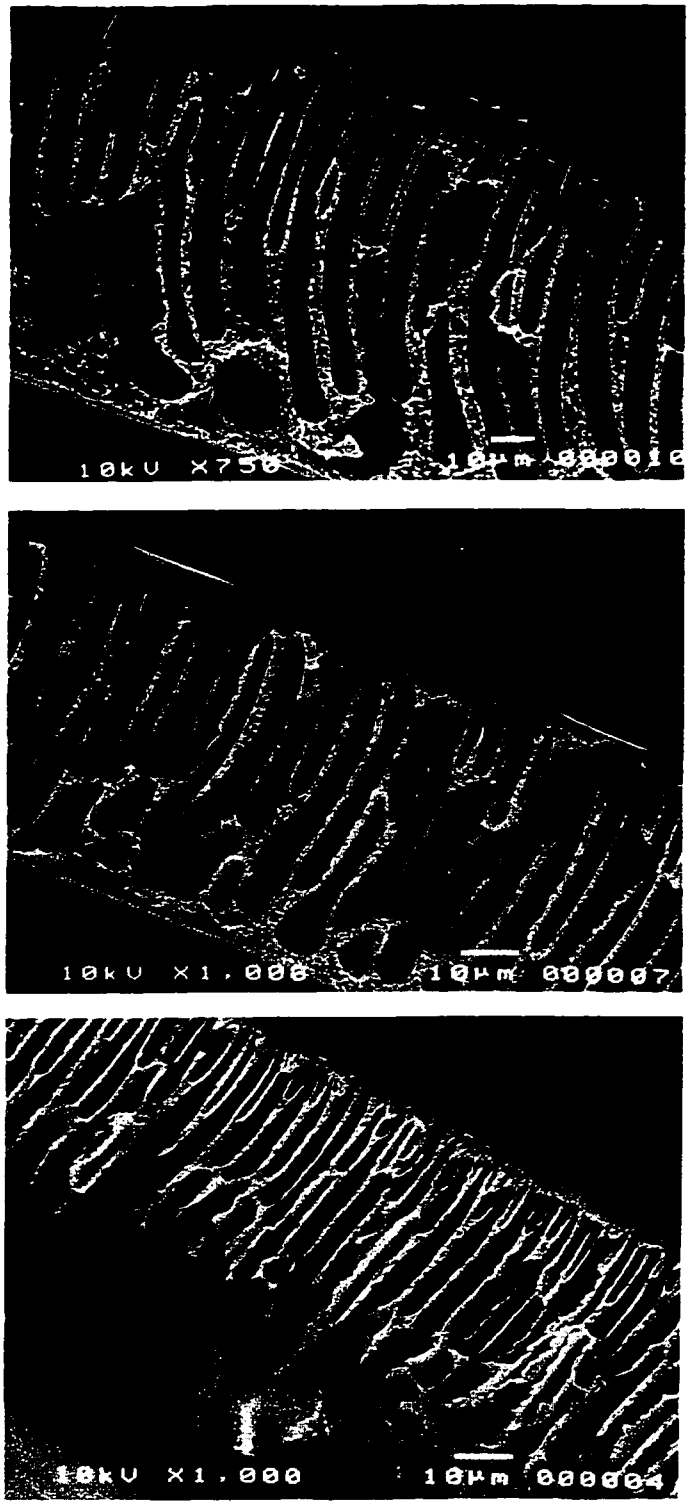

Figure 14. Effect of GBL concentration on the morphological structure of the substrate membranes. PEI concentration = 20 wt%, Solvent = NMP. Content of GBL (wt%) (a) 30 (b) 20 and (c) 10.

The reduction in size of the cavities as the solvent/nonsolvent ratio in the casting solution is increased is due to the faster precipitation of the polymer solution.

During the preparation of PEI hollow fiber membranes from casting solutions of PEI, NMP and GBL, Kneifel and Peinemann (1992) observed, as well, a reduction in the number and size of the cavities with increasing GBL content. At 25% PEI and no GBL a large number of fingerlike cavities which extend over nearly the entire thickness of the wall were obtained. A reduction in the number and size of the cavities was observed by adding 30% GBL and at a concentration of 40% GBL a pure sponge structure was obtained. Park and Lee (1995) also studied the effect of the GBL concentration in the polymer casting solution on the hollow fiber structure. In their study, PEI hollow fibers with an outer skin layer were spun from casting solutions containing different amounts of GBL, 0, 10 and 20 wt%. The polymer concentration was maintained at 25 wt% and NMP was used as the solvent. It was observed that the hollow fiber structure changed from finger to sponge structure as the concentration of GBL in the casting solution increased. In the present study, the change in structure from finger to sponge was not observed. However, the cross-section of the PEI/NMP/GBL:20/50/30 membrane appears to have a larger surface area of sponge structure than the substrate membranes prepared from lower GBL content in the casting solution. Since the polymer concentration of the casting solution in this study was 5 % less than that of the two aforementioned studies, it is possible that the finger to sponge structure transformation would occur at a GBL concentration greater than 30 wt%.

The effect of the polymer concentration on the morphological structure of the substrate membranes was also studied by SEM. The photomicrographs of the substrate

membranes prepared using NMP as the solvent and two polymer concentrations, 20 and 22 wt%, are presented in Figure 15. It was expected that increasing the polymer concentration would result in a densification of the membrane structure; however, no significant differences can be observed in the photomicrographs. The densification in the membrane structure was, on the other hand, more apparent in the permeation fluxes of the substrate membranes (see Figure 12).

The morphological structure of the substrate membrane can also be influenced by the type of solvent used. Figure 16 shows the effect of two different solvents at a PEI concentration of 20wt% and 30 wt% GBL. It is clear that by using NMP as a solvent, a structure with fingerlike cavities is obtained while the application of DMAc results in a spongelike structure. According to Strathmann (1985), fast precipitation of polymer solution in a nonsolvent tends to produce fingerlike cavities, whereas slow precipitation tends to produce a spongelike structure. When solvent loss on the film surface cannot be compensated by solvent diffusion from the film interior to the surface, phase separation in the surface region takes place. As a result, the resistance to the solvent-nonsolvent exchange in the later gelation step increases and, consequently, polymer precipitation slows down, resulting in a spongelike structure. The diffusion coefficients of each solvent used was calculated using equation 1 to determine whether NMP diffused through water faster than DMAc. The results of these calculations are given in Table 4.

a)

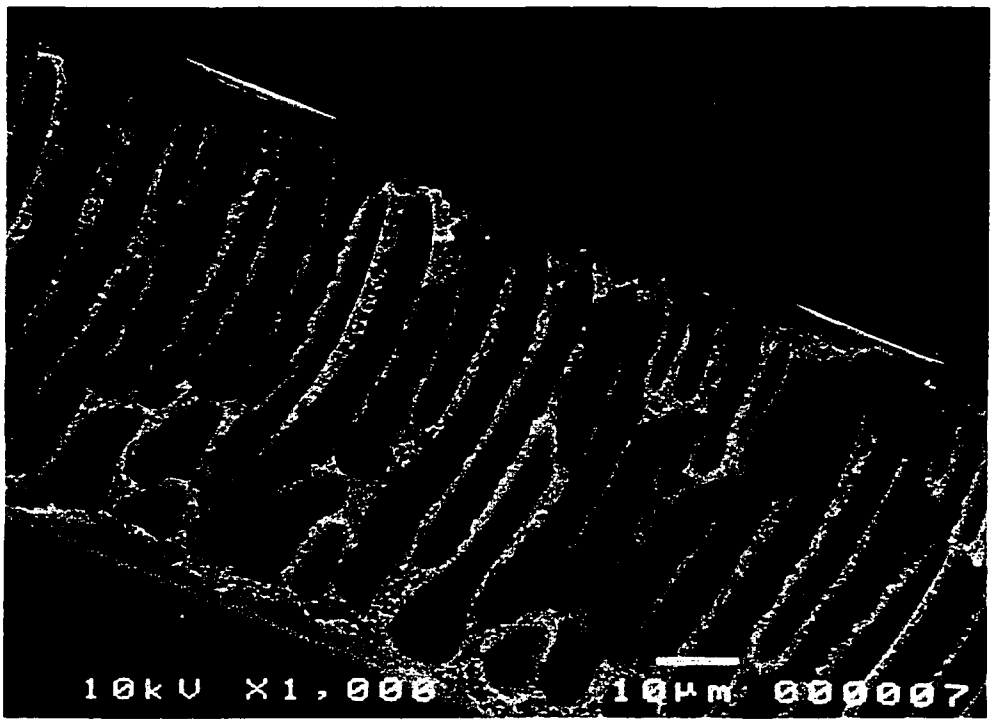

b)

Figure 15. Effect of PEI concentration on the morphological structure of the substrate membranes. Nonsolvent = GBL, Solvent = NMP. Concentration of PEI % (a) 20 (b) 22.

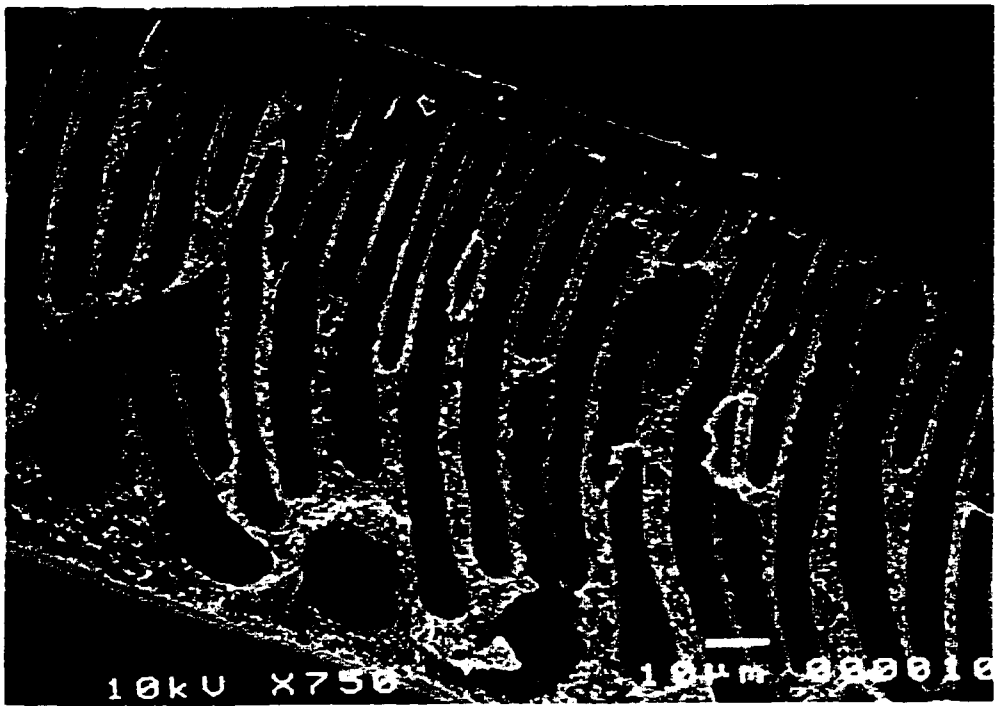

a)

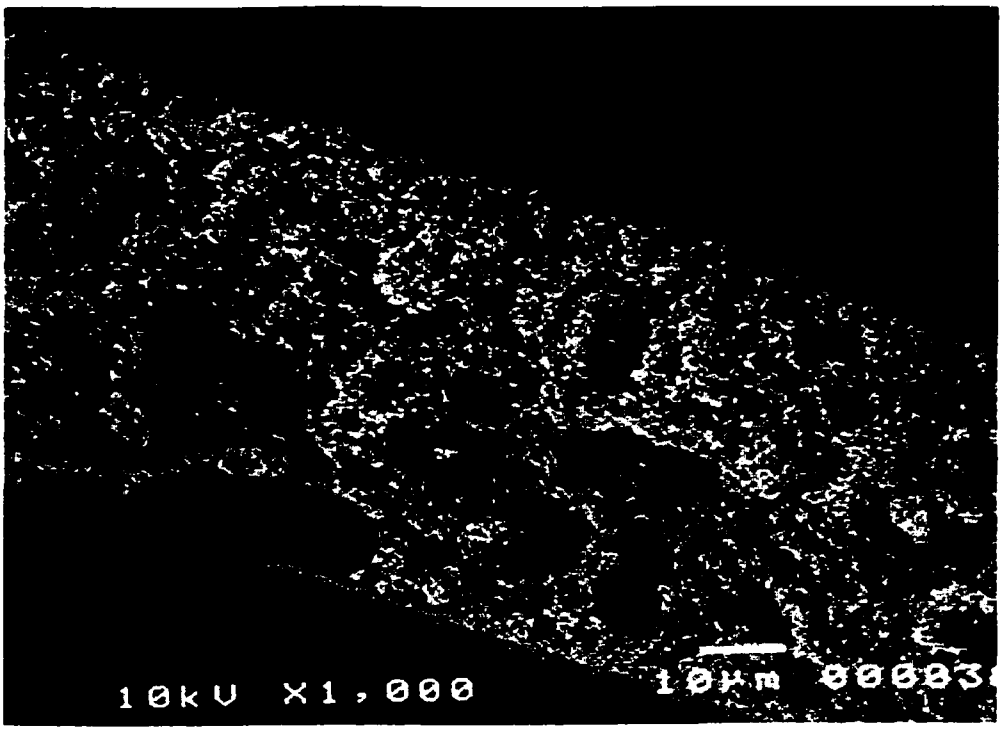

b)

Figure 16. Effect of the solvent on the morphological structure of the substrate membranes. PEI/solvent/GBL:20/50/30. Solvent = (a) NMP (b) DMAc.

Table 4. Estimation of binary liquid diffusion coefficients at infinite dilution of solvents in water.

Solvents and Additive	Diffusion Coefficient (cm^2/s)
NMP	9.757×10^{-6}
DMAc	9.944×10^{-6}
GBL	11.115×10^{-6}

There is hardly any difference between the diffusion coefficients of each solvent. The fingerlike structure obtained using NMP as the solvent can be better explained by the solvent power. As was discussed in section 4.3., NMP is a much more potent solvent than DMAc for PEI polymer and therefore, more water will be imbibed in the polymer precipitate, rendering the membrane structure more open and porous.

4.5. Effect of Coating the Substrate Membrane on the Characterization of the Thin Film Composite Membranes

SPPO, with an ion exchange capacity of 1.8 meq/g, was dissolved in methanol and coated on the substrate membranes to prepare thin film composite membranes. The substrate membranes prepared using NMP as the solvent in the casting solution were coated with one layer of 0.5wt% SPPO whereas the substrate membranes prepared using DMAc as the solvent had one layer of 1wt% SPPO applied to the skin of the porous substrate membranes. It was discussed in the previous sections that by utilizing different solvents and by varying the ratio of solvent to nonsolvent in the polymer casting solution, substrate membranes which possess different molecular weight cutoffs, mean pore sizes

and surface porosities could be produced. In this section, an attempt will be made to understand how these properties will change when the substrate membranes are coated.

The MWCO of the thin film composite membranes as a function of the MWCO of the corresponding substrate membranes was first investigated. The results of this study are presented in Figure 17. The first observation that can be made is that the MWCOs of the thin film composite membranes are always smaller than those of the corresponding substrate membranes. This implies that coating the substrate membranes with a thin layer of SPPO has the effect of decreasing the MWCO of the resulting thin film composite membranes. This can result from: (a) pore blockage by SPPO; (b) pore size reduction due to coating of the pore walls; or (c) development of a polymer network over the preexisting pores (Figure 18).

Figure 17 shows as well that for the MWCO values of the substrate membranes situated in the limited range of approximately 45 000 and 80 000 Da, thin film composite membranes having a variety of MWCOs can be produced. The MWCO values of the resulting TFC membranes extend from 4 400 Da to nearly 37000 Da. This observation implies that the MWCO of the TFC membranes depend on the morphology of the substrate membranes, and the morphology can not be characterized effectively by MWCO values of the substrate membranes.

Another interesting observation is that even for the three PEI/DMAc/GBL:22/58/10 substrate membranes tested which had a very large average MWCO,166 500 Da, the corresponding value for the thin film composite membrane attains a value of only 41 860 Da. This value is not much greater than those obtained for

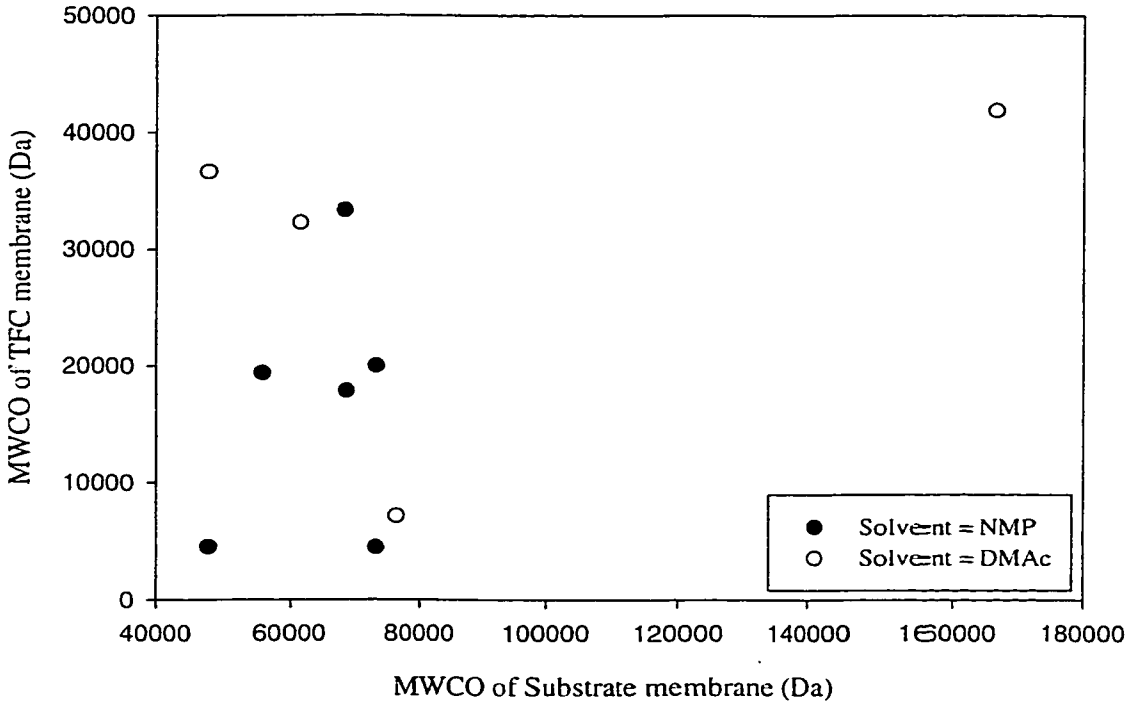

Figure 17. Molecular weight cutoff of the thin film composite membranes versus the molecular weight cutoff of the corresponding substrate membranes.

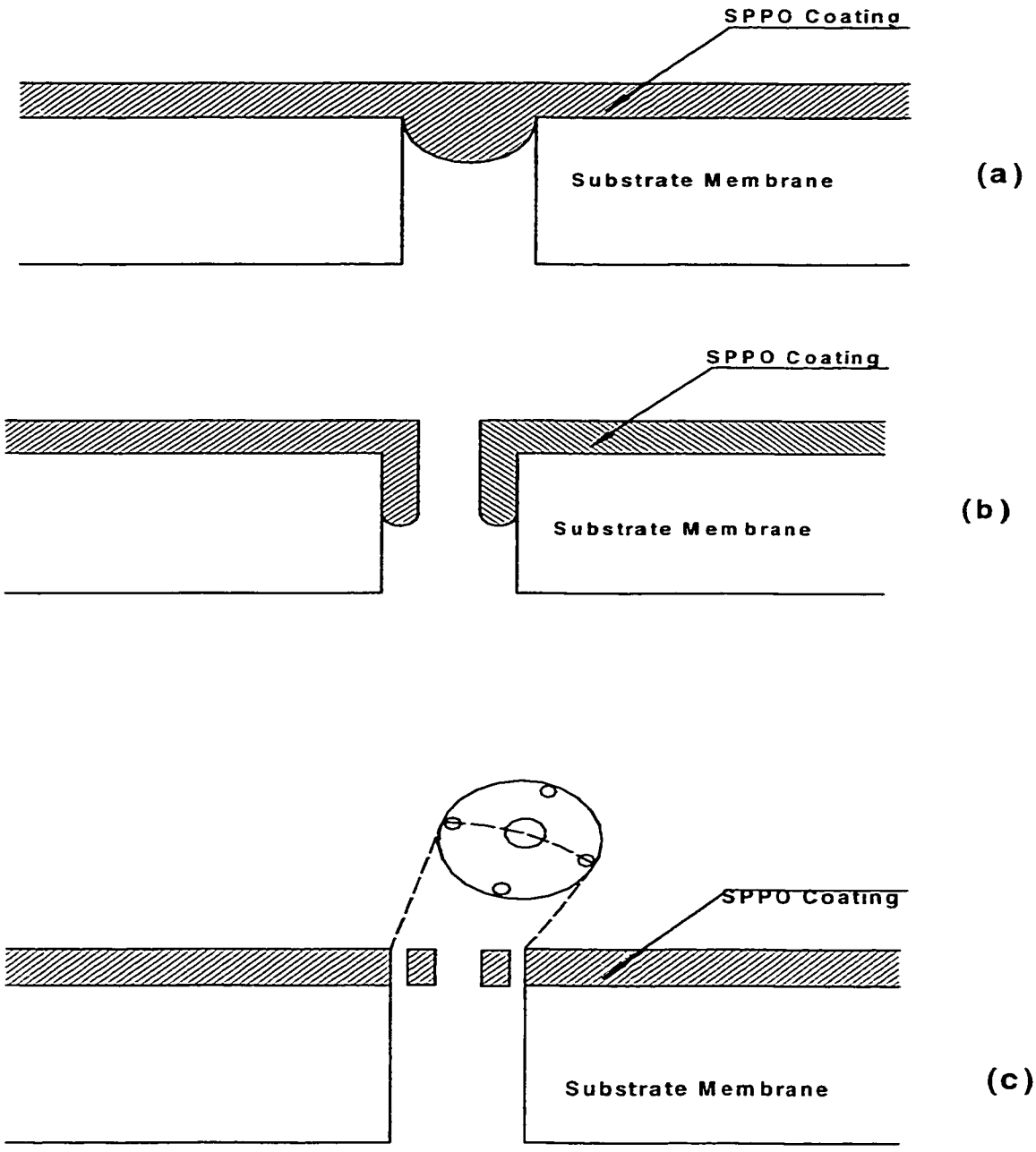

Figure 18. Coating of substrate membranes. (a) pore blockage; (b) pore size reduction due to coating of the pore walls; and (c) development of polymer network over the preexisting pores.

TFC membranes produced from substrate membranes which had much lower MWCOs. This suggests that there seems to be an upper limit which the MWCO of the TFC membranes can achieve. The available data does not permit one to visualize the effect of the MWCO of the substrate membranes on the MWCO of the TFC membranes for substrate molecular weight cutoffs below 48 000 Da.

The effect of the mean pore radius of the substrate membranes on those of the thin film composite membranes was also studied in order to obtain more insight into the role of the substrate membrane. Figure 19 displays these results. No obvious trend was noticed; however it was observed that thin film composite membranes with a mean pore radius smaller than 5.15×10^{-10}m could not be produced by coating substrate membranes of any mean pore radii.

A parameter, N/δ, representing the pore density divided by the total thickness of both the thin coated film of the TFC membrane and the skin of the porous substrate membrane, was calculated using equation 10 for both the substrate and the thin film composite membranes. The calculated results are given in Table 5. A general trend that can be observed is that the membranes produced using DMAc as the solvent in the casting solution produced substrate membranes with lower N/δ values. This is due to the weaker solvation power of DMAc in comparison to NMP for polyetherimide as was discussed in the section concerning the effect of the solvent on the substrate membrane. The relationship between the N/δ parameters for the substrate and for those of the thin film composite membranes is illustrated in Figure 20. The figure shows that there is a maximum in N/δ of the TFC membrane at an N/δ of 50 pores/μm^3 of the substrate membrane. The substrate membranes whose N/δ values are either below 30 pores/μm^3 or

above 75 pores/μm^3 resulted in a very low N/δ of the TFC membranes. A large pore density with a small effective membrane thickness will lead to a membrane of high flux. Therefore, in order to produce high flux thin film composite membranes, substrate membranes with N/δ values must be chosen within the aforementioned range.

Table 5. Parameter N/δ for the substrate and corresponding thin film composite membranes.

Substrate Membrane Composition	N/δ of substrate membrane (# pores/μm^3)	N/δ of TFC membrane (# pores/μm^3)
PEI/NMP/GBL:22/58/20	27	20
PEI/NMP/GBL:20/70/10	48	11 009
PEI/NMP/GBL:20/65/15	31	2
PEI/NMP/GBL:20/60/20	101	18
PEI/NMP/GBL:20/55/25	77	4
PEI/NMP/GBL:20/50/30	38	3 931
PEI/DMAc/GBL:20/50/30	2	847
PEI/DMAc/GBL:22/68/10	1	0.2
PEI/DMAc/GBL:22/58/20	1	607
PEI/DMAc/GBL:22/48/30	17	3

The relationship between the MWCO of the thin film composite membranes and the N/δ parameter for the corresponding substrate membranes is presented in Figure 21. The lowest MWCOs of the TFC membranes appeared in the same N/δ range of the substrate membranes where large N/δ values were obtained for the TFC membranes. Therefore, based on the data presented in Figures 20 and 21, it would appear that in order to produce TFC membranes of high flux and high separation, substrate membranes with N/δ values within the 30 to 75 pores/μm^3 are the best candidates. Investigation on the effect of the N/δ parameter of the substrate membrane on the performance of the TFC membranes will

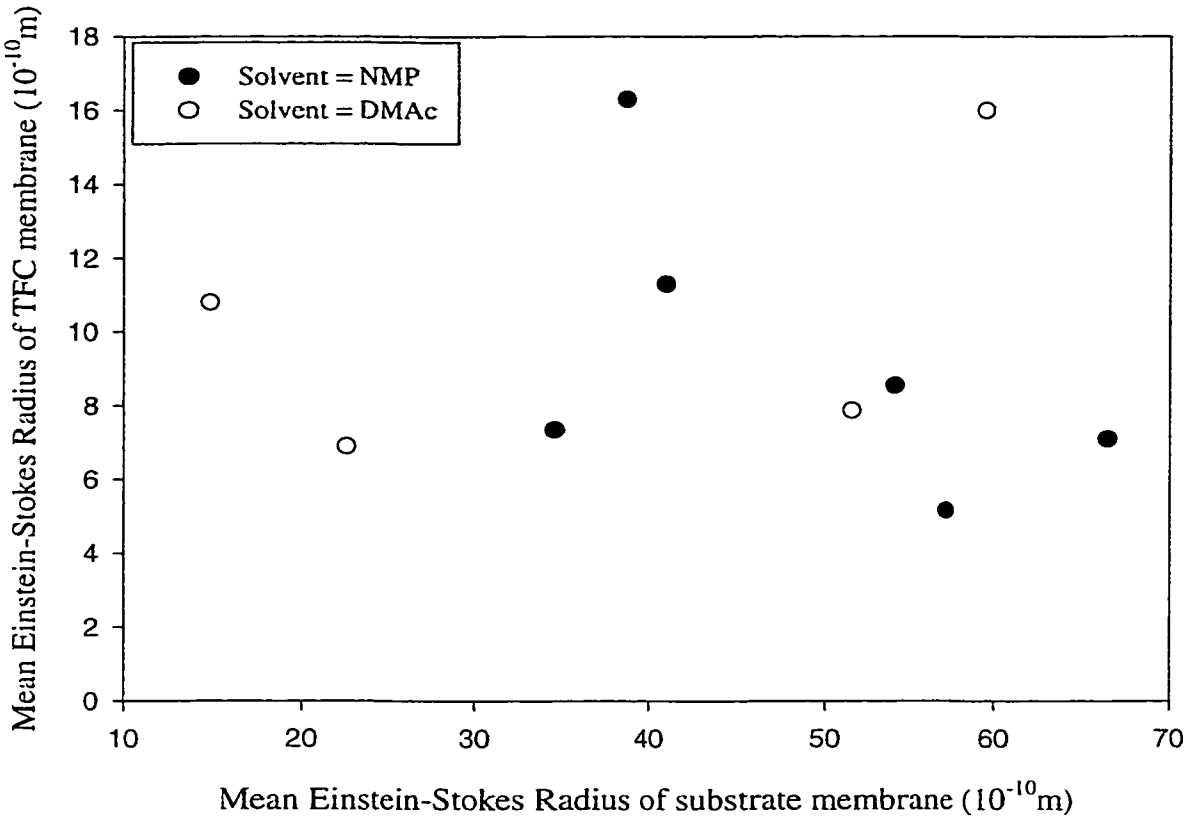

Figure 19. Mean Einstein-Stokes radius of TFC membranes versus the mean Einstein-Stokes radius of the corresponding substrate membranes.

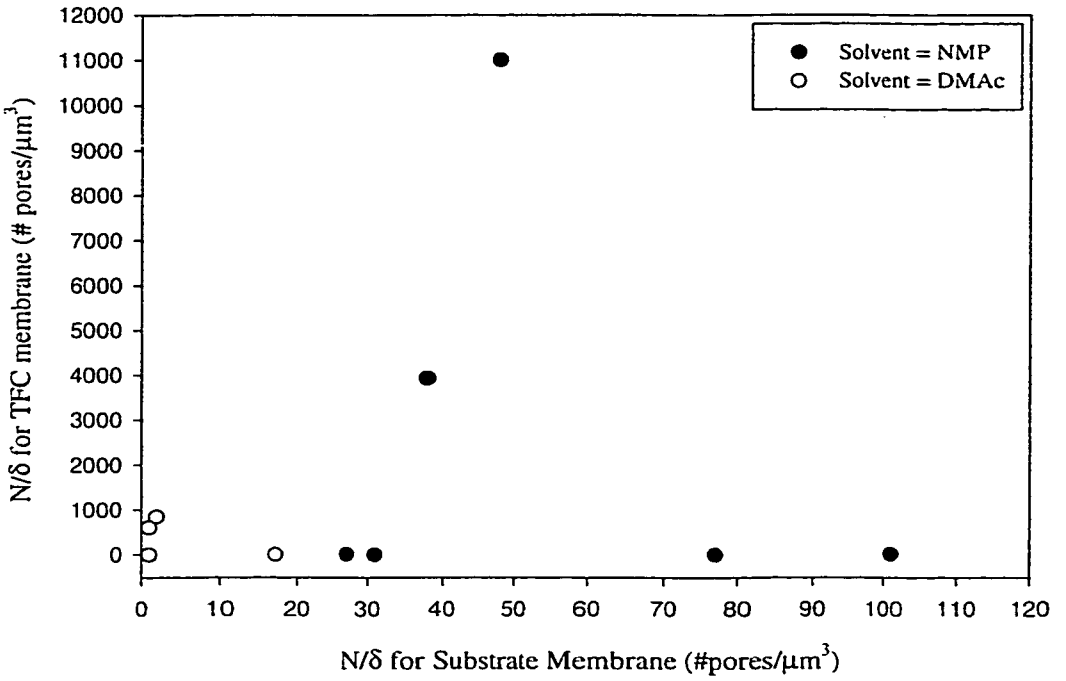

Figure 20. Parameter N/δ for the thin film composite membranes versus the parameter N/δ for the corresponding substrate membranes.

be discussed in the following section.

The dependency of the parameter N/δ for the TFC membranes on the MWCO of the TFC membranes was investigated. The results are illustrated in Figure 22. A very clear correlation was found, where the N/δ values of the TFC membranes are inversely proportional to the MWCO of the TFC membranes. For MWCO values below 7000 Da, the N/δ values of the TFC membranes are very large. However, for MWCO values greater than 7000 Da the N/δ for the TFC membranes remains consistently low. This indicates that increasing the MWCO above 7000 Da of the TFC membranes has no significant effect on the N/δ of the TFC membranes.

No clear correlation was found between the MWCO of the thin film composite membranes and the pure water flux of the substrate membranes. It can be seen in Figure 23, however, that although NMP-formed substrate membranes had higher pure water permeation fluxes, the MWCO of the resulting TFC membranes was not significantly different than those of the TFC membranes prepared from DMAc-formed substrate membranes.

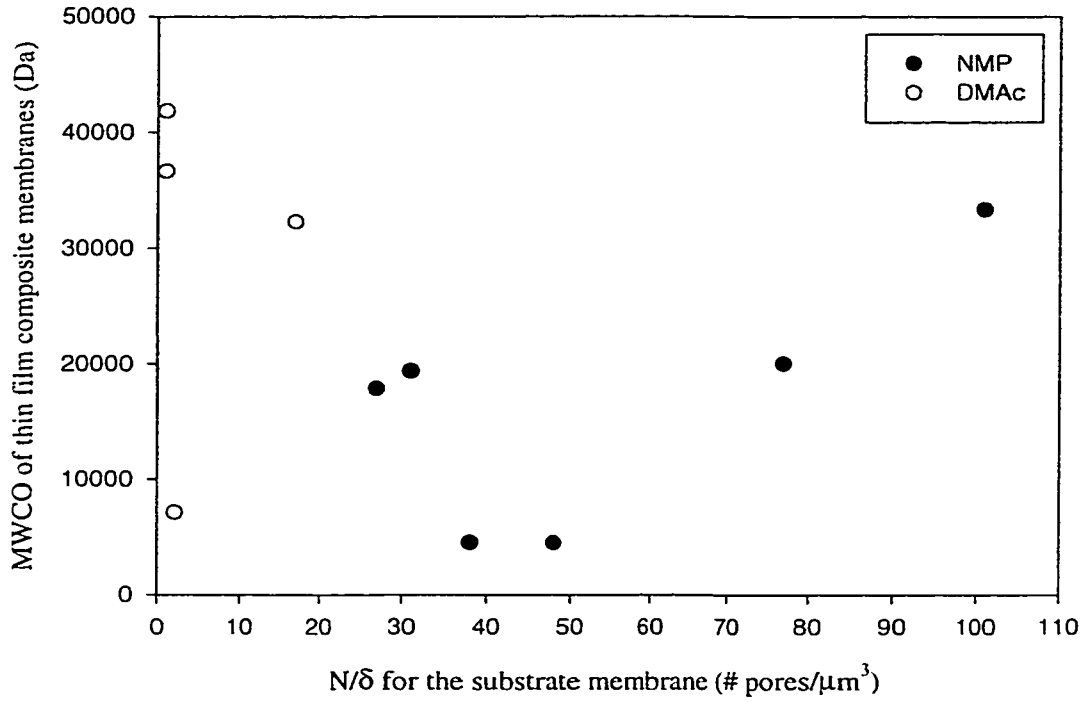

Figure 21. Molecular weight cutoff of the thin film composite membrane versus the number of pores per effective thickness of the membrane.

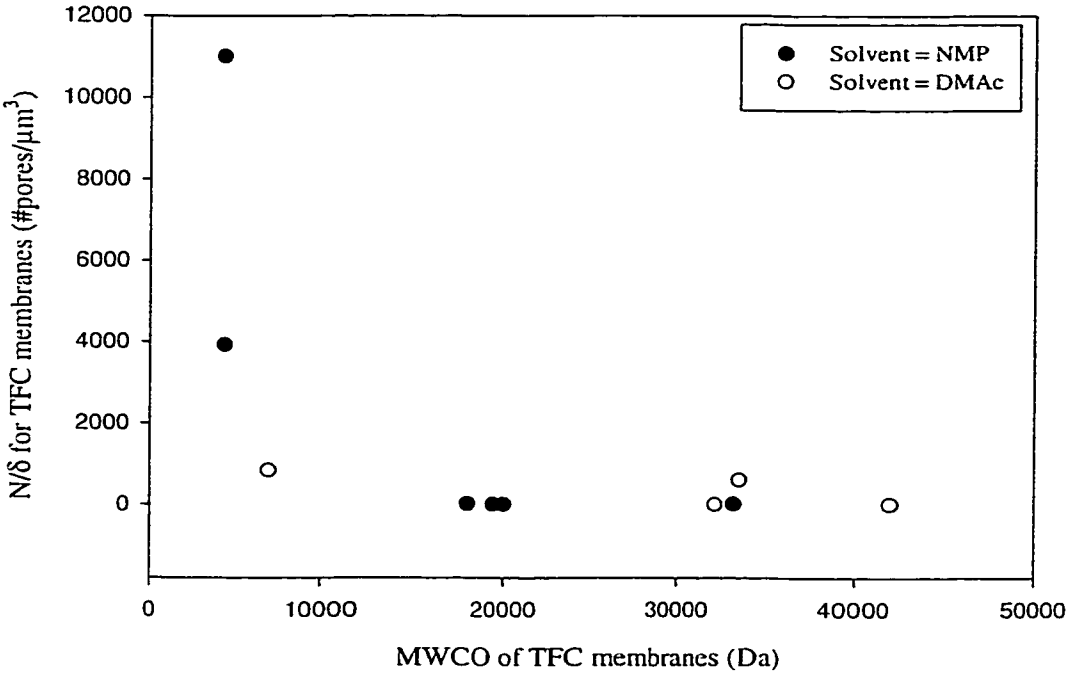

Figure 22. Parameter N/δ for the thin film composite membranes versus the molecular weight cutoff of the thin film composite membranes.

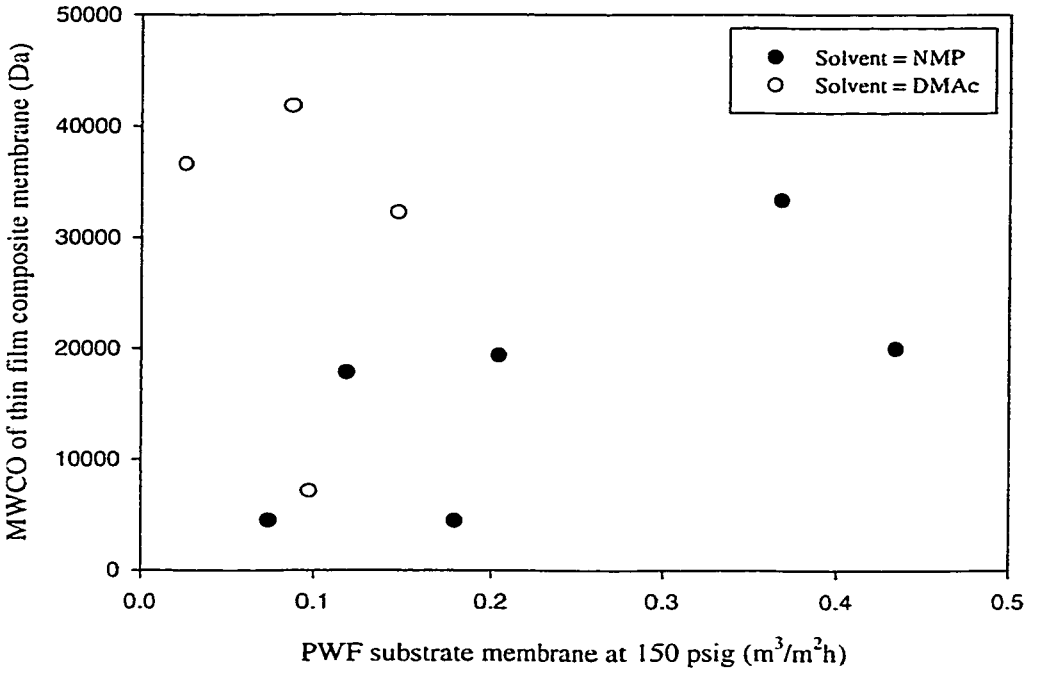

Figure 23. Molecular weight cutoff of thin film composite membranes versus the pure water permeation flux of the corresponding substrate membranes.

4.6. Effect of Mean pore size, Molecular Weight Cutoff and Pore Size Distribution of the Substrate Membrane on the Final Performance of Thin Film Composite Membranes.

The following two tables display the reverse osmosis performance data of the SPPO-PEI composite membranes composed of substrate membranes prepared using NMP as the solvent, Table 6, and substrate membranes prepared using DMAc as the solvent, Table 7, in the polymer casting solution. The tables also include the MWCO data of the substrate and TFC membranes. Both Table 6 and Table 7 show that separation data of NaCl solutions (500 ppm) and $MgSO_4$ solutions (1500 ppm) fall in narrow ranges of 47-63 % and 21-39 % respectively. On the other hand, the MWCO changed almost ten fold from 4 500 Da to 42 000 Da, and correspondingly the average pore size changed from 0.52 to 1.63 nm (see Table 8). It was concluded, therefore, that

Table 6. Performance data for thin-film composite membranes prepared from PEI/NMP/GBL substrate membranes.

PEI/NMP/GBL Substrate	Salt	PWF (m^3/m^2h)	PF (m^3/m^2h)	% Separation	MWCO TFC membrane (Da)	MWCO Substrate (Da)
22/58/20	$MgSO_4$ (500)	-	-	-	17 870	69 650
	$MgSO_4$ (1500)	.022 ± .007	.024 ± .005	22 ± 6		
	NaCl (500)	.024 ± .005	.020 ± .003	48 ± 6		
20/70/10	$MgSO_4$ (500)	-	-	-	4465	73 160
	$MgSO_4$ (1500)	.124 ± .010	.084 ± .005	21 ± 5		
	NaCl (500)	.122 ± .005	.122 ± .008	53 ± 5		
20/65/15	$MgSO_4$ (500)	.059 ± .037	.059 ± .037	41 ± 8	19 370	55 878
	$MgSO_4$ (1500)	.059 ± .039	.056 ± .039	29 ± 7		
	NaCl (500)	.058 ± .041	.063 ± .046	52 ± 10		
20/60/20	$MgSO_4$ (500)	.071 ± .025	.070 ± .024	42 ± 27	33 340	68 350
	$MgSO_4$ (1500)	.081 ± .027	.075 ± .022	30 ± 17		
	NaCl (500)	.081 ± .029	.085 ± .020	47 ± 23		
20/55/25	$MgSO_4$ (500)	.049 ± .012	.048 ± .012	44 ± 16	20 000	73 170
	$MgSO_4$ (1500)	.048 ± .012	.048 ± .012	34 ± 14		
	NaCl (500)	.049 ± .012	.054 ± .012	54 ± 18		
20/50/30	$MgSO_4$ (500)	-	-	-	4510	48 010
	$MgSO_4$ (1500)	.076 ± .019	.070 ± .019	22 ± 5		
	NaCl (500)	.076 ± .019	.080 ± .020	49 ± 12		

All thin-film composite membranes were prepared with one layer of 0.5 wt% SPPO-H in methanol solution unless otherwise stated.

Table 7. Performance data for TFC membranes prepared from PEI/DMAc/GBL substrate membranes.

PEI/DMAc/GBL Substrate	Salt	PWF (m³/m²h)	PF (m³/m²h)	% Separation	MWCO TFC membrane (Da)	MWCO Substrate (Da)
20/50/30	$MgSO_4$ (500)	-	-	-	7 135	76 250
	$MgSO_4$ (1500)	.015 ± .034	.109 ± .032	25 ± 7		
	NaCl (500)	.019 ± .037	.122 ± .036	59 ± 9		
22/68/10	$MgSO_4$ (500)	.034 ± .017	.032 ± .017	55 ± 18	41 860	166 500
	$MgSO_4$ (1500)	.036 ± .015	.037 ± .017	39 ± 14		
	NaCl (500)	.039 ± .019	.044 ± .020	63 ± 12		
22/58/20	$MgSO_4$ (500)	.034 ± .024	.032 ± .024	36 ± 8	36 650	48 010
	$MgSO_4$ (1500)	.034 ± .024	.032 ± .024	23 ± 5		
	NaCl (500)	.034 ± .025	.034 ± .025	62 ± 9		
22/48/30	$MgSO_4$ (500)	.015 ± .020	.015 ± .012	40 ± 19	32 270	61 400
	$MgSO_4$ (1500)	.015 ± .012	.015 ± .012	26 ± 12		
	NaCl (500)	.015 ± .014	.015 ± .014	50 ± 21		

All thin-film composite membranes were prepared with one layer of 1 wt% SPPO-H in methanol solution unless otherwise stated.

the MWCO of the substrate membrane is not the primary factor governing the solute separation performance of the thin film composite membranes. The MWCO data of the substrate membranes cover also a very wide range of 48 000 Da to 166 500 Da. Therefore, it can also be concluded that the MWCO of the substrate membranes does not have much effect on the electrolyte separation. It should be noted that the separation of sodium chloride was higher than that of magnesium sulfate for all thin film composite membranes. This phenomenon can be explained by Donnan exclusion and will be discussed in more detail in a latter section.

Comparing the performance results for all TFC membranes, the flux varied significantly although the separation of electrolyte solutes remained unaffected. Figure 24 shows that there is hardly any correlation between the pure water permeation flux of the TFC membranes and the mean Einstein-Stokes radius of the substrate membranes. As well, there is hardly any correlation between the pure water permeation flux of the TFC

membranes and the geometric standard deviation of the pore size distribution of the substrate membranes (Figure 25). Therefore, the mean pore size and pore size distribution of the substrate membranes do not appear to control the performance of the thin film composite membranes in terms of flux.

Table 8. Mean Einstein-Stokes radii of thin film composite membranes.

TFC membrane	Mean Einstein-Stokes Radius (10^{10}m)
PEI/NMP/GBL:22/58/20 - 1 layer 0.5 wt% SPPO	11.3
PEI/NMP/GBL:20/70/10 - 1 layer 0.5 wt% SPPO	8.55
PEI/NMP/GBL:20/65/15 - 1 layer 0.5 wt% SPPO	5.15
PEI/NMP/GBL:20/60/20 - 1 layer 0.5 wt% SPPO	16.3
PEI/NMP/GBL:20/55/25 - 1 layer 0.5 wt% SPPO	7.1
PEI/NMP/GBL:20/50/30 - 1 layer 0.5 wt% SPPO	7.35
PEI/DMAc/GBL:20/50/30 - 1 layer 1 wt% SPPO	6.9
PEI/DMAc/GBL:22/68/10 - 1 layer 1 wt% SPPO	7.87
PEI/DMAc/GBL:22/58/20 - 1 layer 1 wt% SPPO	11.0
PEI/DMAc/GBL:22/48/30 - 1 layer 1 wt% SPPO	16.0

The effect of the N/δ parameter on the pure water flux of the thin film composite membranes was also examined. As shown in Figure 26, a broad correlation can be visualized, where an increase in N/δ of the substrate membrane is accompanied by a corresponding increase in the pure water flux of the thin film composite membranes with a maximum occurring at a N/δ value of approximately 50 pores/μm^3. This relationship is to be expected, as an increase in the pore density per thickness of the selective layer will lead to an increased flux.

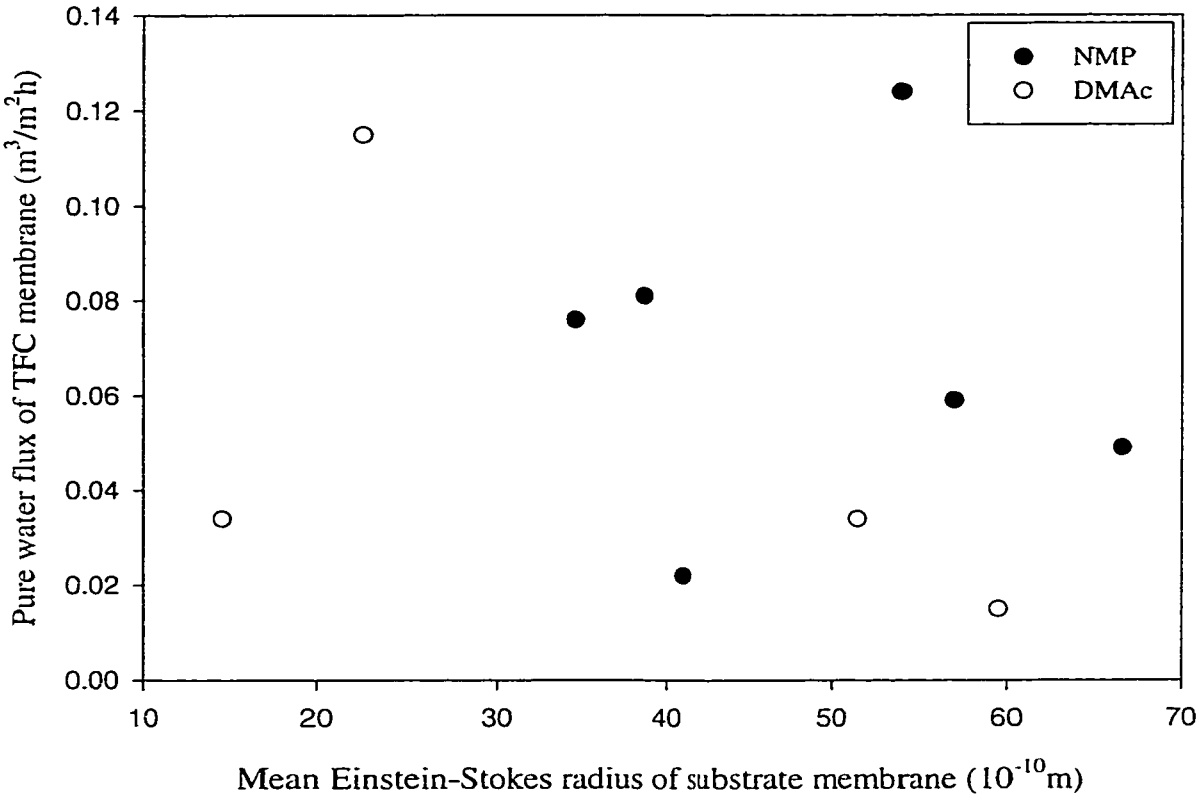

Figure 24. Pure water flux of thin film composite membranes versus of the mean Einstein-Stokes radii of the substrate membranes.

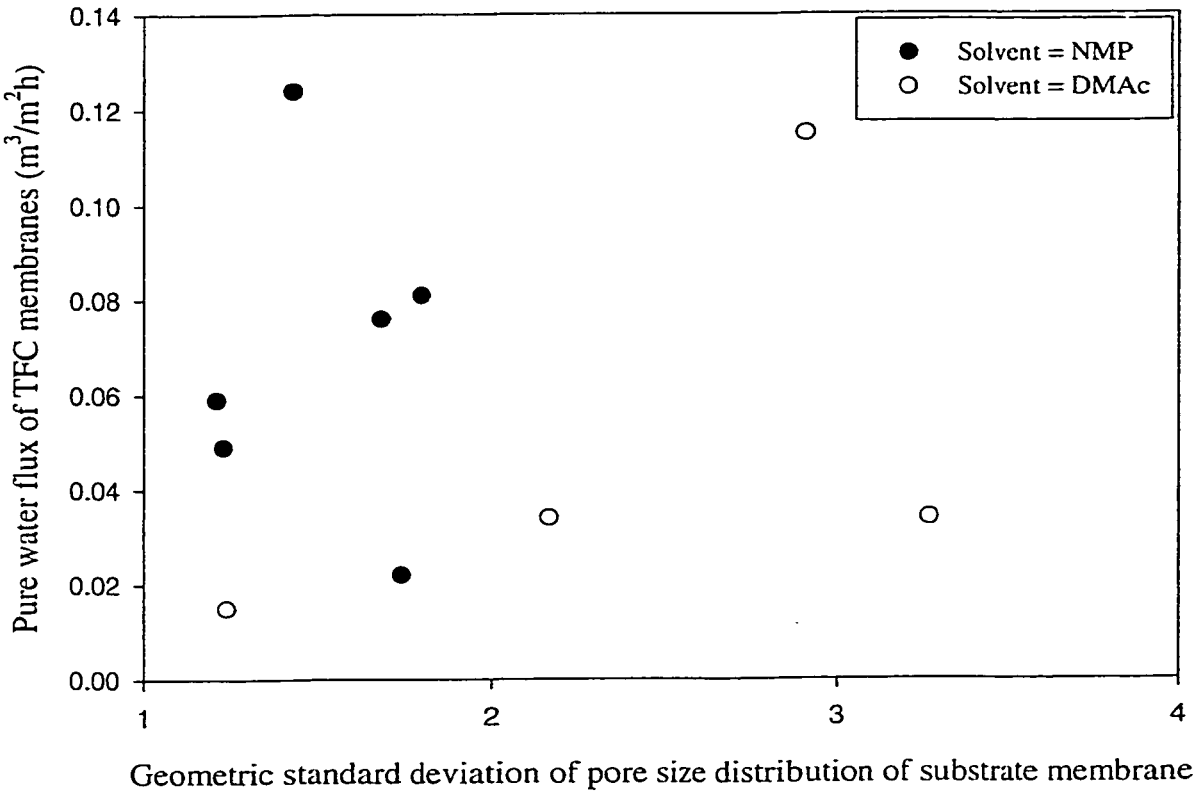

Figure 25. Pure water flux of the thin film composite membranes versus the geometric standard deviation of the pore size distribution of the substrate membranes.

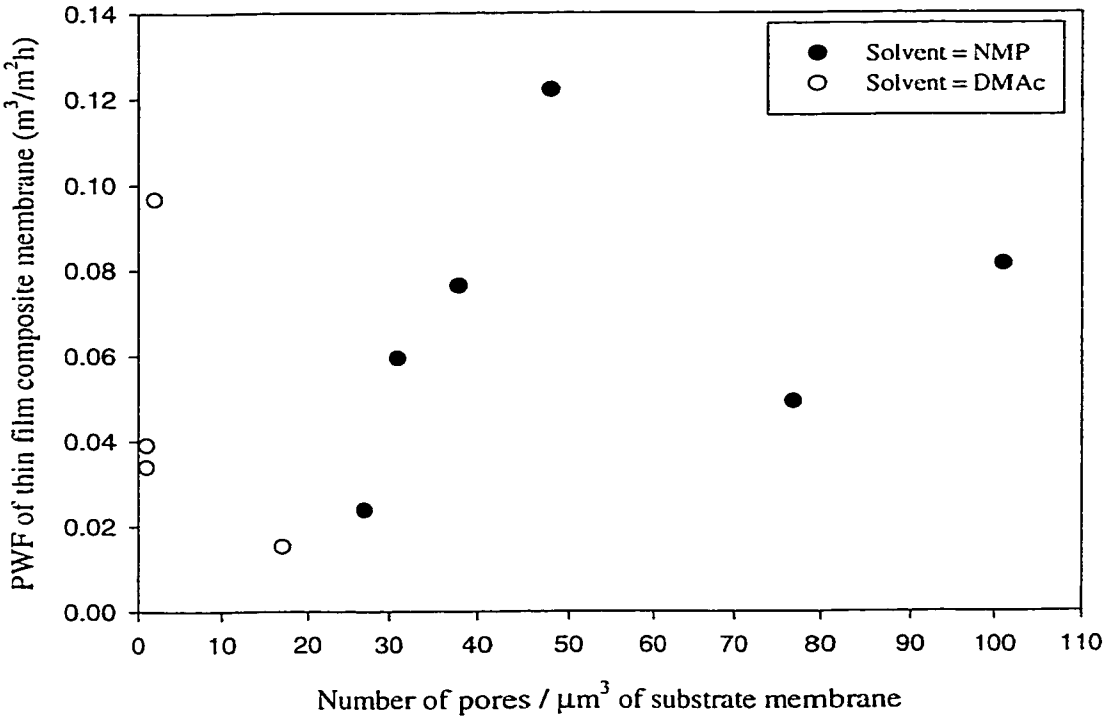

Figure 26. Pure water flux of the thin film composite membranes versus the parameter N/δ for the corresponding substrate membranes.

In Table 5 (section 4.5) large differences in the value of the N/δ parameter were observed for different membranes, yet it is shown here that these differences have little effect on the solute separation performance and only a mild effect on the pure water flux of the TFC membranes. Thus, although the N/δ parameter provides some useful information for characterizing membranes, the parameter does not realistically reflect the morphology of the membranes as it is an indirect parameter.

4.7. Comparison of the Macromolecular Radius of SPPO in Coating Solutions with Membrane Pore Radius

For a given polymer chain length, the configuration of the chain and hence its size in various solvent systems can vary with the relative strength of competing polymer-polymer and polymer-solvent interactions. If the macromolecular radius is smaller than the average pore radius of the substrate membranes, then membrane pores may be plugged with macromolecules during the preparation of thin film composite membranes. If this occurs, the resistance to the transport of fluid across the membrane will increase and hence the flux will decrease. Pore plugging by the coating solution should therefore be avoided by using a solvent in which the dimensions of the polymer molecules are at their largest.

In order to verify whether pore plugging of the substrate membrane by the coating solution was occurring during the preparation of thin film composite membranes, the macromolecular radius of SPPO polymer in dilute methanol solution was determined by intrinsic viscosity measurements and applying equation 14. The intrinsic viscosity was

determined using both the traditional Huggins' method (1942) and an alternative method proposed by Kozicki and Kuang (1996) as was outlined in Chapter 3. A comparison of the intrinsic viscosity of SPPO using both methods is shown in Table 9. There is a slight difference in the intrinsic viscosities. As Kozicki and Kuang's method does not involve extrapolation and does not suffer from a magnification error at low concentrations it was decided that the intrinsic viscosity of SPPO obtained using this method would be employed in the calculation of the macromolecular radius in dilute solution.

Table 9. Intrinsic viscosity of SPPO in methanol determined using two methods.

Huggins' Method	Kozicki and Kuang's Method
12.065 dL/g	15.363 dL/g

As can be seen Table 10, the molecular radius of SPPO in methanol is more than five times larger than the average pore radius of the substrate membrane bearing the largest mean pore size. Even though the radius of macromolecules will become smaller in the coating solution than in a solution of infinite dilution, the radius of the latter is still a good approximation since the concentration of the casting solution is not more than 1 wt%. It can therefore be concluded that pore penetration of the coating solution did not occur in the preparation of thin film composite membranes.

Table 10. Comparison of macromolecular radius of SPPO in dilute methanol solution with the average pore radius of PEI/NMP/GBL:20/55/25 substrate membrane.

SPPO radius in dilute solution (nm)	Average pore radius of PEI/NMP/GBL:20/55/25 (nm)
33.7	6.7

4.8. Effect of the Electrolyte Solutes in the Feed Solutions on the Performance of the Thin Film Composite Membranes

An appreciation of a membrane's surface chemistry and steric exclusion character is necessary to truly understand and predict membrane performance. The interpreter of membrane characterization data must consider both factors in the assessment of separation potential. Nanofiltration is widely used to describe the pressure-driven separation of electrolytes. The exact mechanism of selective separation by these membranes is thus still a matter of debate. Several hypotheses have been made, including a combination of steric and hydrodynamic forces or a combination of steric exclusion and surface force interactions. These hypotheses reflect the heterogeneity of the membrane's structure and composition. Mass transport occurs by convection in ultrafiltration membranes and by diffusion in reverse osmosis membranes. As the nanofiltration process lies between reverse osmosis and ultrafiltration for both pressure and porosity, the transfer can be convective or diffusive.

In this study, experiments were conducted with single salt solutions; i.e. sodium chloride and magnesium sulfate, for all thin film composite membranes. Two different

concentrations, 500 ppm and 1500 ppm, were tested for the magnesium sulfate solutions. The results obtained are given in Tables 6 and 7. If one compares the rejection of magnesium sulfate and sodium chloride for the same concentration of the feed solution (500 ppm), it can be noticed that the rejection of sodium chloride was always greater than that of magnesium sulfate. Since the membranes are negatively charged, it is the anion repulsion which mainly determines the solute retention of salt solutions. In general, the degree of retention increases with increasing valency of the anion due to the increased repulsion by the membrane. The cations are rejected to the same extent as the anions. This is because anions and cations cannot permeate independently, but permeate the membrane while maintaining electroneutrality. This phenomenon was not exhibited here, rather the retention decreased with increasing valency of the anion. These results suggest that the polyvalent cations effectively mask the charge character of the thin film composite membranes.

The degree of hydration can also influence the retention (Rios et al., 1996). In water solutions, ions are surrounded by fixed water molecules which increase the effective size of the ions. The effective diameter of the unhydrated ions as well as the effective radius of the hydrated ions is presented in the following table. The retention of

Table 11. Ionic size and hydrated radii of inorganic ions obtained from Kielland (1937).

Ion	Effective diameter of unhydrated ion (10^{10}m)	Effective radius of hydrated ion (10^{10}m)
Na^{+}	1.0	4.7
Mg^{2+}	0.9	7.0
Cl-	1.9	3.9
SO_4^{2-}	-	5.5

magnesium sulfate is lower than sodium chloride because the sulfate ion is more hydrated in aqueous solution than the chloride ion. This reduces its effective charge, which in turn reduces the retention.

Another interesting observation that can be made which is characteristic of charged membranes, is that although the electrolytes were of small dimensions, all were significantly rejected. The average of the MWCOs of all thin film composite membranes produced was 21 747 Da, which corresponds to 41.32×10^{-10}m, close to six times larger than the effective hydrated radius of Mg^{2+}. Therefore, if smaller MWCOs had been obtained for the thin film composite membranes, the retention of the ions would have been greater, as separation would occur due to both electrostatic interactions and steric exclusion.

Upon comparison of the flux obtained for the aqueous sodium chloride and magnesium sulfate feed solutions for the same feed concentration, it was observed that the flux of sodium chloride was always greater than that of magnesium sulfate. The flux of single salt solutions is generally higher for the monovalent salts than the divalent, partly due to a lower osmotic pressure difference, as the sizes of the monovalent salts are smaller than those of the divalent salts.

The influence of the electrostatic interactions can be determined by studying the influence of ionic concentration on the rejection rate. The solute separations of magnesium sulfate were studied for two concentrations; i.e. 500 ppm and 1500 ppm, at 150 psig. As can be seen in Tables 6 and 7, the rejection is strongly dependent on the solute concentration, which is a characteristic phenomenon of charged membranes. It

was observed that the rejection diminished as the concentration in the feed solution increased. This is because the charges of the thin film composite membrane are screened to a greater degree by solution charges when the ionic concentration is increased. Ions are therefore not repelled by the membrane and can transfer across more easily.

CHAPTER FIVE

CONCLUSIONS

The conclusions drawn from the experimental results and discussions will now be summarized.

The casting solution composition:

- affects the MWCO, mean pore size, surface porosity, N/δ parameter and the PWF of the substrate membranes;
- affects the structure of the substrate membranes.

In terms of the relationship between the substrate membrane and the TFC membrane:

- MWCO of the substrate membrane:
  - does not affect the MWCO of the TFC membrane;
  - does not affect the solute separation performance of the TFC membrane.
- Mean pore radius of the substrate membrane:
  - does not affect the mean pore radius of the TFC membrane;
  - does not affect the PWF of the TFC membrane.
- Geometric standard deviation of the pore size distribution of the substrate membrane:
  - does not affect the PWF of the TFC membrane.

- N/δ parameter of the substrate membrane:
  - affects the N/δ parameter of the TFC membrane;
  - affects the MWCO of the TFC membrane;
  - has a very mild effect on the PWF of the TFC membrane.
- Morphology of the substrate membrane:
  - affects the PWF of the TFC membrane.

In this work, TFC membranes were successfully prepared for water treatment using PEI as the polymer for the substrate membranes. Previous work by researchers focused on using PEI membranes only for gas-gas separations, organic vapor-gas separations and pervaporation separations. As well, this study was a step forward to gaining a better understanding of the role of the substrate membrane on the overall performance of TFC membranes. This was achieved through a detailed analysis of characterization and performance measurements of substrate and TFC membranes. It was found that the N/δ parameter provides some useful information for characterizing membranes. However, this parameter does not realistically reflect the morphology of the membranes. Further studies should be performed on defining a parameter, or combination of parameters, which will reflect the actual morphology of the membranes and hence reflect performance of the membranes. Based on the results and discussions presented in this work, one cannot conclude that the substrate membrane has a significant effect on the performance of TFC membranes. However, one cannot rule out this possibility either as this work raises even more questions and ideas for future investigations.

CHAPTER SIX

RECOMMENDATIONS

1. The substrate membranes produced in this study varied in MWCO from 48 000 to 167 000 Da. It was concluded in this study that the MWCO of the substrate membrane was not a factor contributing to the separation performance of the TFC membranes. However, this conclusion may be different if substrate membranes with very low MWCOs are used to prepare the TFC membranes. The effect of the substrate membranes on the overall performance of thin film composite membranes could be further investigated by preparing substrate membranes bearing MWCOs in the 1000 to 20 000 Da region. This could be achieved by varying the casting conditions of the substrate membranes.

2. The separation performance of the TFC membranes in this study was not high enough to generate commercial interest. This could be increased by crosslinking the thin polymeric coating of the TFC membranes. Experiments could be conducted to crosslink the SPPO coating.

REFERENCES

Bai, J., Fouda, A.E., Matsuura, T., and Hazlett, J.D., "A Study on the Preparation and Performance of Polydimethylsiloxane-Coated Polyetherimide Membranes in Pervaporation", J. Appl. Polym. Sci., 48, 999-1008 (1993).

Cadotte, J.E., U.S. Patent 3, 926, 798, December 16 (1975).

Cadotte, J., Forester, R., Kim, M., Petersen, R., and Stocker, T., "Nanofiltration Membranes Broaden the Use of Membrane Separation Technology", Desalination, 70, 77-88 (1988).

Chowdhury, G., Matsuura, T., and Sourirajan, S., "A Study of Reverse Osmosis Separation and Permeation Rate for Sulfonated Poly(2,6-dimethyl-1,4-phenylene oxide) Membranes in Different Cationic Forms", J. Appl. Polym. Sci., 51, 1071-1075 (1994).

Dean, J.A. ed., "Lange's Handbook of Chemistry", McGraw Hill Book Company, Thirteenth Edition (1985).

Deng, S., Sourirajan, S., and Matsuura, T., "Study of Volatile Hydrocarbon Emission Control by an Aromatic Poly(ether imide) Membrane", Ind. Eng. Chem. Res, 34, 4494-4500 (1995).

Deng, S., Liu, T., Sourirajan, S., and Matsuura, T., "Study of Volatile Hydrocarbon Emission Control by an Aromatic Polyetherimide Hollow Fibers Membranes", J. Polym. Eng., 14, no. 4, 219-235 (1995).

Eriksson, P., "Nanofiltration Extends the Range of Membrane Filtration", Env. Prog., 7, no. 1, 58-62 (1988).

Flory, P.J., Principles of Polymer Chemistry, Cornell University Press, Ithaca (1953).

Fouda, A., Bai, J., Zhang, S.Q., Kutowy, O., and Matsuura, T., "Membrane Separation of non Volatile Organic Compounds by Pervaporation and Vapor Permeation", Desalination, 90, 209-223 (1993).

Francis, P.S., "Fabrication and Evaluation of New Ultra Thin Reverse Osmosis Membranes", NTIS Report No. PB-177083, available from National Technical Information Service, U.S. Department of Commerce, Springfield, VA 22161 (February 1996).

Gazicki, M. and Yasuda, H., "An Atomic Aspect of Plasma Polymerization: The Role of Elemental Composition of the Monomer", J. Appl. Polym. Sci., Appl. Polym. Symp., 38, 35-44 (1984).

Hamza, A., Chowdhury, G., Matsuura, T., and Sourirajan, S., "Study of Reverse Osmosis Separation and Permeation Rate for Sulfonated Poly(2,6-dimethyl-1,4-phenylene oxide) Membranes of Different Ion Exchange Capacities", J. Appl. Polym. Sci., 58, 613-620 (1995).

Hamza, A., Chowdhury, G., Matsuura, T., and Sourirajan, S., "Sulphonated poly(2,6-dimethyl-1,4-phenylene oxide) - Polyethersulfone Composite Membranes. Effects of Composition of Solvent System, used for Preparing Casting Solution, on Membrane-Surface Structure and Reverse Osmosis Performance", J. Membrane Sci., 129, 55-64 (1997).

Ho, W. S., and Sirkar, K. K., Eds., "Membrane Handbook", Chapman and Hall, New York, NY (1992).

Htsieh, F. U., Matsuura, T., and Sourirajan, S., "Reverse Osmosis Separations of Polyethelene Glycols in Dilute Aqueous Solutions Using Porous Cellulose Acetate Membranes", J. Appl. Polym. Sci., 23, 561-573 (1979).

Huang, R. Y. M., and Feng, X., "Resistance Model Approach to Asymmetric Polyetherimide Membranes for Pervaporation of Isopropanol/Water Mixtures", J. Membrane Sci., 84, 15-27 (1993).

Huang, R. Y. M., and Feng, X., "Dehydration of Isopropanol by Pervaporation Using Aromatic Polytherimide Membranes", Sep. Sci. Tech., 28 , nos. 11 & 12, 2035-2048 (1993).

Huang, R. Y. M., and Feng, X., "Studies of Solvent Evaporation and Polymer Precipitation Pertiment to the Formation of Asymmetric Polyetherimide Membranes", J. Appl. Polym. Sci, 57, 613-621 (1995).

Huang, R.Y.M, and Kim, J.J., "Synthesis and Transport Properties of Thin Film Composite Membranes. I. Synthesis of Poly(phenylene oxide) Polymer and its Sulfonation", J. Appl. Polym. Sci., 29, 4017-4027 (1984).

Huang, R.Y.M. and Kim, J.J., "Synthesis and Transport Properties of Thin Film Composite Membranes. II. Preparation of Sulfonated Poly(phenylene oxide) Thin Film Composite Membranes for the Purification of Alberta Tar Sands Waste Waters", J. Appl. Polym. Sci., 29, 4029-4035 (1984).

Huggins, M.L., "The Viscosity of Dilute Solutions of Long-chain Molecules, IV. Dependence on Concentration", J. Amer. Chem. Soc. 64, 2716-2718 (1942).

Ikeda, K., Nakano, T., Ito, H., Kubota, T., and Yamamoto, S., "New Composite Charged Reverse Osmosis Membrane", Desalination, 68, 109-119 (1988).

Jitsuhara, I. and Kimura, S., "Structure and Properties of Charged Ultrafiltration Membranes Made of Sulfonated Polysulfone", J. Chem. Eng. Japan, 16, no. 5, 389-393 (1983).

Jitsuhara, I. and Kimura, S., "Rejection of Inorganic Salts by Charged Ultrafiltration Membranes Made of Sulfonate Polysulfone", J. Chem. Eng. Japan, 16, no. 5, 394-399 (1983).

Kesting, R.E., "The Nature of Pores in Integrally-Skinned Phase Inversion Membranes", in Advances in Reverse Osmosis and Ultrafiltration, T. Matsuura and S. Sourirajan, eds., National Research Council Canada, 3-14 (1989).

Kielland, J., "Individual Activity Coefficients of Ions in Aqueous Solutions", J. Amer. Chem. Soc., 59, 1675-1678 (1937).

Kneifel, K., and Peinemann, K.V., "Preparation of Hollow Fiber Membranes from Polyetherimide for Gas Separation", J. Membrane Sci., 65, 295-307(1992).

Kozicki, W. and Kuang, P.Q., " An Alternative Method for Evalutation of Intrinsic Viscosity" Can. J. Chem. Eng., 74, 429-432 (1996).

Kurihara, M., Karamaru, N., Harumiya, N., Yoshimura, K., and Hagiwara, S., "Spiral-Wound New Thin Film Composite Membrane for Single Stage Seawater Desalination by Reverse Osmosis", Desalination, 32, 13 (1980).

LaConti, A. B., "Advances in Development of Sulfonated PPO and Modified PPO Membrane Systems for some Unique Reverse Osmosis Applications", in S. Sourirajan ,ed., Reverse Osmosis and Synthetic Membranes, National Research Council of Canada, Ottawa, 211-229 (1977).

Linde, K., and Jönsson, A. S., "Nanofiltration of Salt Solutions and Landfill Leachate", Desalination, 103, 223-232 (1995).

Loeb, S., and Sourirajan, S., "Advanced Chemical Series", 38, 117 (1962).

Loeb, S., and Sourirajan, S., US Patent 3, 133, 132, May 12 (1964).

Londsdale, H.K., Riley, R.L., Lyons, C.R., and Carosella Jr, O.P., "Membrane Processes in Industry and Biomedicine", M. Bier, ed., Plenum Press, New York, p.101 (1971).

Meireles, M., Bessieres, A., Rogissart, I., Aimar, P., and Sanchez, V., "An Appropriate Molecular Size Parameter for Porous Membranes Calculation", J. Membrane Sci., 103, 105-115 (1995).

Michaels, A. S., "Analysis and Prediction of Sieving Curves for Ultrafiltration Membranes: A Universal Correlation?" Sep. Sci. Tech., 15, 1305-1322 (1980).

Morgan, P.W., "Condensation Polymers: By Interfacial and Solution Methods", Interscience Publishers, NY (1965).

Nakao, S., "Review: Determination of Pore Size and Pore Size Distribution. 3. Filtration membranes", J. Membrane Sci., 96, 131-165 (1994).

Nakao, S., Osada, H., Kurata, H., Tsuru, T., and Kimura, S., "Separation of Proteins by Charged Ultrafiltration Membranes" Desalination, 70, 191-205 (1988).

Page, C.A., Fouda, A.E., Tyagi, R., and Matsuura, T., "Pervaporation Performance of Polyetherimide Membranes Spin and Dip-Coated with Polydimethylsiloxane", J.Appl. Polym. Sci., 54, 975-989 (1994).

Park , Y.I., and Lee, K. H., " The Permeation of CO2 and N2 Gases Through Asymmetric Polyetherimide Membrane", Energy Convers. Mgmt., 36, no. 6-9, 423-426 (1995).

Petersen, R. J., "Composite Reverse Osmosis and Nanofiltration Membranes", J. Membrane Sci., 83, 1-150 (1993).

Petersen, R. J., and Cadotte, J.E., " Thin Film Composite Reverse Osmosis Membranes, in: M.C.. Porter (Ed.), Handbook of Industrial Membrane Technology, Noyes Publications, Park Ridge, NJ, p.307 (1990).

Plummer, C.W., Kimura, G., and LaConti, A.B., "Development of Sulfonated Polyphenylene Oxide Membrane for Reverse Osmosis", Research and Development Progress Report #551, Office of Saline Water, United States Department of Interior (1970).

Rautenbach, R., and Gröschl, A., "Separation Potential of Nanofiltration Membranes", Desalination, 77, 73-84 (1990).

Riley, R.L., Londsdale, H.K., and Lyons, C.R., "Composite Membranes for Seawater Desalination by Reverse Osmosis", J. Appl. Polym. Sci., 15, 1267 (1971).

Rios, G. M., Joulie, R., Sarrade, S. J., and Carles, M., "Investigation of Ion Separation by Microporous Nanofiltration Membranes", AIChE Journal, 42, no. 9, 2521-2528 (1996).

Rosa, M. J., and Depinho, M. R., "Separation of Organic Solutes by Membrane Pressure-driven Processes", J. Membrane Sci., 89, 235-243 (1994).

Rozelle, L.T., Cadotte, J.E., Cobian, K.E., and Kopp Jr., C.V., "Nonpolysaccharide Membranes for Reverse Osmosis: NS-100 Membranes, in S. Sourirajan, ed., Reverse Osmosis and Synthetic Membranes, National Research Council Canada, Ottawa, p. 249 (1977).

Rudie, B. J., Ross, G. S., Harrold, S. J., and Paulson, D. J., "Effects of Surface Force Interactions on an NF/UF Membrane", Desalination, 90, 107-118 (1993).

Serfaty, I.W., "Polyetherimide: A Versatile, Processable Thermoplastic", Polymides: Synthesis, Characterization and Applications, Mittal, K.L., ed., Plenum Press, New York (1984).

Singh, S., Khulbe, K. C., Matsuura, T., and Ramamurthy, P., "Membrane Characterization by Solute Transport and Atomic Force Microscopy", J. Membrane Sci., 142, 111-127(1998).

Smolders, C.A., Reuvers, A.J., Boom, R. M., and Wienk, I.M., "Microstructures in Phase Inversion Membranes. Part A Formation of Macrovoids" J. Membrane Sci., 73, 259-275 (1992).

Sourirajan, S. and Matsuura, T., "Reverse Osmosis / Ultrafiltration Process Principles", Division of Chemistry, National Research Council Canada, Ottawa (1985).

Strathmann, H., Production of Microporous Media by Phase Inversion Processes, in : D.R. Llyod(Ed.), Materials Science by Synthetic Membranes, ACS Symp. Ser No. 269, American Chemical Society, Washington, DC, 165-195 (1985).

Strathmann, H., "Electrodialysis – Theory" in Membrane Handbook, Eds. W.S. Ho and K.K. Sirkar, 1992.

Toi, K., Morel, G., and Paul, D.R., "Gas Sorption and Transport in Poly(phenylene oxide) and Comparisons with other Glassy Polymers", J. Appl. Polym. Sci., 27, 2997-3005 (1982).

Tsuru, T., Shutou, T., Nakao, S., and Kimura, S., "Peptide and Amino Acid Separation With Nanofiltration Membranes" Sep. Sci. Tech., 29, 971(1994).

Weast, R.C. ed., "CRC Handbook of Chemistry and Physics" The Chemical Rubber Company, OH (1972).

Wilke, C.R. and P. Chang, "Correlation of Diffusion Coefficients in Dilute Solutions", AIChE Journal, 1 (2), 264-270 (1955).

Wood, H., and Sourirajan, S., "The Effect of Additives, Solvent Type, and Polymer Concentration on Macromolecular Dimensions", J. Appl. Polym. Sci., 43, 213-217 (1991).

Yasuda, H., (Ed.), "Plasma Polymerization and Plasma Treatment", J. Appl. Polym. Sci., Appl. Polym. Symp., 38, John Wiley & Sons, New York, NY (1984).

Yasuda, H. and Lamaze, C.E., "Preparation of Reverse Osmosis Membranes by Plasma Polymerization of Organic Compounds", J. Appl. Polym. Sci., 17, 201-222 (1973).

Zhang,H., Lau, W.W.Y., and Sourirajan, S., "Factors Affecting the Production of Polyethersulfone Microfiltration Membranes by Immersion Phase Inversion Process" Sep. Sci. Tech., 30, 33-52 (1995).

APPENDIX A Experimental Reverse Osmosis Performance Raw Data for Substrate Membranes

Substrate Membrane: PEI/DMAc/GBL:22/48/30
Operating Pressure: 150 psig for PWF and 50 psig for PEGs

Feed Solution	Time (min)	Temp (°C)	Volume Permeating (ml)			% Separation by TOC Analysis		
			Memb. 1	Memb. 2	Memb. 3	Memb. 1	Memb. 2	Memb. 3
Pure Water	5	25.0	14.5	17.5	15.5	-	-	-
PEG 10000	15	25.0	23.5	20.5	19.5	0	0	0
PEG 20000	15	25.0	21.0	19.0	18.0	17.10	32.34	15.78
PEG 35000	17	24.6	20.5	19.5	18.0	39.88	62.10	38.55
PEG 100000	17	25.0	18.5	21.0	16.5	93.81	96.37	94.69

Substrate Membrane: PEI/NMP/GBL:20/60/20
Operating Pressure: 150 psig for PWF and 50 psig for PEGs

Feed Solution	Time (min)	Temp (°C)	Volume Permeating (ml)		% Separation by TOC Analysis	
			Memb. 1	Memb. 2	Memb. 1	Memb. 2
Pure Water	5	25.0	28.0	43.0	-	-
PEG 10000	15	25.0	18.0	37.0	49.37	23.65
PEG 20000	15	25.0	17.0	35.5	65.77	44.92
PEG 35000	17	24.6	18.0	36.0	66.38	48.78
PEG 100000	17	25.0	17.0	26.5	95.06	96.25

Substrate Membrane: PEI/NMP/GBL:20/65/15
Operating Pressure: 150 psig for PWF and 50 psig for PEGs

Feed Solution	Time (min)	Temp (°C)	Volume Permeating (ml)			% Separation by TOC Analysis		
			Memb. 1	Memb. 2	Memb. 3	Memb. 1	Memb. 2	Memb. 3
Pure Water	5	25.0	46.5	26.0	18.0	-	-	-
PEG 10000	15	25.0	41.5	12.1	8.6	0	0	0
PEG 20000	15	25.0	40.5	11.2	8.1	15.25	45.47	49.91
PEG 35000	17	24.6	41.0	11.9	8.6	15.06	76.36	72.33
PEG 100000	17	25.0	29.0	12.5	8.5	96.5	97.57	96.3

Substrate Membrane: PEI/NMP/GBL:20/55/25
Operating Pressure: 150 psig for PWF and 50 psig for PEGs

Feed Solution	Time (min)	Temp (°C)	Volume Permeating (ml)			% Separation by TOC Analysis		
			Memb. 1	Memb. 2	Memb. 3	Memb. 1	Memb. 2	Memb. 3
Pure Water	5	25.0	40.5	47.0	45.5	-	-	-
PEG 10000	15	25.0	31.5	53.0	46.5	0	0	0
PEG 20000	15	25.0	30.5	51.0	46.0	9.18	5.13	9.96
PEG 35000	17	24.6	32.5	54.0	49.5	9.81	0.38	6.73
PEG 100000	17	25.0	21.5	29.5	30.5	95.36	96.58	96.76

Substrate Membrane: PEI/NMP/GBL:22/58/20
Operating Pressure: 150 psig for PWF and 50 psig for PEGs

Feed Solution	Time (min)	Temp (°C)	Volume Permeating (ml)			% Separation by TOC Analysis		
			Memb. 1	Memb. 2	Memb. 3	Memb. 1	Memb. 2	Memb. 3
Pure Water	10	29.5	29.0	15.8	33.0	-	-	-
PEG 3400	10	26.6	10.0	5.0	12.8	40.14	38.16	45.62
PEG 10000	20	25.7	17.5	8.6	24.6	42.74	35.11	30.34
PEG 20000	30	28.3	26.0	12.8	36.5	47.09	47.96	31.85
PEG 35000	50	27.5	39.0	19.0	56.0	67.42	66.66	45.32
PEG 100000	60	27.0	47.0	21.5	61.0	96.44	94.41	96.72

Substrate Membrane: PEI/DMAc/GBL:20/50/30
Operating Pressure: 150 psig for PWF and 50 psig for PEGs

Feed Solution	Time (min)	Temp (°C)	Volume Permeating (ml)			% Separation by TOC Analysis		
			Memb. 1	Memb. 2	Memb. 3	Memb. 1	Memb. 2	Memb. 3
Pure Water	10	29.5	9.8	35.5	19.0	-	-	-
PEG 3400	10	26.6	3.6	13.0	8.1	36.86	59.15	50.75
PEG 10000	20	25.7	7.0	27.0	14.0	42.23	58.10	57.56
PEG 20000	30	28.3	9.3	38.0	19.0	49.80	65.60	68.44
PEG 35000	50	27.5	14	58.5	39.0	60.93	72.50	78.67
PEG 100000	60	27.0	16.0	62.0	37.0	94.45	96.80	97.37

Substrate Membrane: PEI/DMAc/GBL:22/68/10
Operating Pressure: 150 psig for PWF and 50 psig for PEGs

Feed Solution	Time (min)	Temp (°C)	Volume Permeating (ml)			% Separation by TOC Analysis		
			Memb. 1	Memb. 2	Memb. 3	Memb. 1	Memb. 2	Memb. 3
Pure Water	10	29.5	26.0	20.0	12.4	-	-	-
PEG 3400	10	26.6	8.2	6.4	4.1	10.53	11.12	4.00
PEG 10000	20	25.7	16.1	12.3	8.1	16.34	31.84	10.08
PEG 20000	30	28.3	25.2	18.8	12.5	24.23	46.29	18.16
PEG 35000	50	27.5	40.0	30.0	19.6	42.35	65.07	39.22
PEG 100000	60	27.0	42.0	32.5	20.0	88.52	88.13	79.04
PEO 200000	36	27.0	25.4	18	12.4	90.87	90.17	85.28

Substrate Membrane: PEI/DMAc/GBL:22/58/20
Operating Pressure: 150 psig for PWF and 50 psig for PEGs

Feed Solution	Time (min)	Temp (°C)	Volume Permeating (ml)			% Separation by TOC Analysis		
			Memb. 1	Memb. 2	Memb. 3	Memb. 1	Memb. 2	Memb. 3
Pure Water	10, 10, 30	29.5	9.5	7.4	3.2	-	-	-
PEG 3400	30	26.6	11.3	8.3	1.2	51.07	59.52	-
PEG 10000	60	25.7	23.2	15.3	2.0	62.01	74.38	-
PEG 20000	75	28.3	28.0	19.0	2.6	74.59	80.96	82.59
PEG 35000	120	27.5	41.0	27.0	3.4	81.19	88.23	83.14
PEG 100000	123	27.0	40.0	29.5	3.7	96.69	96.62	91.72

APPENDIX B Experimental Reverse Osmosis Performance Raw Data for Thin Film Composite Membranes

Thin Film Composite Membrane: PEI/NMP/GBL:20/50/30 - 1 layer 0.5 wt% SPPO
Operating Pressure: 150 psig

Feed Solution	Time (min)	Temp (°C)	Volume Permeating (ml)			
			Memb. 1	Memb. 2	Memb. 3	Memb. 4
Pure Water	10	24.4	18	14.5	12.5	15
1500 ppm $MgSO_4$	31	26.7	54.5	43.5	36.5	44
500 ppm NaCl	10	26.0	19.5	15.5	13.5	15.5
PEG 400	5	28.2	8.05	6.5	5.4	6.6
PEG 600	5	27.4	7.7	6	5.1	6.2
PEG 1000	5	26.2	6.8	5.4	4.45	5.6
PEG 2000	5	27.9	5.8	4.5	3.6	4.9
PEG 3400	5	27.8	5.4	4.15	3.2	4.5

Feed Solution	Permeate Conductivity				Feed Conductivity µS/cm
	Memb. 1	Memb. 2	Memb. 3	Memb. 4	
1500 ppm $MgSO_4$	1570	1533	1497	1522	1999
500 ppm NaCl	473	493	496	498	1050
	% Separation by TOC Analysis				
PEG 400	25.91	28.21	26.12	29.95	
PEG 600	38.99	41.28	34.94	45.66	
PEG 1000	52.41	47.29	38.42	56.18	
PEG 2000	80.35	74.26	57.88	81.85	
PEG 3400	91.40	86.79	77.48	90.90	

Thin Film Composite Membrane: PEI/NMP/GBL:20/70/10 - 1 layer 0.5 wt% SPPO
Operating Pressure: 150 psig

Feed Solution	Time (min)	Temp (°C)	Volume Permeating (ml)				
			Memb. 1	Memb. 2	Memb. 3	Memb. 4	Memb. 5
Pure Water	5	27.0	12.5	13.0	13.5	14.5	12.5
1500 ppm $MgSO_4$	20	27.0	34.0	36.0	36.0	39.0	34.5
500 ppm NaCl	20	26.5	48.5	51.0	52.0	56.0	49.0
PEG 600	5	26.4	11.0	11.5	11.5	12.5	11.0
PEG 1000	5	26.3	9.0	9.5	9.5	11.0	9.0
PEG 2000	5	25.4	6.0	6.7	6.8	7.5	6.1
PEG 3400	10	27.3	14.5	15.0	14.5	15.5	13.5
PEG 6000	10	25.8	14.0	14.0	14.0	15.0	13.5

Feed Solution	Permeate Conductivity					Feed Conductivity µS/cm
	Memb. 1	Memb. 2	Memb. 3	Memb. 4	Memb. 5	
1500 ppm $MgSO_4$	1464	1470	1600	1643	1595	1974
500 ppm NaCl	447	498	484	545	560	1072
	% Separation by TOC Analysis					
PEG 600	33.33	31.69	18.18	13.75	23.33	
PEG 1000	57.30	46.74	38.27	23.69	43.32	
PEG 2000	85.58	77.56	83.40	54.18	74.00	
PEG 3400	90.98	85.90	92.53	79.71	87.27	
PEG 6000	93.77	90.99	96.10	86.71	91.63	

Thin Film Composite Membrane: PEI/NMP/GBL:22/58/20 - 1 layer 0.5 wt% SPPO
Operating Pressure: 150 psig

Feed Solution	Time (min)	Temp (°C)	Volume Permeating (ml)				
			Memb. 1	Memb. 2	Memb. 3	Memb. 4	Memb. 5
Pure Water	10	25.2	4.25	4.2	3.9	4.2	6.3
1500 ppm $MgSO_4$	54	27.0	26.5	24.5	23.5	24.5	35.5
500 ppm NaCl	60	26.4	25.5	24.0	24.5	24.5	31.0
PEG 600	15	26.9	6.8	6.4	6.1	6.3	9.6
PEG 1000	15	26.7	6.2	5.8	5.4	5.6	8.6
PEG 2000	15	27.4	5.6	5.5	4.8	5.2	8.1
PEG 3400	15	27.0	5.3	5.0	4.4	4.8	7.1
PEG 6000	15	26.0	4.8	4.6	3.9	4.4	6.5
PEG 10000	20	27.4	6.0	5.9	4.9	5.6	7.9

Feed Solution	Permeate Conductivity					Feed Conductivity µS/cm
	Memb. 1	Memb. 2	Memb. 3	Memb. 4	Memb. 5	
1500 ppm $MgSO_4$	1551	1525	1352	1529	160 7	1941
500 ppm NaCl	582	596	483	611	600	1111
	% Separation by TOC Analysis					
PEG 600	26.98	25.66	38.67	27.70	21.19	
PEG 1000	29.81	32.12	39.83	31.65	26.45	
PEG 2000	42.43	40.87	43.11	36.87	35.34	
PEG 3400	78.01	75.23	77.17	77.08	68.01	
PEG 6000	77.88	76.86	74.62	72.69	67.79	
PEG 10000	85.66	83.91	82.00	78.41	75.04	

Thin Film Composite Membrane: PEI/NMP/GBL:20/65/15 - 1 layer 0.5 wt% SPPO
Operating Pressure: 150 psig

Feed Solution	Time (min)	Temp (°C)	Volume Permeating (ml)					
			Memb. 1	Memb. 2	Memb. 3	Memb. 4	Memb. 5	Memb. 6
Pure Water	10	27.4	28.5	9.2	18.0	9.1	4.5	10.2
500 ppm $MgSO_4$	8, 20, 8, 20, 30, 20	27.2	22.5	18.5	14.5	18.0	13.0	20.5
1500 ppm $MgSO_4$	30	27.8	84.0	27.0	54.0	25.0	7.0	29.5
500 ppm NaCl	30	28.3	99.5	30.5	61.0	28.0	7.8	34.5
PEG 2000	15, 15, 15, 15, 30, 15	26.9	41.5	10.4	23.0	10.4	4.2	13.0
PEG 3400	15, 15, 15, 15, 30, 15	26.9	39.0	9.8	21.3	9.6	4.1	12.6
PEG 10000	15, 15, 15, 15, 40, 15	25.8	36.0	9.7	20.0	9.3	4.6	12.1
PEG 20000	15, 15, 15, 15, 50, 15	28.5	42.5	12.3	24.0	12.3	6.7	16.1

Feed Solution	Permeate Conductivity						Feed Conductivity µS/cm
	Memb. 1	Memb. 2	Memb. 3	Memb. 4	Memb. 5	Memb. 6	
500 ppm $MgSO_4$	620	479	617	577	525	468	921
1500 ppm $MgSO_4$	1673	1420	1719	1638	1648	1366	2220
500 ppm NaCl	725	487	763	604	690	472	1288
	% Separation by TOC Analysis						
PEG 2000	54.13	72.44	50.85	68.31	49.65	87.27	
PEG 3400	58.08	88.33	59.77	85.62	99.48	92.33	
PEG 10000	69.19	96.43	69.34	91.75	91.92	96.03	
PEG 20000	74.99	98.06	75.55	95.34	94.94	97.56	

Thin Film Composite Membrane: PEI/NMP/GBL:20/55/25 - 1 layer 0.5 wt% SPPO
Operating Pressure: 150 psig

Feed Solution	Time (min)	Temp (°C)	Volume Permeating (ml)					
			Memb. 1	Memb. 2	Memb. 3	Memb. 4	Memb. 5	Memb. 6
Pure Water	15	25.1	20.8	13.0	21.3	14.8	9.6	14.4
500 ppm $MgSO_4$	20	25.0	26.5	16.0	26.5	18.5	12.5	18.0
1500 ppm $MgSO_4$	20	25.0	25.5	16.5	27.0	19.0	12.0	18.5
500 ppm NaCl	20	25.0	25.5	21.0	30.5	22.5	12.5	24.0
PEG 2000	15	26.0	16.8	13.4	19.8	14.6	7.8	15.2
PEG 3400	30	26.8	30.5	23.5	34.0	26.0	13.1	28.0
PEG 10000	30	26.0	30.0	22.5	31.5	24.5	11.8	26.5
PEG 20000	30	27.0	29.5	22.0	30.0	24.0	11.5	26.0

Feed Solution	Permeate Conductivity						Feed Conductivity µS/cm
	Memb. 1	Memb. 2	Memb. 3	Memb. 4	Memb. 5	Memb. 6	
500 ppm $MgSO_4$	714	350	570	414	517	390	881
1500 ppm $MgSO_4$	1849	1108	1605	1232	1493	1177	2140
500 ppm NaCl	890	356	667	450	543	367	1190
	% Separation by TOC Analysis						
PEG 2000	22.33	77.68	37.81	70.09	40.98	86.15	
PEG 3400	55.21	91.22	67.17	87.63	88.55	92.65	
PEG 10000	54.76	93.36	77.63	92.01	88.70	93.27	
PEG 20000	70.90	95.61	83.05	95.61	95.36	96.93	

Thin Film Composite Membrane: PEI/NMP/GBL:20/60/20 - 1 layer 0.5 wt% SPPO
Operating Pressure: 150 psig

Feed Solution	Time (min)	Temp (°C)	Volume Permeating (ml)		
			Memb. 1	Memb. 2	Memb. 3
Pure Water	10	27.5	18.4	16.6	13.9
500 ppm $MgSO_4$	20	27.1	35.0	32.0	27.0
1500 ppm $MgSO_4$	20	26.7	35.5	35.0	29.0
500 ppm NaCl	20	25.5	40.0	39.5	33.5
PEG 2000	10	25.7	16.4	17.3	13.0
PEG 3400	15	25.5	20.2	23.0	16.2
PEG 10000	10	26.6	12.2	12.2	9.7
PEG 20000	16	25.5	17.6	17.6	14.4
PEG 35000	20	26.6	21.6	22.4	17.6

Feed Solution	Permeate Conductivity			Feed Conductivity µS/cm
	Memb. 1	Memb. 2	Memb. 3	
500 ppm $MgSO_4$	595	412	563	909
1500 ppm $MgSO_4$	1683	1415	1679	2260
500 ppm NaCl	692	498	684	1173
	% Separation by TOC Analysis			
PEG 2000	34.66	24.23	45.56	
PEG 3400	54.74	35.88	60.72	
PEG 10000	74.59	66.65	74.55	
PEG 20000	84.69	84.18	79.36	
PEG 35000	91.11	93.30	88.29	

Thin Film Composite Membrane: PEI/DMAc/GBL: 22/68/10 - 1 layer 1wt% SPPO
Operating Pressure: 150 psig

Feed Solution	Time (min)	Temp (°C)	Volume Permeating (ml)					
			Memb. 1	Memb. 2	Memb. 3	Memb. 4	Memb. 5	Memb. 6
Pure Water	10	26.7	10.5	8.5	13.0	7.0	3.1	4.1
500 ppm $MgSO_4$	32 (1-3) & 62 (4-6)	27.0	30.5	26.0	41.0	38.5	12.5	20.5
1500 ppm $MgSO_4$	27 (1-3) &51 (4-6)	25.5	29.5	24.5	35.5	37.0	16.0	24.0
500 ppm NaCl	25 (1-3) & 45 (4-6)	25.3	34.0	25.5	38.0	36.0	16.5	25.0
PEG 600	25	24.8	32.5	26.5	39.0	19.5	8.05	12.5
PEG 1000	25	25.5	32.0	25.5	39.0	18.5	7.7	12.0
PEG 2000	30	26.0	35.0	29.0	44.5	21.0	8.0	14.5
PEG 3400	30	25.4	29.0	24.5	37.5	18.0	6.2	10.0
PEG 10000	30	26.2	26.0	22.0	34.5	17.0	5.6	8.8

Feed Solution	Permeate Conductivity						Feed Conductivity µS/cm
	Memb. 1	Memb. 2	Memb. 3	Memb. 4	Memb. 5	Memb. 6	
500 ppm $MgSO_4$	410	521	560	555	255	196	917
1500 ppm $MgSO_4$	1307	1506	1576	1497	1154	842	2140
500 ppm NaCl	453	483	546	549	334	215	1166
	% Separation by TOC Analysis						
PEG 600	43.27	40.98	33.72	41.52	39.68	60.67	
PEG 1000	47.13	50.57	39.24	50.22	41.19	63.75	
PEG 2000	-	56.78	42.16	56.85	42.67	64.55	
PEG 3400	70.07	79.39	68.89	80.69	81.17	88.23	
PEG 10000	73.66	73.46	59.29	74.32	80.69	85.69	

Thin Film Composite Membrane: PEI/DMAc/GBL:22/58/20 - 1 layer 1 wt% SPPO
Operating Pressure: 150 psig

Feed Solution	Time (min)	Temp (°C)	Volume Permeating (ml)					
			Memb. 1	Memb. 2	Memb. 3	Memb. 4	Memb. 5	Memb. 6
Pure Water	10	26.0	18.0	5.6	5.0	5.6	5.5	3.5
500 ppm $MgSO_4$	22 (1) & 65 (2-6)	25.3	38.5	35.0	30.0	35.0	35.0	21.5
1500 ppm $MgSO_4$	20 (1) & 64 (2-6)	25.7	34.0	35.5	30.0	34.5	33.5	21.5
500 ppm NaCl	17 (1) & 40 (2-6)	26.5	32.0	22.5	20.5	23.0	20.0	15.0
PEG 1000	30	27.0	38.0	11.5	10.5	11.5	9.5	7.0
PEG 2000	30	26.0	34.0	11.0	10.0	10.5	9.0	6.5
PEG 3400	20	26.1	20.5	7.0	5.9	6.2	5.7	3.7
PEG 10000	30	26.4	25.0	9.0	7.4	7.7	6.9	4.9
PEG 20000	40	25.9	30.5	12.0	9.5	10.0	8.5	6.0

Feed Solution	Permeate Conductivity						Feed Conductivity µS/cm
	Memb. 1	Memb. 2	Memb. 3	Memb. 4	Memb. 5	Memb. 6	
500 ppm $MgSO_4$	607	645	527	520	575	462	867
1500 ppm $MgSO_4$	1681	1741	1580	1593	1685	1463	2110
500 ppm NaCl	579	574	448	356	473	346	1205
	% Separation by TOC Analysis						
PEG 1000	30.79	45.32	44.55	46.26	52.91	59.14	
PEG 2000	40.32	42.27	48.28	51.83	57.37	65.10	
PEG 3400	43.13	64.56	52.90	55.26	60.91	70.46	
PEG 10000	60.76	70.48	67.22	74.43	66.29	76.43	
PEG 20000	78.12	89.28	81.93	88.04	85.96	89.38	

Thin Film Composite Membrane: PEI/DMAc/GBL:22/48/30 - 1 layer 1 wt% SPPO
Operating Pressure: 150 psig

Feed Solution	Time (min)	Temp (°C)	Volume Permeating (ml)					
			Memb. 1	Memb. 2	Memb. 3	Memb. 4	Memb. 5	Memb. 6
Pure Water	30	27.4	26.5	13.0	3.0	9.0	5.7	4.7
500 ppm $MgSO_4$	30, 60, 120, 60, 90, 120	28.0	26.5	26.0	11.0	19.0	18.5	18.5
1500 ppm $MgSO_4$	30, 60, 120, 60, 90, 120	26.8	25.0	26.0	11.0	15.0	175	18.5
500 ppm NaCl	30, 60, 120, 60, 90, 120	26.8	26.0	28.5	11.5	16.0	17.5	20.0
PEG 1000	30 (1,2) & 60 (3-6)	28.6	24.5	12.5	4.9	14.0	9.5	8.7
PEG 2000	30 (1,2) & 60 (3-6)	28.0	21.0	10.5	4.0	12.5	8.4	7.2
PEG 3400	45 (1,2) & 90 (3-6)	28.4	26.0	12.0	4.9	17.0	11.5	8.5
PEG 10000	45 (1,2) & 90 (3-6)	27.7	20.5	10.0	3.9	14.5	9.6	7.1
PEG 20000	45 (1,2) & 90 (3-6)	27.9	19.5	9.5	3.6	14.5	7.7	6.8

Feed Solution	Permeate Conductivity						Feed Conductivity µS/cm
	Memb. 1	Memb. 2	Memb. 3	Memb. 4	Memb. 5	Memb. 6	
500 ppm $MgSO_4$	580	465	421	755	758	384	936
1500 ppm $MgSO_4$	1717	1518	1485	1957	1966	1352	2250
500 ppm NaCl	597	439	459	916	940	365	1248
	% Separation by TOC Analysis						
PEG 1000	21.88	34.12	42.69	5.75	5.21	40.72	
PEG 2000	19.37	36.02	79.83	0.00	2.53	42.06	
PEG 3400	52.76	68.64	51.67	32.64	38.42	77.04	
PEG 10000	60.35	71.54	78.34	66.62	71.87	87.95	
PEG 20000	78.39	84.91	83.43	82.19	82.39	91.45	

Thin Film Composite Membrane: PEI/DMAc/GBL:20/50/30 - 1 layer 1 wt% SPPO
Operating Pressure: 150 psig

Feed Solution	Time (min)	Temp (°C)	Volume Permeating (ml)					
			Memb. 1	Memb. 2	Memb. 3	Memb. 4	Memb. 5	Memb. 6
Pure Water	10	26.5	30.5	12.5	29.5	28.0	18.5	28.5
1500 ppm $MgSO_4$	18	25.0	41.5	29.0	40.5	39.0	41.5	40.0
500 ppm NaCl	18	25.8	48.5	34.5	47.0	45.5	44.5	44.5
PEG 600	10	25.0	28.5	11.0	28.5	27.5	15.0	28.0
PEG 1000	10	26.0	27.0	10.0	26.5	26.5	14.5	27.0
PEG 2000	10	25.0	22.5	8.5	21.5	21.5	12.5	22.5
PEG 3400	10	26.3	20.0	8.0	20.5	21.5	12.5	22.0
PEG 10000	10	25.0	16.0	6.5	16.5	17.0	9.5	17.5

Feed Solution	Permeate Conductivity						Feed Conductivity µS/cm
	Memb. 1	Memb. 2	Memb. 3	Memb. 4	Memb. 5	Memb. 6	
1500 ppm $MgSO_4$	1514	1229	1512	1490	1567	1600	1987
500 ppm NaCl	402	287	509	489	539	545	1120
	% Separation by TOC Analysis						
PEG 600	33.78	53.03	35.17	36.98	44.11	31.19	
PEG 1000	51.48	69.37	48.64	53.40	63.18	46.43	
PEG 2000	74.78	88.30	67.21	73.58	85.23	62.51	
PEG 3400	83.04	93.42	75.47	77.43	90.75	71.65	
PEG 10000	93.34	94.71	88.79	91.81	96.03	82.83	

APPENDIX C Sample calculation of Permeation Rate (PR) and Solute Separation (f) of SPPO-PEI Composite Membranes

The following calculations were performed using the raw data for SPPO-PEI thin film composite membrane found in Appendices A and B.

The permeation flux is calculated as follows:

$$PF = (\frac{V}{At})(T_c)$$

where **V** is the volume of the permeating the membrane of the area ***A*** in time ***t*** and T_c is the temperature correcting factor (from temperature T °C to temperature 25 °C.) estimated based on pure water properties as:

$$T_c = (\frac{\mu_{T°C}}{\mu_{25°C}})(\frac{\rho_{25°C}}{\rho_{T°C}})$$

The water density and viscosity values were taken from "Lange's Handbook of Chemistry", J.A. Dean Ed., McGraw-Hill Book Company, Thirteen Edition (1985).

For an operating temperature of 27 °C, water properties are:

$\mu_{25°C} = 0.890 \times 10^{-3}$ Ns/m^2
$\mu_{27°C} = 0.851 \times 10^{-3}$ Ns/m^2
$\rho_{25°C} = 997.0$ Kg/m^3
$\rho_{27°C} = 996.5$ Kg/m^3

Thus, the temperature correction factor is

$$T_c = 0.957$$

The membrane area for each of the six cells used in the experimental setup are:

Membrane Areas for Cells Used in Experimental Setup

Cell	Membrane Area (cm^2)
Cell 1	13.20
Cell 2	12.57
Cell 3	13.20
Cell 4	13.20
Cell 5	10.75
Cell 6	11.34

Thus the permeation flux for PEI/NMP/GBL:20/70/10 - 1 layer 0.5 wt% SPPO membrane 1 is

$$PF = \left(\frac{12.5}{13.2(5)}\right)0.6 = 0.114\ m^3/m^2h$$

where 0.6 is a conversion factor to obtain the results in SI units.

In the range of salt concentrations studied, relationship between the solution concentration and its conductivity is linear enabling direct calculations of solute separation from conductivity measurements.

The solute separation is calculated as follows:

$$f = 1 - \frac{C_p}{C_f} \times 100$$

Thus the solute separation of feed solution of 1500 ppm $MgSO_4$ for PEI/NMP/GBL:20/70/10 - 1 layer 0.5 wt% SPPO Membrane 1 is:

$$f = 1 - \frac{1464}{1974} \times 100 = 25.84\%$$

The solute separation for PEG solutions was by the % total organic carbon (TOC) in the permeate and the TOC in the feed obtained by a Total Organic Carbon Analyzer (see Chapter 3).

APPENDIX D Log-normal Probability Plots of all Membranes

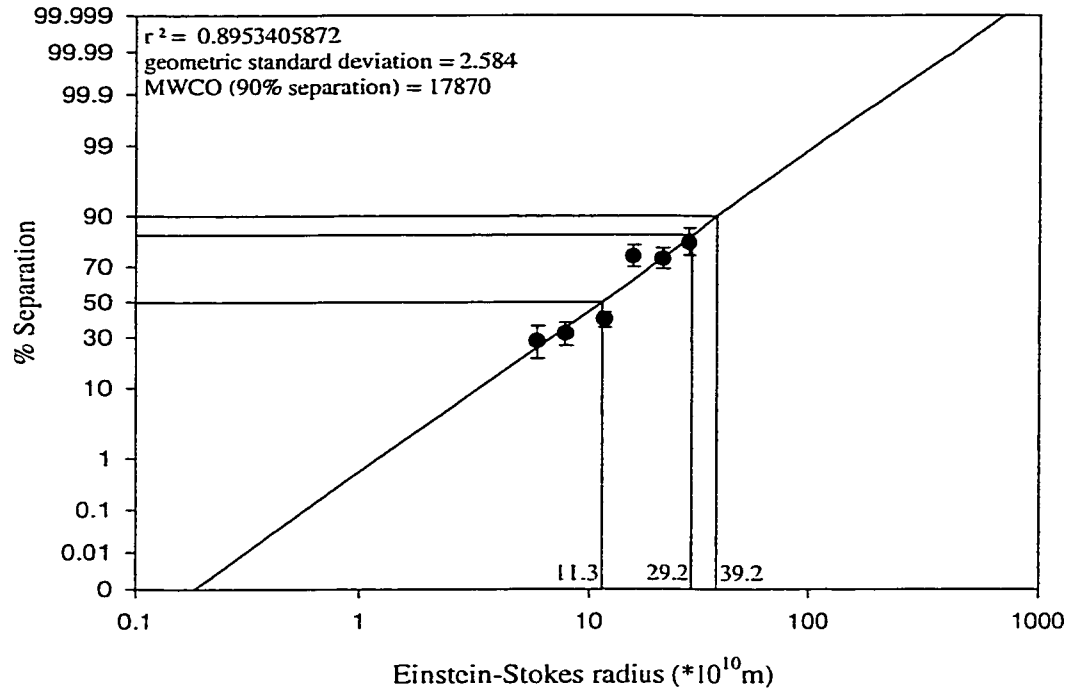

Log-normal probability plot of PEG separation versus Einstein-Stokes radius for PEI/NMP/GBL:22/58/20 - 1 layer 0.5 wt% SPPO-H.

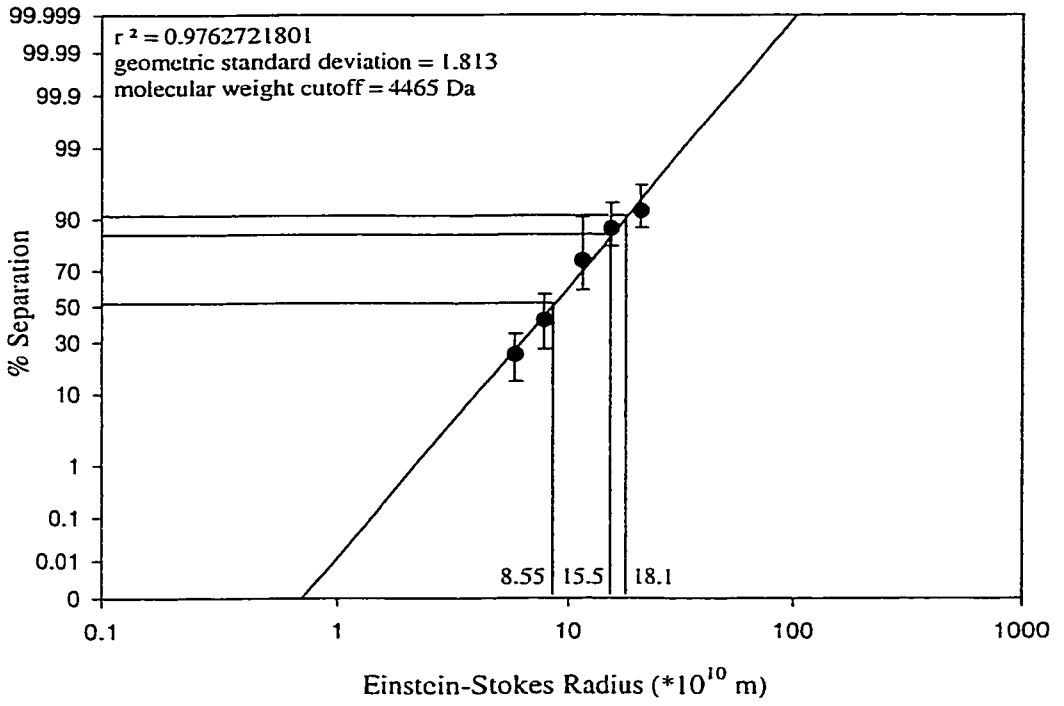

Log-normal probability plot of PEG separation versus Einstein-Stokes radius for PEI/NMP/GBL:20/70/10 - 1 layer 0.5 wt% SPPO-H.

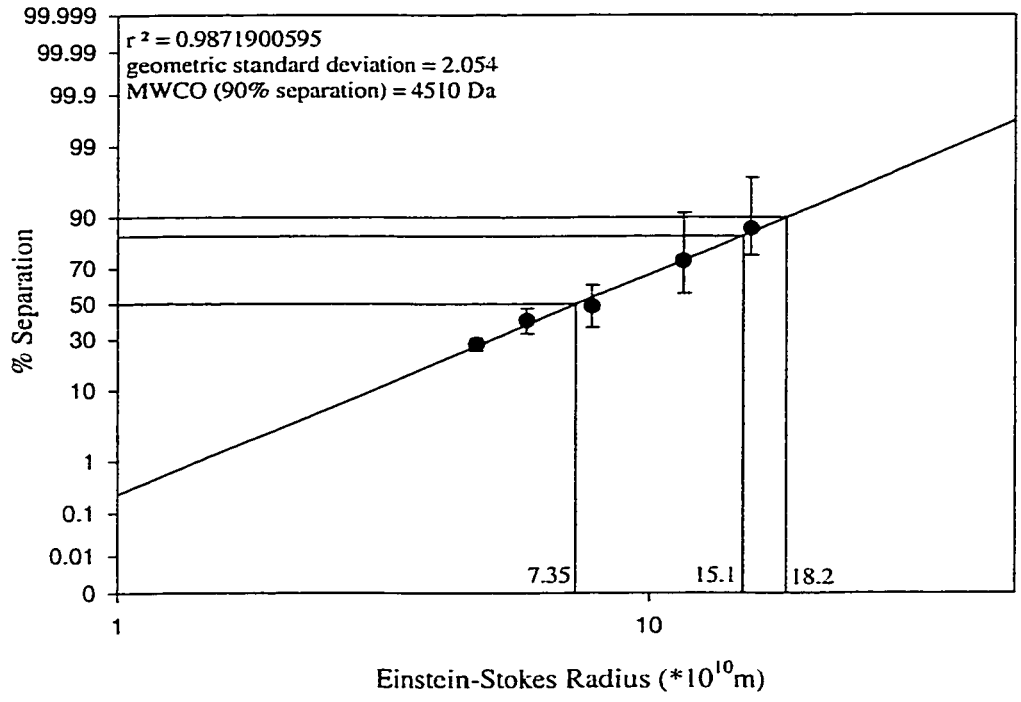

Log-normal probability plot of PEG separation versus Einstein-Stokes radius for PEI/NMP/GBL:20/50/30 - 1 layer 0.5 wt% SPPO-H

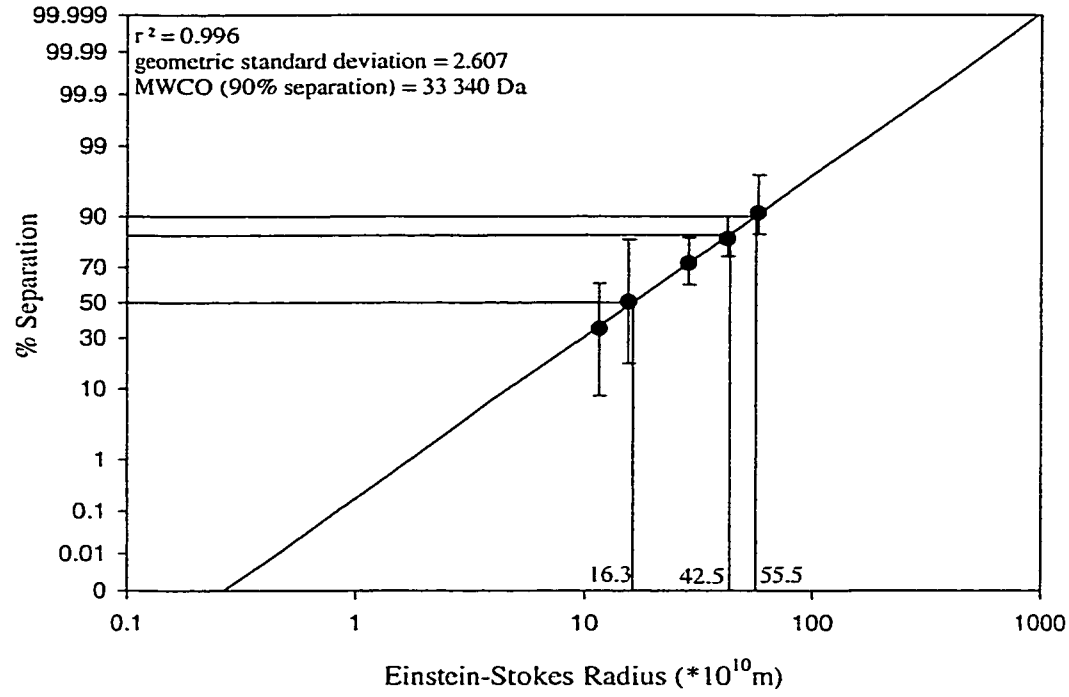

Log-normal probability plot of PEG separation versus Einstein-Stokes radius for PEI/NMP/GBL:20/60/20 - 1 layer 0.5 wt% SPPO-H.

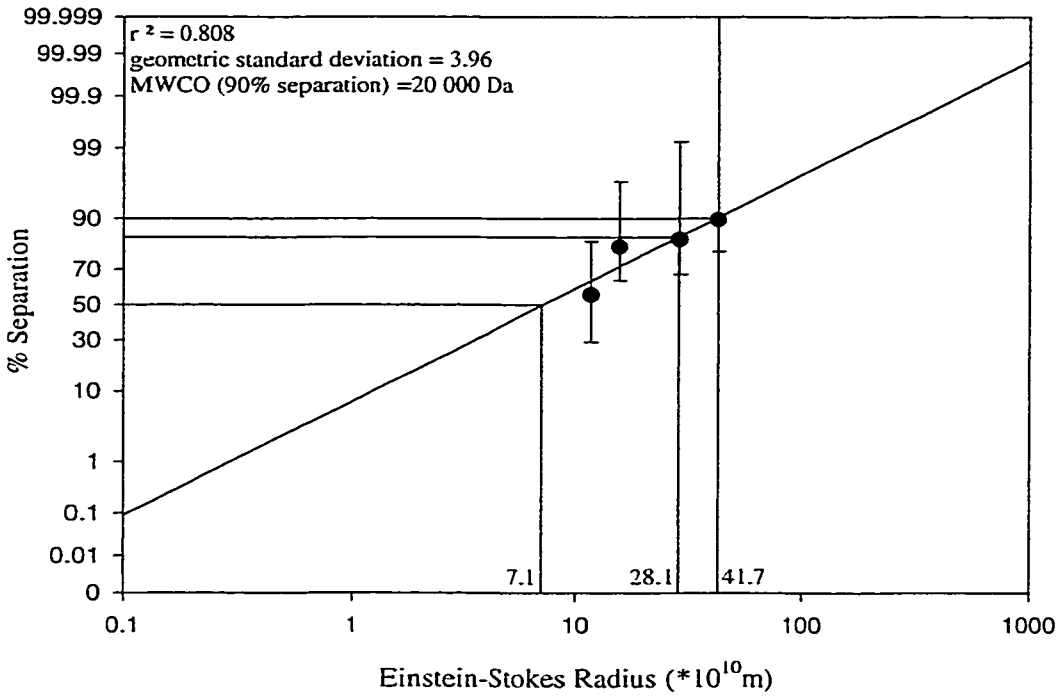

Log-normal probability plot of PEG separation versus Einstein-Stokes radius for PWI/NMP/GBL:20/55/25 - 1 layer 0.5 wt% SPPO-H.

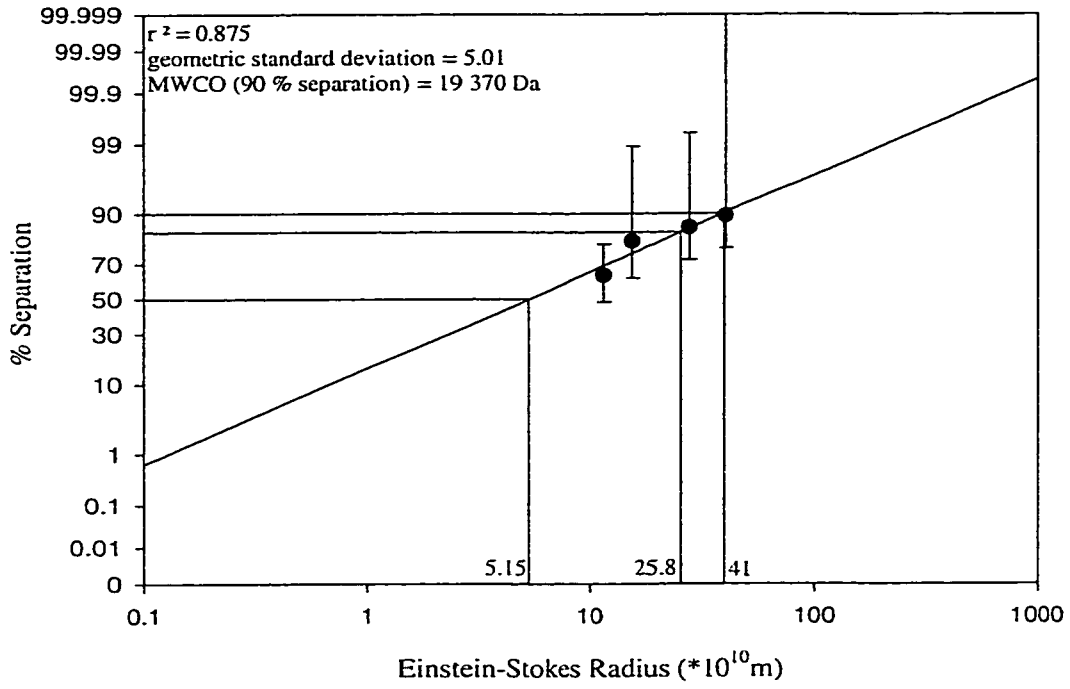

Log-normal probability plot of PEG separation versus Einstein-Stokes radius for PEI/NMP/GBL:20/65/15 - 1 layer 0.5 wt% SPPO-H.

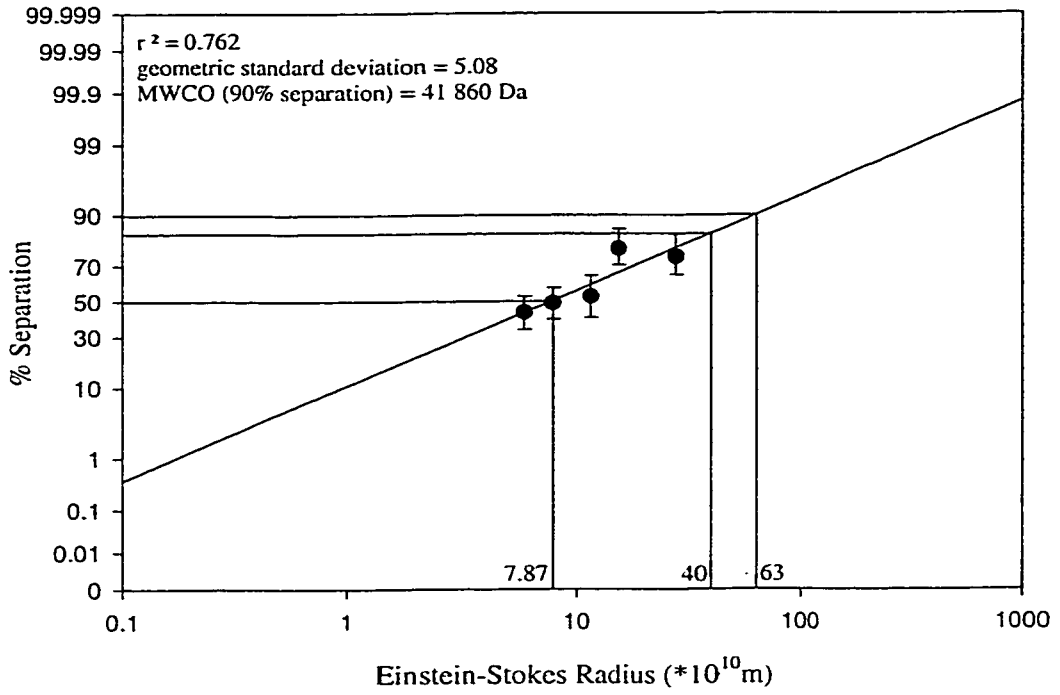

Log-normal probability plot of PEG separation versus Einstein-Stokes radius for PEI/DMAc/GBL:22/68/10 - 1 layer 1 wt% SPPO-H.

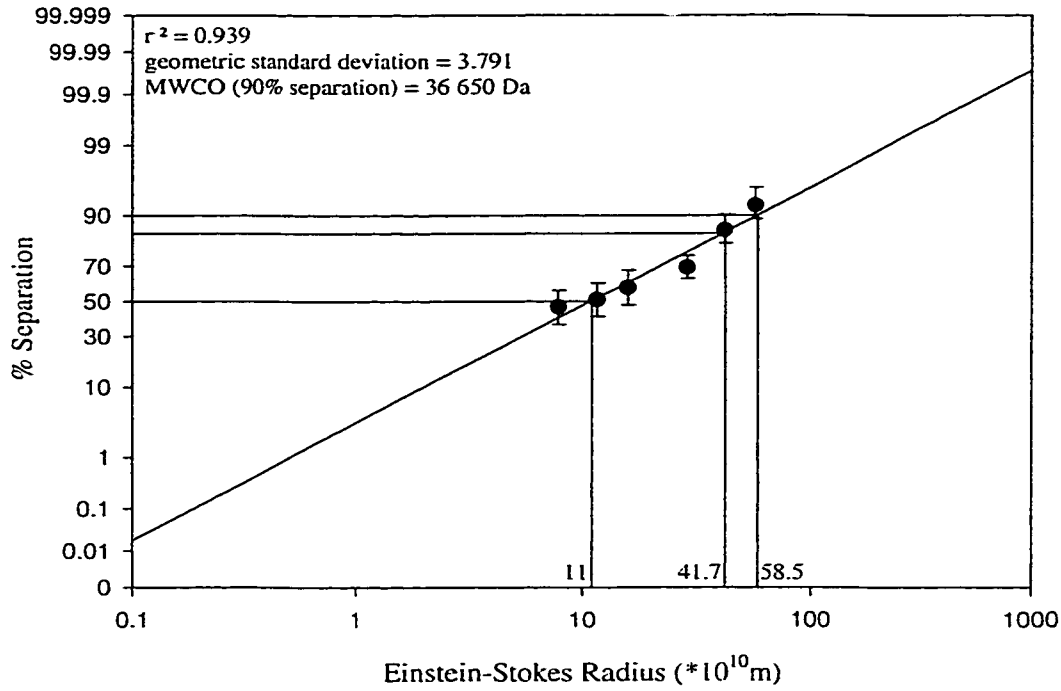

Log-normal probability plot of PEG separation versus Einstein-Stokes radius for PEI/DMAc/GBL:22/58/20 - 1 layer 1 wt% SPPO-H.

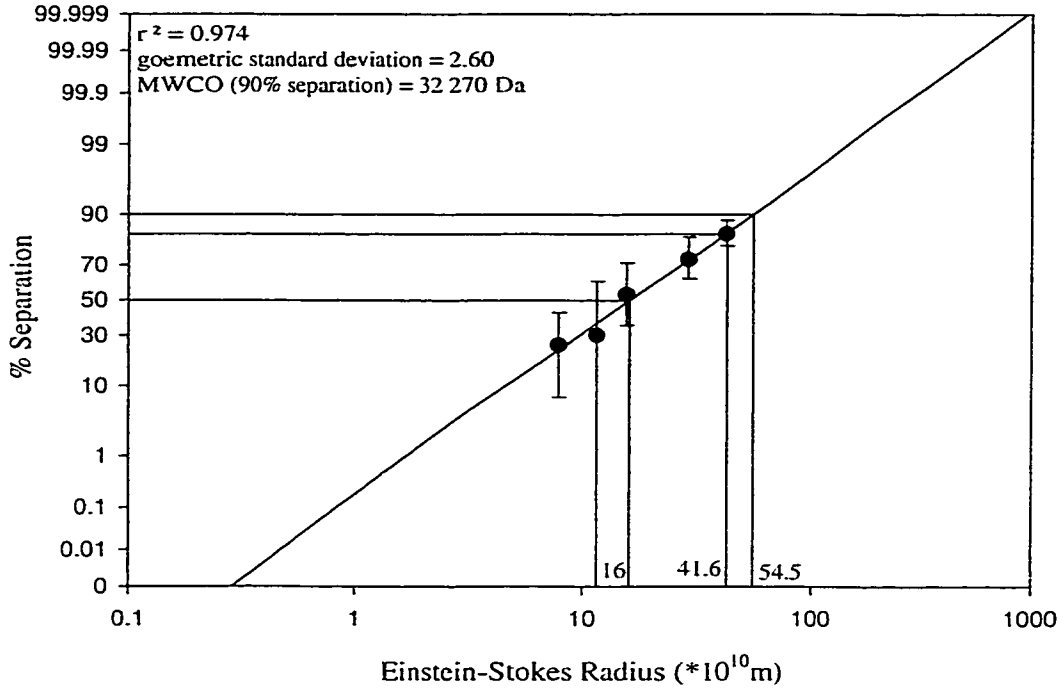

Log-normal probability plot of PEG separation versus Einstein-Stokes radius for PEI/DMAc/GBL:22/48/30 - 1 layer 1 wt% SPPO-H.

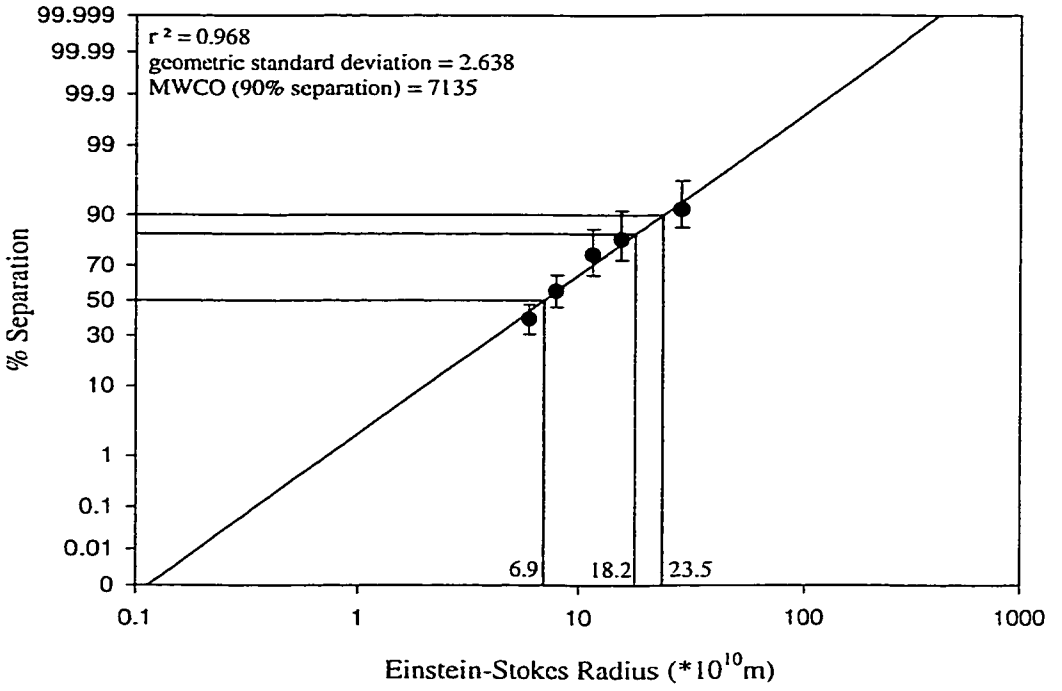

Log-normal probability plot of PEG separation versus Einstein-Stokes radius for PEI/DMAc/GBL:20/50/30 - 1 layer 1 wt% SPPO-H.

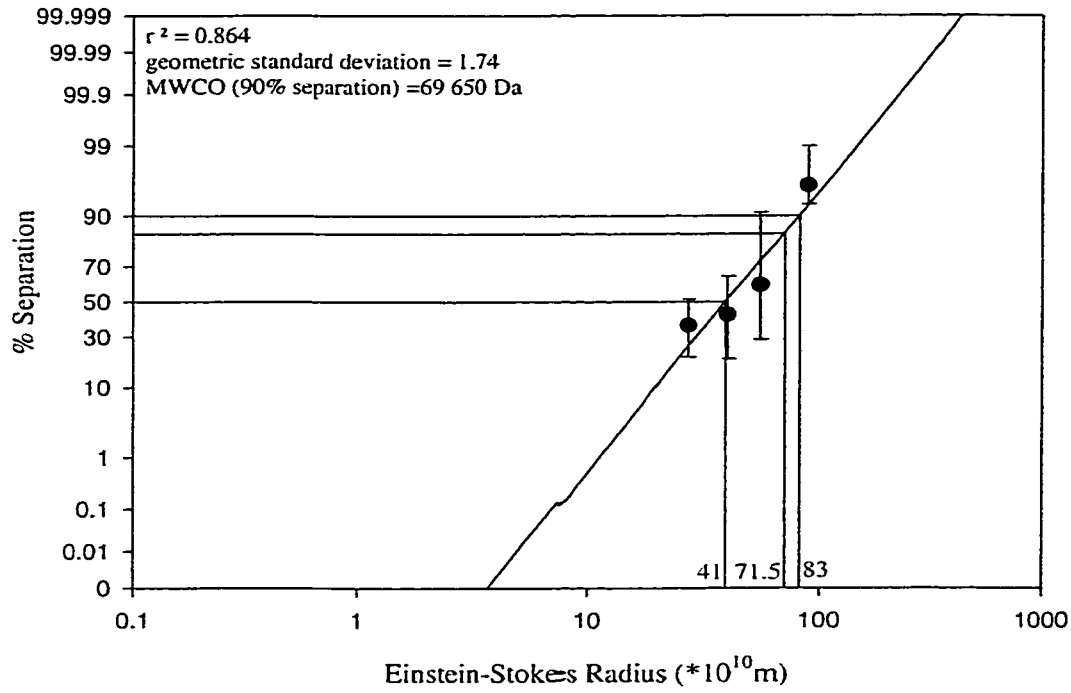

Einstein-Stokes radius versus PEG separation for PEI/NMP/GBL:22/58/20 substrate membranes.

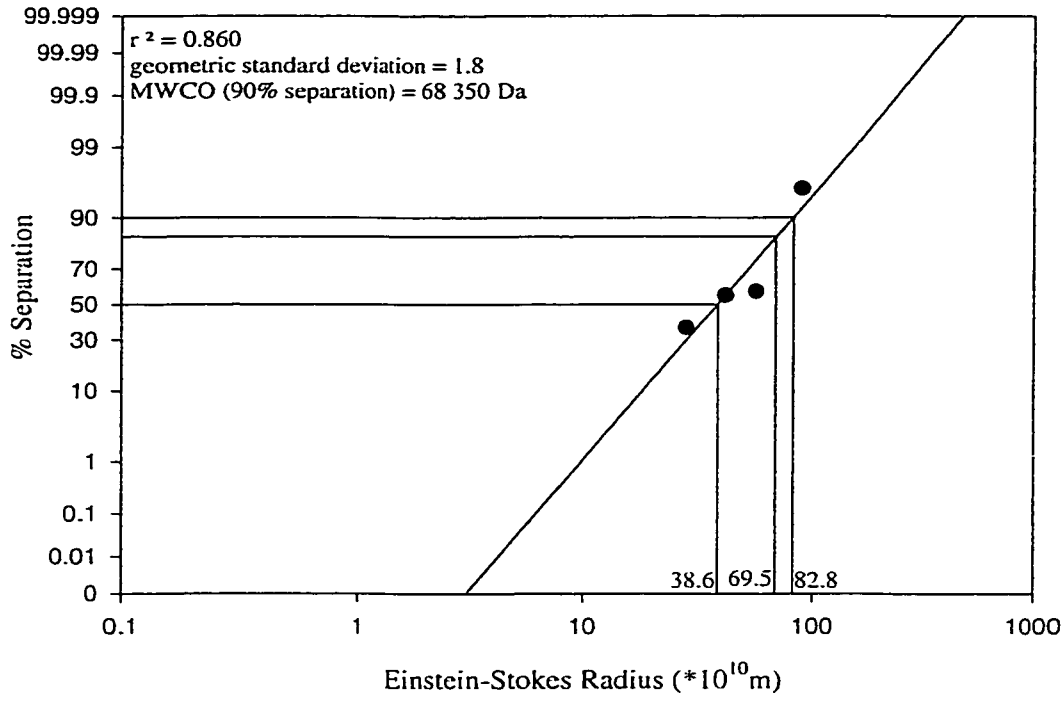

Log-normal probability plot of PEG separation versus Einstein-Stokes radius for PEI/NMP/GBL:20/60/20 substrate membranes.

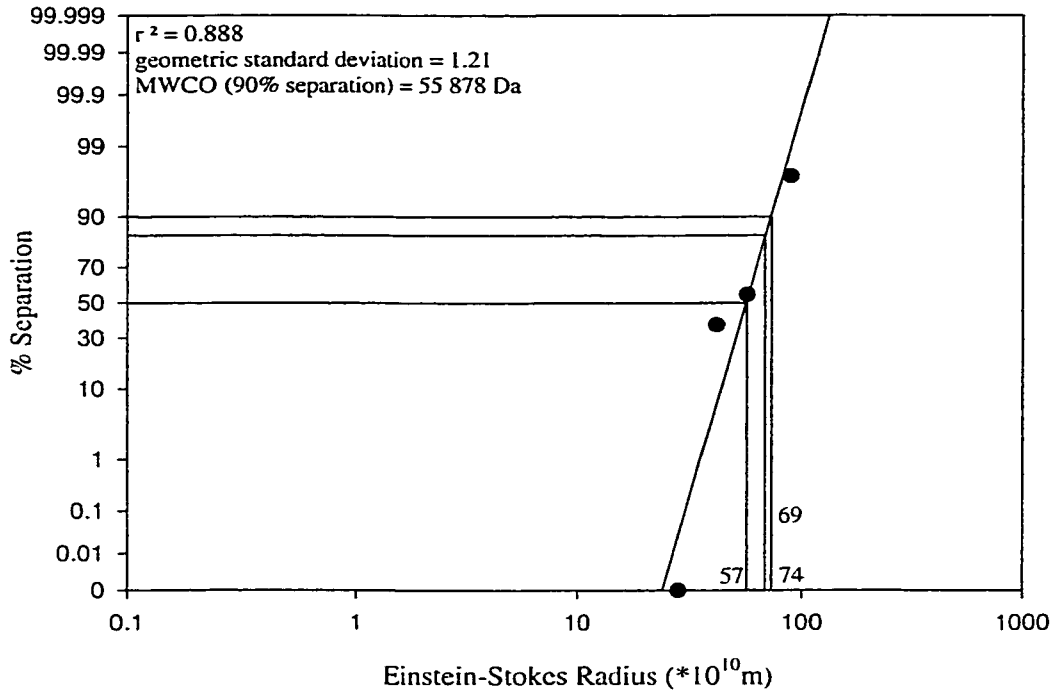

Log-normal probability plot of PEG separation versus Einstein-Stokes radius for PEI/NMP/GBL:20/65/15 substrate membranes.

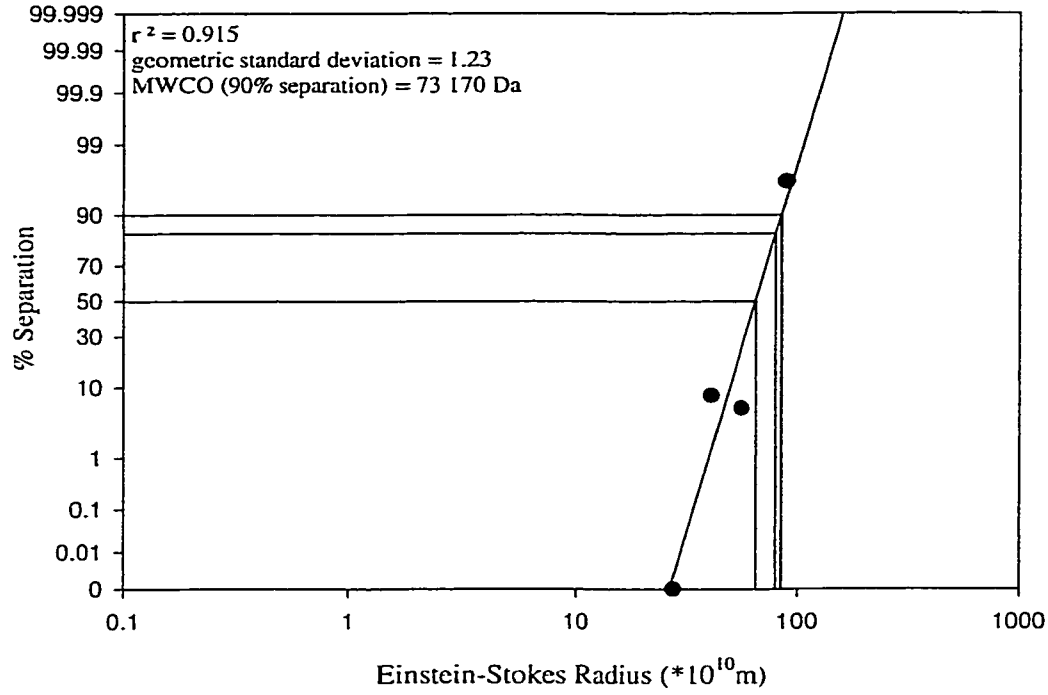

Log-normal probability plot of PEG separation versus Einstein-Stokes radius for PEI/NMP/GBL:20/55/25 substrate membranes.

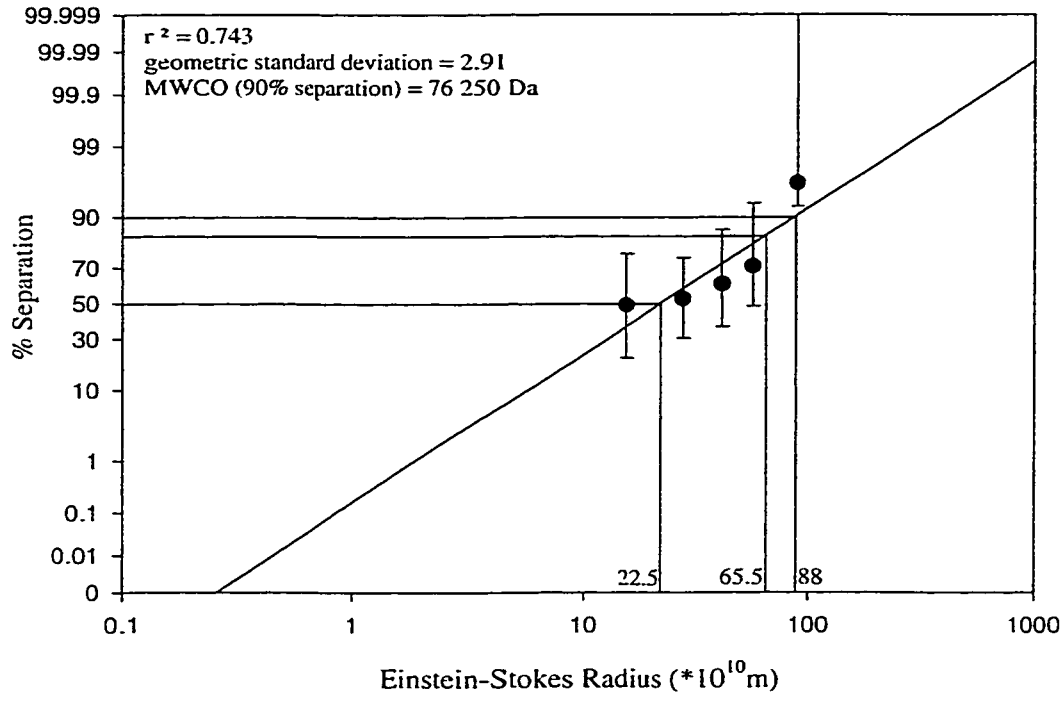

Einstein-Stokes radius versus PEG separation for PEI/DMAc/GBL:20/50/30 substrate membranes.

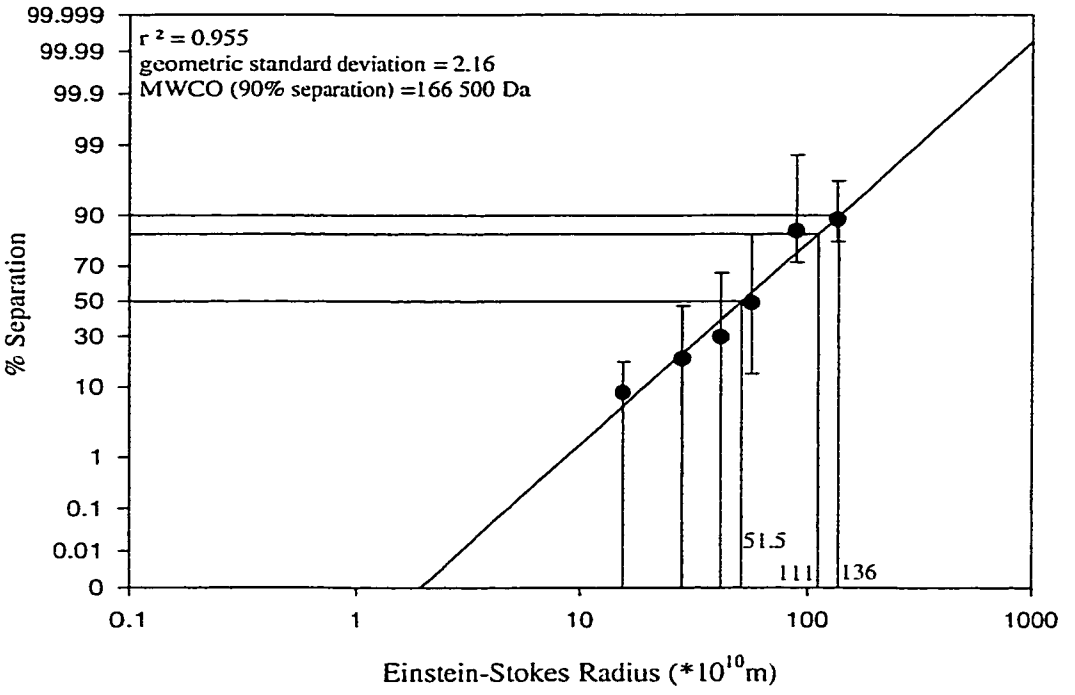

Einstein-Stokes radius versus PEG separation for PEI/DMAc/GBL:22/68/10 substrate membranes.

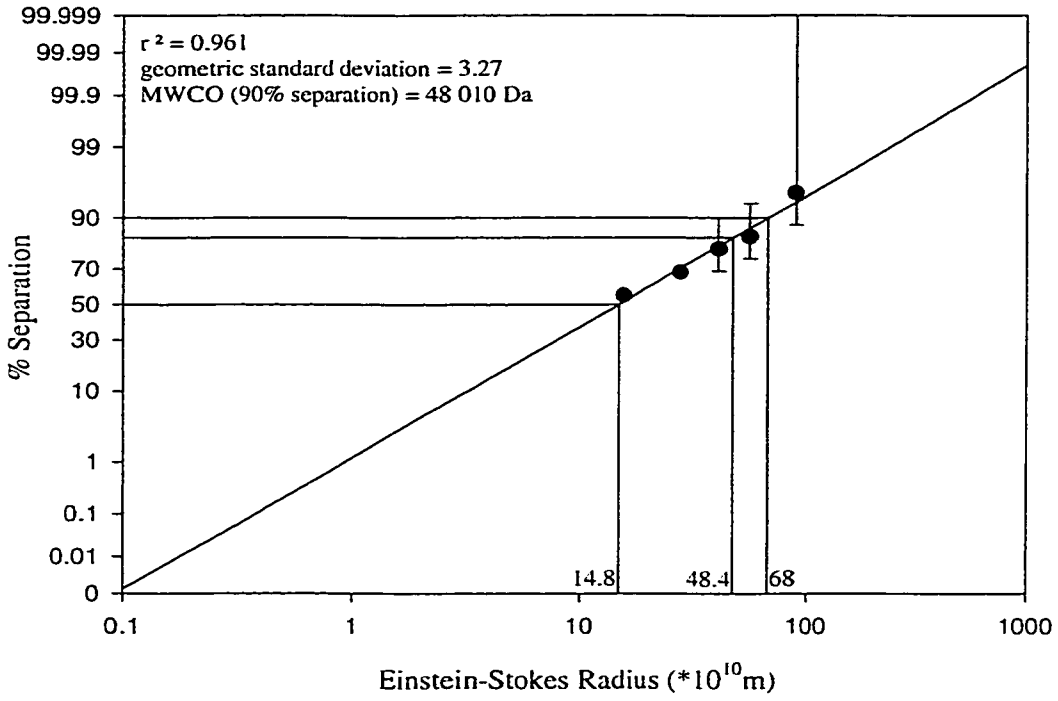

Einstein-Stokes radius versus PEG separation for PEI/DMAc/GBL:22/58/20 substrate membranes.

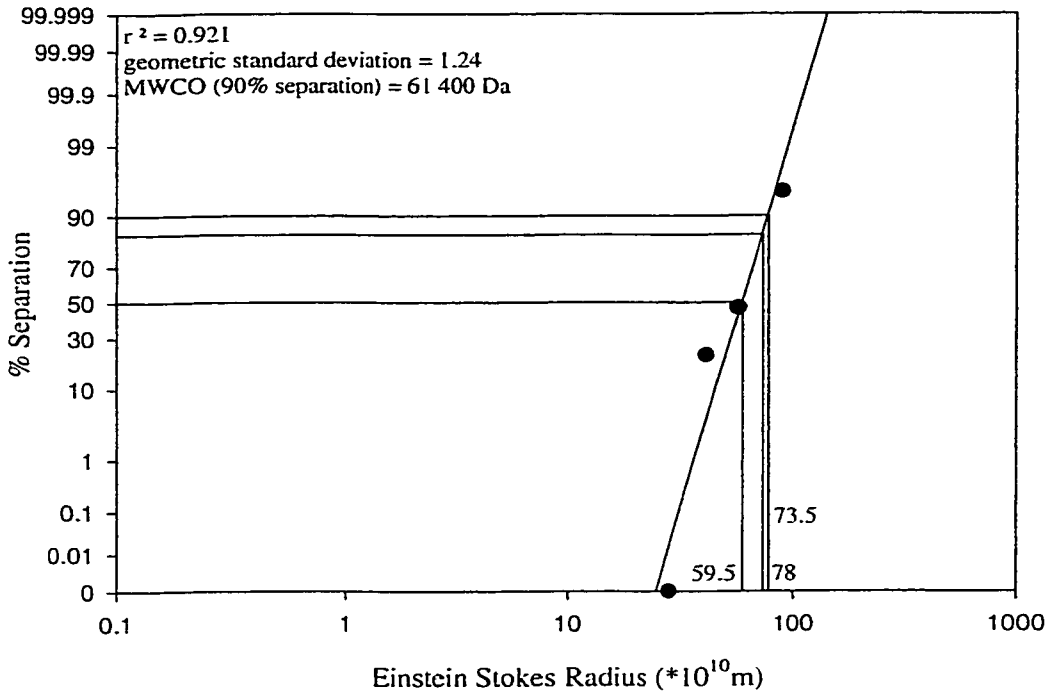

Log-normal probability plot of PEG separation versus Einstein-Stokes radius for PEI/DMAc/GBL:22/48/30 substrate membranes.

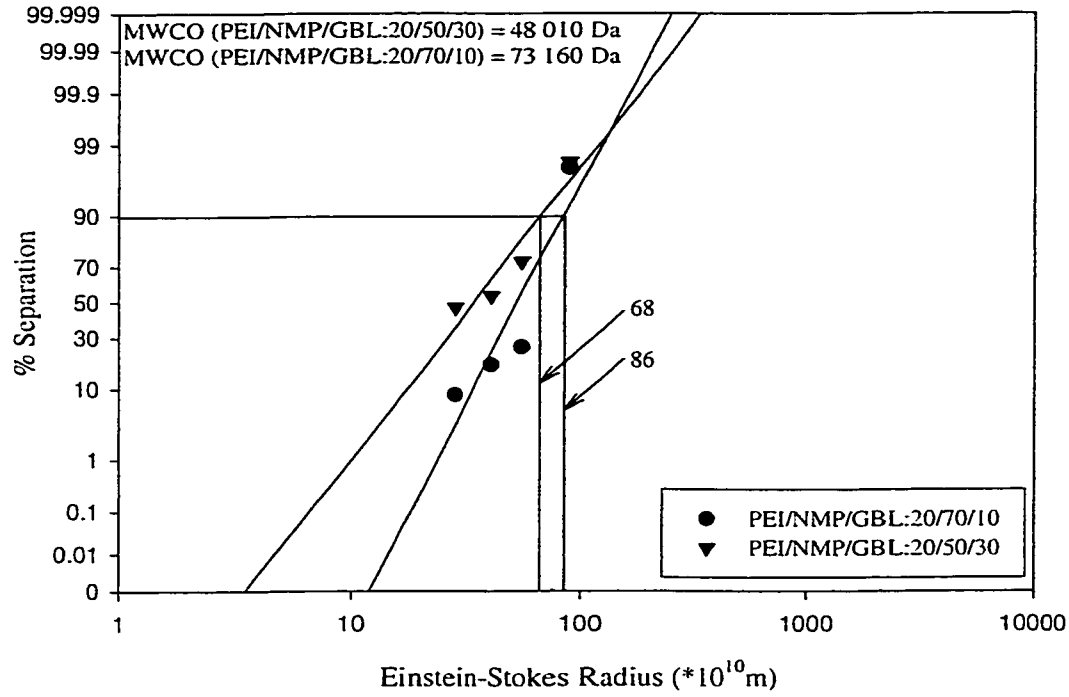

Log-normal probability plot of Einstein-Stokes radius versus separation for 2 PEI substrate membranes.

APPENDIX E Estimation of Binary Liquid Diffusion Coefficients

The binary liquid diffusion coefficients for NMP, DMAc, and GBL in water were estimated by using the molecular weights and densities at 25 °C of each which were obtained from the CRC Handbook of Chemistry and Physics (Weast, 1972) and equation 1.

Solvent	Molecular Weight (g/mol)	Density (g/cm^3)
γ-butyrolactone	86.09	1.120
N-methylpyrrolidinone	99.13	1.033
Dimethylacetamide	87.12	0.937

Thus, the estimated binary liquid diffusion coefficient at infinite dilution for NMP is calculated as follows:

$$D_{NMP/H_2O} = \frac{7.4\times10^{-10}(\phi M_B)^{1/2}T}{\eta_B V_A^{0.6}}$$

$$= \frac{7.4\times10^{-10}[(2.6)(18)]^{0.5}298}{0.01(95.963)^{0.6}}$$

$$= 9.757\times10^{-6}\ cm^2/s$$

APPENDIX F Determination of N/δ and Surface Porosity

The parameter N/δ and the surface porosity of the membranes were determined by using equations 10 and 11 respectively as well as the log-normal probability plots for the corresponding membranes.

A spreadsheet was prepared in order to calculate the f_i's, d_i's, N/δ and % surface porosities. An example is given for PEI/NMP/GBL:20/70/10 substrate membrane along with an explanation of how the numbers in each column is obtained.

% of pores < pore size	fraction of pores of diameter (fi)	log of pore radius (A) from graph	log of pore radius (A) for fraction	pore diameter di (m)	fi*di^4 (m^4)	fi*di^2 (m^2)	PWP(gfd)	number of pores/m^2	number of pores/um^2 (N)	Surface porosity %
1	0.01	1.375	1.375	4.74E-09	5.06E-36	2.25E-19	105.638	2.8764E+13	28.764426	0.340037
5	0.04	1.4825	1.42875	5.37E-09	3.32E-35	1.15E-18				
10	0.05	1.54	1.51125	6.49E-09	8.87E-35	2.11E-18	PWP			
20	0.1	1.605	1.5725	7.47E-09	3.12E-34	5.59E-18	(m^3/m^2s)		N/delta	
30	0.1	1.655	1.63	8.53E-09	5.3E-34	7.28E-18	4.9762E-05		47.940711	
50	0.2	1.735	1.695	9.91E-09	1.93E-33	1.96E-17				
70	0.2	1.815	1.775	1.19E-08	4.03E-33	2.84E-17				
80	0.1	1.865	1.84	1.38E-08	3.67E-33	1.91E-17				
90	0.1	1.93	1.8975	1.58E-08	6.22E-33	2.49E-17				
95	0.05	1.985	1.9575	1.81E-08	5.41E-33	1.64E-17				
98	0.03	2.0475	2.01625	2.08E-08	5.57E-33	1.29E-17				
99	0.01	2.09	2.06875	2.34E-08	3.01E-33	5.49E-18				
99.9	0.009	2.21	2.15	2.3E-08	5.73E-33	7.18E-18				
				Sums -->	3.65E-32	1.51E-16				

The example will look at the row beginning with % of pores less than 5%. Using the log-normal probability plot for this substrate membrane, the log of pore radius (column 3) is obtained by reading the log Einstein-Stokes radius corresponding to 5% separation from the fitted line (1.4825). The log of the pore radius for the fraction is then the mean of the log of the pore radii for this fraction of pores and the previous one, i.e. (1.375+1.4825)/2 = 1.42875. The fifth column, pore diameter di, is obtained by taking the antilog of the previous column and converting it to metres by multiplying by 10^{-10}. Now, we have obtained the f_i's and d_i's. The summations of $f_i d_i^4$ and $f_i d_i^2$ are found at the bottom of columns 6 and 7 respectively. Using the pure water permeation flux of the membrane, the number of pores can be calculated as follows:

$$N = \frac{128\eta\delta J}{\pi\Delta P \sum_{d\,min}^{d\,max} f_i d_i^4}$$

$$= \frac{128(0.0008937)(0.6\times10^{-6})(4.9762\times10^{-5})}{3.14159(1034214)(3.65\times10^{-32})}$$

$$= 28.76 \text{ pores}/\mu m^2$$

where δ, the membrane thickness, was taken as 0.6 microns. The surface porosity can thus by calculated as follows:

$$S_p = \left(\frac{N\pi}{4}\sum_{d\,min}^{d\,max} f_i d_i^2\right)\times 100$$

$$= \frac{0.2876\times10^{14}(3.14159)(1.51\times10^{-16})(100)}{4}$$

$$= 0.340\%$$

The parameter N/δ can be easily obtained by simply dividing N by the membrane thickness:

$$\frac{N}{\delta} = \frac{28.76}{0.6} = 47.9 \text{ pores}/\mu m^3$$

APPENDIX G Intrinsic Viscosity Measurement

Intrinsic viscosity was measured by two methods. In the first method, Huggin's Method, the intrinsic viscosity is determined by plotting η_{sp}/c versus c and linearly extrapolating to c=0, where c is the concentration of the polymer in solvent and η_{sp} is defined as

$$\eta_{sp} = \frac{\bar{t} - t_o}{t_o}$$

where $\bar{t}$ is the capillary pass time of the pure solvent, methanol, and t_o is the capillary pass time of SPPO of concentration c.

Concentration of SPPO in methanol (g SPPO/100 ml solvent)	Capillary pass time (s)
pure methanol	188.10
0.5010	690.30
0.2556	560.33
0.2009	523.67
0.1683	498.33
0.1426	477.67

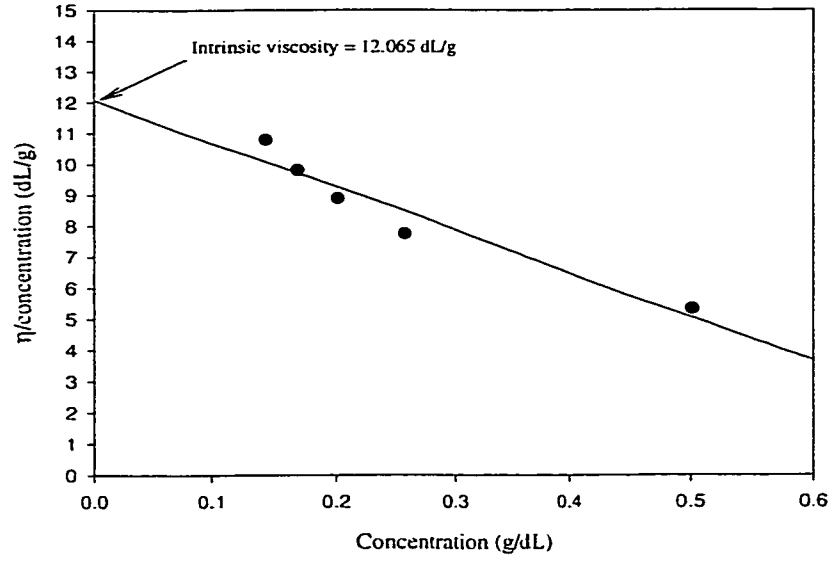

Intrinsic viscosity of SPPO ([η]=1.58, I.E.C.=1.73 meq/g) in methanol.

The intrinsic viscosity was also determined by Kozicki and Kuang's method by plotting η_{sp} by the concentration, applying an analytical expression containing the point $\eta_{sp}=0$ at c=0 which provides a good fit of the experimental data and yields a first derivative at c=0 and solving for the coefficients. In this case a third order equation best fitted the experimental points,

$$\eta_{sp} = 15.363c - 39.379c^2 + 38.585c^3$$

and the intrinsic viscosity was found to be 15.363 dL/g after solving for the coefficients.

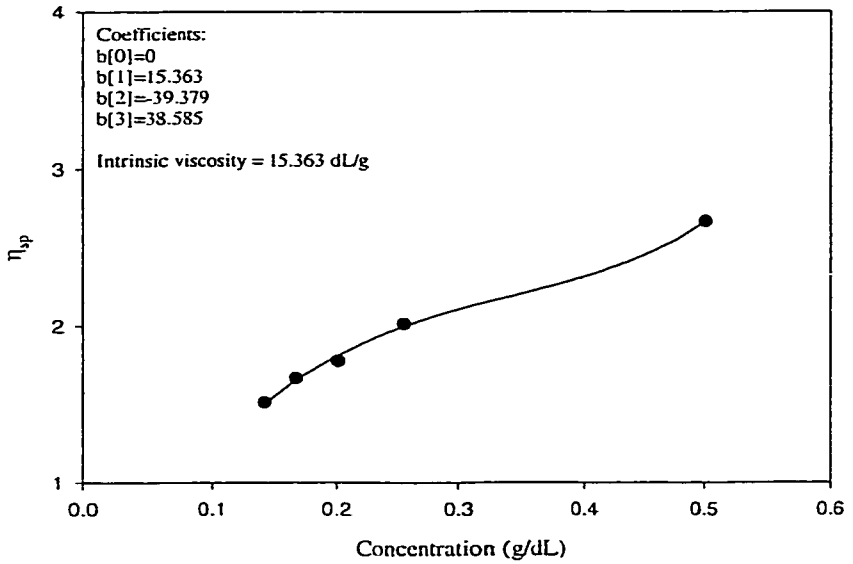

Intrinsic viscosity of SPPO ([η] = 1.58 , IEC = 1.8 meq/g) in methanol.

APPENDIX H Determination of Macromolecular Radius of SPPO at Infinite Dilution

The macromolecular radius of SPPO in solution of infinite dilution was calculated using the intrinsic viscosity obtained by Kozicki and Kuang's method (see Appendix G) as follows:

$$R_o^3 = \frac{3[\eta]M}{2.5N_o(4\pi)}$$

where M, the number-averaged molecular weight of SPPO, is 157 128 Da and N_o is Avogadro's number, 6.022045×10^{23}/mol,

$$R_o = \left(\frac{(1536.3)(157128)(3)}{2.5(6.02245\times10^{23})(4\pi)}\right)^{1/3}$$

$$R_o = 3.3699\times10^{-6}\ \text{cm} = 33.7\ \text{nm}$$